8-2013

Optimizing SCM Proportions to Meet Multiple Performance Characters of Ternary Concrete Mixtures Using Simplex-Centroid Design and Analysis Techniques

Sujay Math
Clemson University, smath@clemson.edu

Follow this and additional works at: https://tigerprints.clemson.edu/all_dissertations

Part of the Civil Engineering Commons

Optimizing SCM Proportions to Meet Multiple Performance Characters of Ternary Concrete Mixtures Using Simplex-Centroid Design and Analysis Techniques

---

A Dissertation
Presented to
the Graduate School of
Clemson University

In Partial Fulfillment
of the Requirements for the Degree
Doctor of Philosophy
Civil Engineering

---

by
Sujay Math
August 2013

Accepted by:
Dr. Prasad Rangaraju, Committee Chair
Dr. Bradley Putman
Dr. Amir Poursaee
Dr. William Bridges

Abstract

High performance concrete mixtures often contain multiple cementitious components. Among these, cement is the most expensive in addition to having a higher carbon footprint. Life cycle assessment of cement production reveals that the cement content is the most important factor in determining a concrete mixture's embodied energy and carbon footprint. Compressive strength, an important property of concrete, is directly related to the quantity of cement used in the mixture. However, higher quantities of cement lead to durability issues. The increased concerns about the durability of concrete over the past decade have increased focus on improving the long-term performance of concrete structures. The goal of reducing the quantity of cement has led the use of supplementary cementitious materials (SCM) such as slag, fly ash, silica fume and others as a replacement.

The traditional method for optimizing high performance concrete mixtures involves systematically varying the individual proportions of the components in small increments and studying the resultant effect. In this method, the basis for selecting SCM dosage is arbitrary and often focuses on a specific set of requirements such as strength or durability. Optimizing the component proportions in the traditional way to achieve the desired properties is time-consuming, requiring a large number of trial batches, making this process expensive and inefficient. The use of statistical mixture design techniques has the potential to reduce the number of test runs needed, especially when multiple cementitious components are used and multiple requirements have to be simultaneously satisfied.

The research reported here investigates the use of a statistical design of experiments approach, specifically the simplex-centroid mixture design, using three cementitious com-

ponents and a minimum of seven design points representing specific mixture proportions. In this study, a ternary blend of portland cement, slag and Class F fly ash was used. The total cementitious content of the concrete was kept constant although the individual proportions were varied. Fresh and hardened properties of concrete were evaluated, including mechanical properties such as compressive strength and split tensile strength and durability indicators such as rapid chloride ion permeability and expansion due to alkali-silica reaction. With the use of statistical design software (JMP), strength and durability prediction equations were developed and subsequently validated using an additional five concrete mixtures. These prediction equations investigated here generated a response surface for a given property as a function of the proportions of the three cementitious components using the seven concrete mixtures. Multiple response surfaces were superimposed on the simplex design region, and optimum cementitious mixtures were identified. The ternary blends were also used to evaluate mortars for alkali-silica reaction potential in mortar bars, and fundamental studies on cementitious paste systems involved pore solution extraction analysis and electrical resistivity.

The results obtained from this study showed that the properties of concrete such as compressive strength and rapid chloride ion permeability had a good correlation between the actual and predicted values whereas properties such as split tensile strength did not a show good correlation. The deleterious effects of alkali-silica reaction in mortar and concrete were evaluated using a threshold expansion value. These evaluations indicated that the mixtures below the threshold expansion contour in the simplex region did not show any alkali-silica reaction distress. The results from the cementitious paste studies showed that the electrical resistivity of the cementitious paste systems increased with decreasing ionic concentrations in the pore solution due to the replacements of cement with SCMs. In addition, the pore solution analysis showed that because of the pozzolanic reaction of SCMs, the alkali ions become trapped in the secondary C-S-H gel and the pore solution alkalinity is reduced with age. At elevated temperatures due to the instability of the calcium sulfo-aluminate phases, the sulfate ions (SO_4^{-2}) dissolved back into the pore solution. Using the simplex centroid

design technique the pore solution results can be used to generate response surface for ionic concentrations of cementitious paste systems.

Results from this research suggest that the simplex-centroid design could be a valuable tool for minimizing the number of trial batches needed to identify the optimal concrete proportions for achieving the desired properties. As an outcome of this research, guidelines were developed for using the simplex-centroid method for concrete mixture design applications. The optimum mixtures obtained for various concrete applications within the simplex region yielded optimum cement dosages, in turn reducing the cost of concrete and its carbon footprint.

Future work in this area should include using different SCMs to optimize desired properties of concrete. In addition, this concept can be extended to include the w/c ratio, another important property of concrete. Various statistical mixture designs techniques can also be explored to improve the predictability power. Ultimately, the research in this area should lead to more cost-effective concrete with a smaller carbon footprint that can be adopted for use in the field.

Dedication

This thesis is dedicated to my loving parents, Prabhudev and Prema Math, for their inspiration and endless support without which none of this would have been possible. This thesis is also dedicated to my caring sister, Sneha Math, for her continous encouragement throughout my graduate studies.

Acknowledgments

I would like to express my gratitude to my advisor, Dr. Prasad Rangaraju, whose expertise, understanding, and patience added considerably to my graduate experience. I appreciate his vast knowledge and skill in many areas, and his assistance scholarship applications, journal publications and this dissertation all of which have helped me achieve my goals. I would like to thank the other members of my committee, Dr. Brad Putman, Dr. Amir Poursaee and Dr. William Bridges, for the assistance they provided at all levels of this research project.

I would like to acknowledge the support provided by Clemson University's faculty and staff from different departments in helping me with my research. I would like to extend my thanks to Dr. Richard Warner from Gelology, Dr. Kathy Moore from the Agricultural Service Laboratory, Mr. Sanjeewa Duminda and Mr. Colin McMillen from Chemistry, Mrs. Kimberly Ivey from Material Science for helping me with different aspects of my research. I would also like to thank Mr. Danny Metz and his team from Civil Engineering, for maintaining the equipment in the concrete lab and helping me with operating the equipment. I also thank Mrs. Barbara Ramirez, the Director of the Class of 1941 Studio for Student Communications, for providing excellent editorial support for my doctoral dissertation.

I would like to thank my fellow graduate students and my lab mates, Harish Kizhakkumodom, Shubhada Gadkar, Enamur Latifee and Kaveh Afshinnia, for helping me in the lab irrespective of their busy schedules. I extend special thanks to my friend Andrew Neptune for our discussions of knowledge, skills, philosophical ideas and our frustrations during my graduate program, which helped enrich my experience.

In conclusion, I recognize that this research would not have been possible without the financial assistance of the US Navy Department of Defense (DOD) and the Department of Civil Engineering at Clemson University through teaching and research assistantships. I express my gratitude to those agencies.

Table of Contents

List of Tables

List of Figures

Chapter 1

Introduction

1.1 Background

The wide-spread use of concrete is a result of its workability when it is freshly mixed and its strength and durability when hardened. These properties explain why this material can be used to construct highways, bridges, skyscrapers, sidewalks, houses and dams. In addition these properties can be modified to suit the type of structure being constructed. For example, highway pavements are constructed to withstand the load of moving traffic and a wide range of environmental conditions. The desirable properties for pavements is low workability and adequate strength with high durability. For buildings using reinforced steel in concrete, a higher workability is desired to allow the concrete to flow through the reinforcement cage. The expectancy of strength and durability for such buildings is higher considering the importance of the lives of people occupying them. These properties of concrete are controlled by changing the proportions of the components making up the mixture. Water, aggregates and cement are the three major components forming the concrete mixture. When selecting these proportions, the primary objective is to meet the desired properties in the most economical way possible.

Of these three components, water is the cheapest, its proportion having a direct influence on the workability, and its quantity inversely affecting the strength of concrete.

Aggregates, the next most inexpensive material, generally vary from 65% to 80% of the total volume of concrete. Their physical and chemical properties such as shape, texture, gradation and reactivity not only influence the properties of fresh concrete but also affect the strength and durability of hardened concrete. Since aggregates form the bulk of the skeleton structure of concrete, it is important to optimize their proportion; however, this does not significantly change the overall cost. Cement, which acts as the filler material between the aggregates in the concrete, is reduced by selecting their optimum gradation.

1.2   Role of Cement in Concrete

Cement is the most expensive component of concrete, accounting for 60% of the overall cost and 10% to 15% of its volume. Cement, when mixed with water, reacts to form a paste which binds the aggregates into a rock-like mass when hardened. The quantity of cement used significantly influences concrete properties: higher cement content usually yields high strength, but this high cement content also leads to durability issues and subsequently higher costs.

Strength in concrete is primarily achieved through the hydration of cement grains. This hydration produces a calcium silicate hydrate (C-S-H) gel and calcium hydroxide (CH) as the reaction products. This gel forms the primary pore structure of the hardened cement paste and with time, the hydration of cement continues, the pore structure becoming more refined as more gel forms. The CH is dispersed throughout the hardened cement matrix, leaching out to the surface of the concrete if in excess. The hydration process is an exothermic reaction; the excess heat thus generated causes a temperature gradient on the concrete surface, leading to the development of micro-cracks. These micro-cracks compromise the durability because they allow easy access of rain and harmful chemicals. In addition, the durability of concrete is affected by the quantity of cement: the more the cement, the higher the alkali content, which increases the pore solution alkalinity in concrete. This higher alkalinity has the potential to react with reactive aggregates, causing alkali-

silica reaction distress. Thus, with increased durability issues at later ages, the longevity of concrete structures is reduced.

A second consideration about the role of cement in concrete is its manufacturing process, which results in high energy-related carbon dioxide (CO_2) emissions that contribute to greenhouse gases. Life cycle assessment of cement production reveals that the cement content is the most important factor in determining a concrete mixture's embodied energy and carbon footprint. Reducing the cement content for per unit volume of concrete produced decreases the overall cost and makes concrete more environmentally friendly. Thus, a reduction in cement usage promotes reduced cement manufacturing, yielding lower CO_2 emissions and greenhouse gases. Organizations such as the EPA and USGBS encourage the reduced use of cement in concrete by providing incentives to contractors and construction companies. The challenge becomes finding the right proportion of cement, one that is environmentally friendly but also provides optimum strength and durability at a reasonable cost. To address these problems, optimizing the proportion of cement by substituting it with supplementary cementitious materials (SCMs) may have potential.

1.3   Supplementary Cementitious Materials

Supplementary cementitious materials include mineral-based materials that possess pozzolanic reactivity and/or latent hydraulic reactivity. The typical SCMs used to replace cement in concrete include slag, fly ash, silica fume, metakaolin and natural pozzolans. Slag is a residue obtained from the steel or iron manufacturing process; its chemical composition does not significantly vary from its source of production. Fly ash is finely divided residue that results from the combustion of coal in power plants; its chemical composition varies significantly based on the type of coal. Silica fume is composed primarily of amorphous silica produced by electric arc furnaces as a byproduct of the production of elemental silicon or ferrosilicon alloys. Similarly, other SCMs are obtained either from different manufacturing processes or are produced for their beneficial characteristics. These

SCMs such as fly ash and slag are industrial by-products, with a smaller carbon footprint than portland cement. Increasing the quantity of SCM while minimizing the total cementitious materials in concrete will, thus, have a net beneficial environmental impact [Bentz et al., 2011, Zhang et al., 2012].

The use of SCMs enhances the overall performance characteristics of the fresh and hardened concrete in terms of strength and durability by undergoing a pozzolanic reaction. SCMs react with the excess CH produced during the cement hydration process producing a secondary C-S-H gel. As a result of this reaction, the pore structure becomes more refined as the connectivity of the pores decreases. This pore structure refining process increases the electrical resistivity of concrete reducing the ion movement in it, making concrete denser and impermeable to harmful chemicals.

As a result, the choice of which SCMs to use in concrete primarily depends on the desired performance of concrete at its various ages. For example, fly ash and slag increase the slump of fresh concrete due to the ball bearing effect whereas silica fume makes concrete sticky, decreasing slump. Silica rich ($SiO_2 \geq 90\%$) SCMs are usually used in lower dosages as they are highly reactive at initial stages of mixing with concrete. Low to moderate siliceous SCMs require higher dosages of cement replacement and under go pozzolanic reaction at later stages. Slag and fly ash are inactive at the initial hardening stage when mixed with cement, causing a reduction in strength whereas silica fume and metakaolin are highly reactive and increase the early age strength. Due to their slow reactivity, slag and fly ash improve the durability of concrete as it ages as compared to pure cement concrete, thus increasing the longevity of concrete structures. While in some cases the early age strength of concrete is compromised with the use of SCMs, its long-term effects are advantageous. Because of these characteristics, ternary blends of SCMs with cement are becoming wide-spread to compensate for these effects; however, the challenge is to choose the optimum dosage levels of these various SCMs.

Currently in industry the dosages of SCMs are selected based on past performance and chemical composition. The conventional approach is to replace cement with an SCM in

small increments and test its performance. For a ternary mixture, this traditional approach becomes difficult as the permutation combination of three materials in small increments yields hundreds of mixtures, requiring numerous time-consuming test runs, making this process expensive. To address this issue, the research reported here investigates the use of a statistical mixture design technique to reduce the number of test runs needed to yield useful information.

1.4 Problem Statement and Research Significance

Increased concerns about the longevity of structures has compelled concrete designer to use SCMs in concrete. While their use has been widely accepted, their proportions as cement replacements has been based on past performance and may not necessarily be the optimum dosages. In addition, the proportion of SCM used to meet one desirable property may not necessarily meet others.

The research reported here focuses on reducing cement content by optimizing the proportions of SCM, in particular slag and class F fly ash, to the amount requiring the fewest number of trial mixtures to meet several desirable properties. This research explores the use of a design of experiment approach, specifically Henry Scheffe's Simplex-Centroid Design technique, to evaluate its potential to achieve this goal.

The results of this study should support a technique to optimize cementitious content in concrete mixtures to meet various performance requirements based on desired properties. This technique will, thus, help a concrete designer develop cost-effective mixtures with a low carbon footprint while at the same time achieving the desired performance.

1.5 Research Objectives

The main objective of this research is to develop a concrete mixture optimization tool that will evaluate ternary concrete mixtures to fulfill both mechanical and durability performance with fewer trials, than are currently needed. To achieve this objective, the

properties of concrete evaluated in this investigation are listed below:

1. Investigate the effectiveness of SCMs (slag and class F fly ash) on the performance of fresh and hardened properties of portland cement concrete.

2. Evaluate the fresh properties including slump, air content and the unit weight of concrete.

3. Evaluate such hardened properties as compressive strength, split tensile strength, rapid chloride-ion permeability and alkali-silica reactivity of concrete.

4. Evaluate the alkali-silica reactivity potential of various aggregates using ternary combinations of cement, slag and class F ash.

5. Investigate the chemical and electrical properties of binary and ternary cementitious paste systems.

6. Evaluate the effect of pore solution alkalinity and hydroxyl ion concentration on alkali-silica reaction expansions in concrete.

7. Evaluate the effect of pore solution chemistry on electrical properties of cementitious systems.

1.6   Scope of the Research

The Simplex-Centroid Design methodology used here requires various materials and standard and modified test methods. The materials selected for this research include aggregates, portland cement, supplementary cementitious material, reagent grade sodium hydroxide (NaOH) and reagent grade sodium chloride (NaCl). The aggregates selected for this research were from different parts of the North America. For the concrete studies one reactive coarse aggregate from North Carolina was used, and the fine aggregate selected was river sand from South Carolina. For mortar studies four aggregates were selected based on their mineralogical content to represent various levels of alkali-silica reactivity under

6

laboratory and field conditions. The cement used was high alkali cement (Type I) with an Na_2O equivalent of 0.86% (Na_2O_{eq}) and an autoclave expansion of 0.12% for all aggregates used here. The total volume of concrete prepared was 11.5 ft^3 (0.325 m^3) which was further cast into 156 concrete cylinders and 36 concrete prisms. For the mortar study, 180 mortar bar specimens were prepared from various reactive aggregates and SCMs.

To evaluate strength performance, the compressive strength and split tensile strength were determined for the concrete cylinders. To evaluate durability performance, the alkali-silica reaction distress and chloride ion permeability of concrete was determined. For the mortar study, only the alkali-silica reaction durability distress was studied using accelerated mortar bar tests. The chemical and electrical properties study of the cementitious paste systems was limited to pore solution elemental analysis and electrical resistivity of the paste samples.

1.7   Organization of the Dissertation

This dissertation includes six chapters.

Chapter 1 provides an introduction to this study stating the problem statement and the need for this research. It also defines its principal objectives and scope.

Chapter 2 is the literature review of the past studies and the state-of-the-art optimization techniques for concrete mixture proportioning in general, the standard test methods used to assess the individual performance of concrete and the various mixture design techniques. This chapter also discusses the various modified test methods used in this study and their advantages and disadvantages.

Chapter 3 discusses the materials used and the standard test methods adopted for this research. Chapter 4 describes the experimental program adopted for evaluating the objectives of this research.

Chapter 5 reports the results of the various tests including their analysis and discussion.

Chapter 6 concludes this dissertation and draws conclusions relating to the principal findings of this study in relation to its objectives. Based on these findings, recommendations for further research are suggested.

Chapter 2

Literature Review

Optimizing concrete mixtures to meet desired requirements for a particular situation involves optimizing either one or several variables at a time. For the research reported here, one of the Design of Experiment (DOE) mixture-design technique namely, Simplex-Centroid Design (SCD) is used. This technique is applied to proportion the cementitious content of concrete by replacing cement with Supplementary Cementitious Materials (SCMs). In addition to discussing on the past research on DOE mixture-design technique, this chapter also reviews the literature related to the basic aspects of the physical, chemical, durability, and mechanical characteristics of cementitious paste systems in concrete. The literature lists the research related to use of SCMs such as slag and fly ash to improve the performance of concrete, along with other SCMs used by different researchers.

2.1   Design of Experiments (DOE)

Design of Experiments involves running experiments to yield the most information from the fewest runs. The methodology of designing experiments was first proposed by Ronald A. Fisher [Fisher and Mackenzie, 1923] in his field trial work dealing with agricultural applications of statistical methods. Since this discovery many other researchers contributed towards the development of various design of experiments techniques.

2.1.1 Experiments with Mixtures

In early 1960's Henry Scheffe introduced the simplex-lattice [Scheff, 1958] designs which are considered to be the genesis of mixture design experiments. Later Scheffe introduced simplex centroid designs for a 3-component mixture design with a mathematical model [Scheffe, 1963]. Experiment with mixture techniques uses a design approach when response changes only as a function of the proportion of component ingredients. The mixture design approach has designs and mathematical models for exploring the entire simplex factor space by factorial design approach. This technique concentrates on fitting of mathematical equations to model the response surface over the entire simplex factor space, so that the empirical prediction of the response to any mixture over the entire simplex is possible. The coefficients obtained from the mathematical model will define synergistic blending effects or antagonistic blending effects and interaction effects of the components.

The mathematical model or the regression equation is postulated to represent the response surface over the entire simplex region. The design is chosen at whose points observations are collected to which the regression equation can be fitted and the coefficients of the regression equation can be estimated. Finally the adequacy of the model is tested to ensure that our fitted equation is a prediction tool with which we can comfortable predict any point within the design space.

In mixture experiments, the property studied depends on the proportions of the components present, but not on the amount of the mixture [Cornell, 2002]. The factors used are the components or ingredients of a mixture, and consequently their levels are not independent. Simplex designs are used to study the effects of mixture components on the response variable. A {p, m} simplex lattice design for p components consists of points defined by the following coordinate settings: the proportions assumed by each component take the m + 1 equally spaced values from 0 to 1, and all possible combinations (mixtures) of the proportions from Equation (2.1) are used.

$$x_i = 0, \frac{1}{m}, \frac{2}{m}, \frac{3}{m}, \ldots \ldots, 1 \qquad i = 1, 2, \ldots, p \qquad (2.1)$$
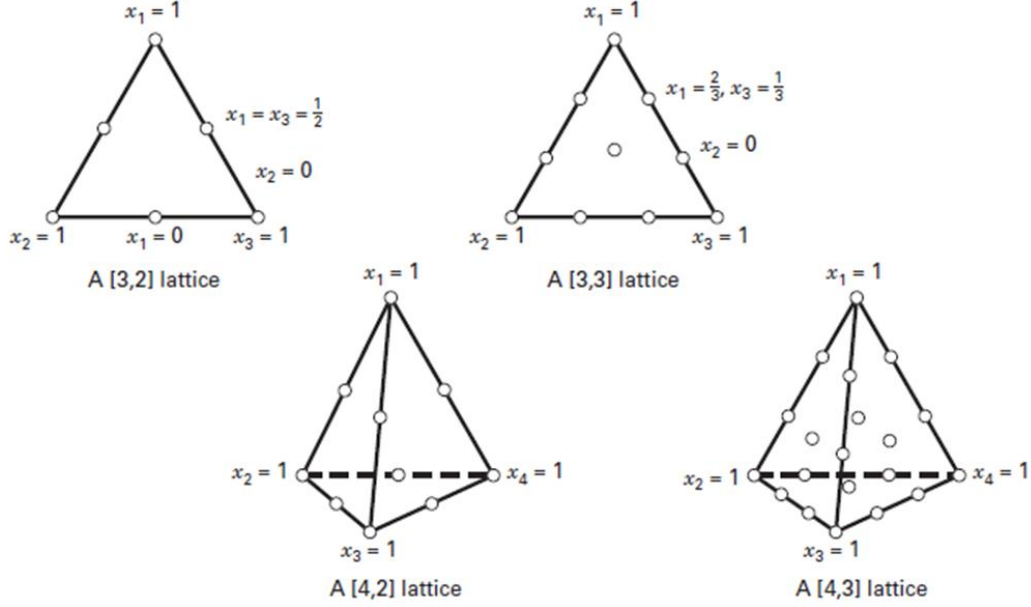
Figure 2.1: Some simplex lattice designs for p = 3 and p = 4 components [Cornell, 2002]

As an example, let p = 3 and m = 2. Then

$$x_i = 0, \frac{1}{2}, 1 \qquad i = 1, 2, 3 \tag{2.2}$$

and the simplex lattice consists of the following six runs:

$$(x_1, x_2, x_3) = (1, 0, 0), (0, 1, 0), (0, 0, 1), (\frac{1}{2}, \frac{1}{2}, 0), (\frac{1}{2}, 0, \frac{1}{2}), (0, \frac{1}{2}, \frac{1}{2}) \tag{2.3}$$

This design is shown in Figure 2.1. The three vertices (1, 0, 0), (0, 1, 0), and (0, 0, 1) are the pure blends, whereas the points $(\frac{1}{2}, \frac{1}{2}, 0), (\frac{1}{2}, 0, \frac{1}{2})$, and $(0, \frac{1}{2}, \frac{1}{2})$ are binary blends or two component mixtures located at the midpoints of the three sides of the triangle. Figure 2.1 also shows the {3, 3},{4, 2}, and {4, 3} simplex lattice designs. An alternative to the simplex lattice design is the simplex centroid design. In a p-component simplex-centroid design, there are $2^p - 1$ points, corresponding to the p permutations.

Mixture models differ from the usual regression polynomials employed in response surface work because of the constraint $\sum x_i = 1$. Due to this constraint of $x_1 + x_2 + ... + x_q =$

1, the form of the regression function that is fit to the data from a mixture experiment is somewhat different from the traditional polynomial fit and is often referred to as the canonical polynomial. The canonical form is derived using the general form of the regression function that can be fit to data collected at the points of a {p, m} simplex-lattice design and substituting into this function the dependence relationship among the x_i terms. For example, the equation that can be fit to the points from a {p, m = 1} simplex-lattice design is

$$E(y) = \beta_0 + \beta_1 x_1 + \ldots\ldots\ldots + \beta_p x_p \tag{2.4}$$

Multiplying β_0 by $(x_1 + x_2 + \ldots + x_p = 1)$, the resulting equation is

$$E(y) = \beta_1^* x_1 + \ldots\ldots + \beta_p^* x_p \tag{2.5}$$

with $\beta_i^* = \beta_0 + \beta_i$ for all $i = 1,\ldots,$p.

This is called the canonical form of the first-order mixture model.The standard canonical forms of the mixture models(with the asterisks removed from the parameters) that are more commonly used are:

Linear:

$$E(y) = \sum_{i=1}^{p} \beta_i x_i \tag{2.6}$$

Quadratic:

$$E(y) = \sum_{i=1}^{p} \beta_i x_i + \sum\sum_{i<j} \beta_{ij} x_i x_j \tag{2.7}$$

Full Cubic:

$$E(y) = \sum_{i=1}^{p} \beta_i x_i + \sum\sum_{i<j}^{p} \beta_{ij} x_i x_j + \sum\sum_{i<j}^{p} \delta_{ij} x_i x_j (x_i - x_j) + \sum\sum\sum_{i<j<k}^{p} \beta_{ij} x_i x_j x_k \tag{2.8}$$

Special Cubic:

$$E(y) = \sum_{i=1}^{p} \beta_i x_i + \sum \sum_{i<j} \beta_{ij} x_i x_j + \sum \sum_{i<j<k} \sum \beta_{ij} x_i x_j x_k \qquad (2.9)$$

From Equations 2.6 through 2.9, the parameter β_i represents the expected response to the pure blend $x_i = 1$ and $x_j = 0$ when $j \neq i$. The portion $\sum_{i=1}^{p} \beta_i x_i$ is called the linear blending portion. When curvature arises from nonlinear blending between component pairs, the parameters β_{ij} represent either synergistic or antagonistic blending. Higher order terms are frequently necessary in mixture models because (1) the phenomena studied may be complex and (2) the experimental region is frequently the entire operability region and therefore large, requiring an elaborate model. For more discussion, see [Cornell, 2002]

2.1.2   Simplex-Centroid Design

Simplex-Centroid design is a type of simplex lattice design that uses boundary-point designs; that is, with the exception of the overall centroid point, all the design points are on the boundaries of the simplex. Points on the vertices represent pure mixtures, points on the edges represent binary blends and any other point within the region is a ternary blend   [Scheff, 1958, Scheffe, 1963]. Figure 2.2(a) shows the simplex region for ternary blend mixture design, in mixture designs the sum of the mixtures adds up to one (1).

The design points in the simplex-centroid design is associated to the special cubic regression polynomial as described in Equation 2.9. At the points of the simplex-centroid design, data on the response are collected and a polynomial is fitted that has the same number number of terms (or parameters to be estimated) as there are points in the associated design. For example, a three (3) component simplex-centroid design of degree 2 {3, 2} would have $2^3 - 1 = 7$ design points and the runs are (1,0,0), (0,1,0), (0,0,1), (0.5,0.5,0), (0.5,0,0.5), (0,0.5,0.5), $(\frac{1}{3}, \frac{1}{3}, \frac{1}{3})$.

The mixture designs often have constraints on the component proportions, these are known as upper and/or lower bound constraints of the form $Li \leq x_i \leq Ui$, $i = 1, 2,..., p$,
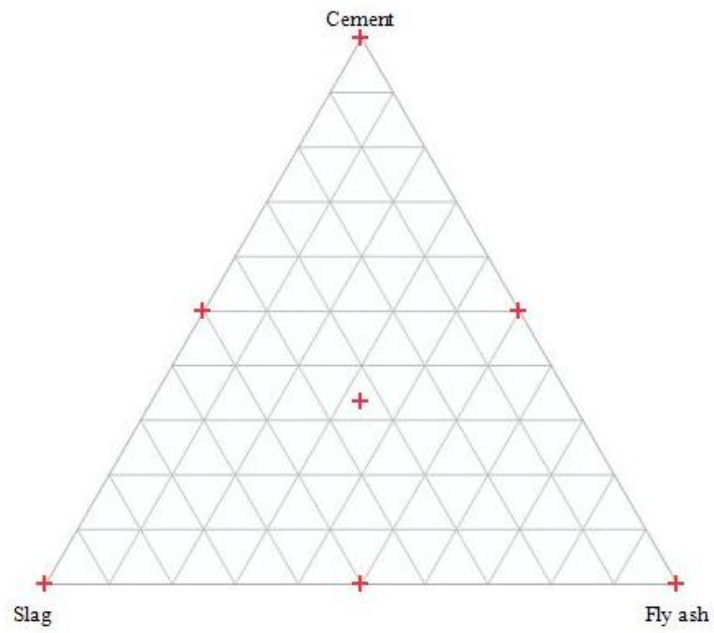
(a) standard
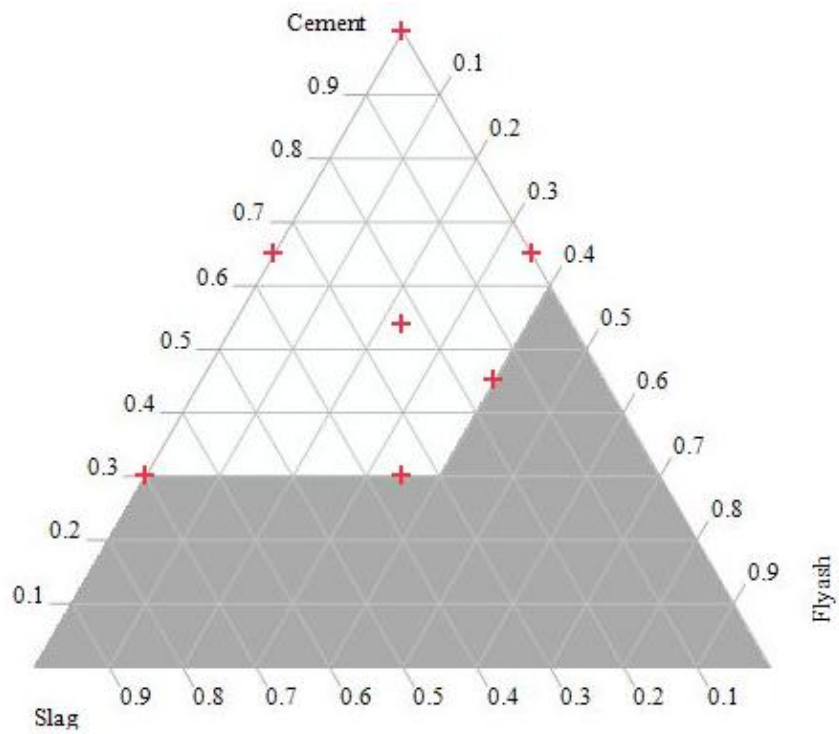
(b) with constraints

Figure 2.2: Simplex-centroid design with test points

where L_i is the lower bound for the i-th component and U_i the upper bound for the i-th component. The simplex region can be transformed into a polygon by adding lower and upper limits to the mixture components. The design space within the region still remains a simplex design but with new set of design points along the transformed region. Figure 2.2(b) shows the transformed simplex region with new design points.

Since the transformed region is still a simplex design, it is possible to define a new set of components that take on the values from 0 to 1 over the transformed simplex region. By doing this, the the simplex-centroid design model can be constructed with new components and fit with the special cubic regression polynomial. These new components (x_i^*) are called pseudo components and are defined using the following formula:

$$x_i^* = \frac{x_i - L_i}{1 - L} \tag{2.10}$$

where L = $\sum\limits_{i=1}^{p} L_i < 1$, denoting the sum of all the lower bounds.

The pseudo components represent the design points in terms of the (x_i^*) of the simplex region. Rearranging the equation 2.10 the original components of the mixtures can be derived by Equation 2.11 shown below:

$$x_i = L_i + (1 - L)x_i^* \tag{2.11}$$

In certain cases while transforming the pseudo components into original mixture components the component proportions tend to exceed their upper bounds. In such cases the component proportions are replaced their upper bounds and relatively increasing the remaining component proportions by equal amounts. In cases with several upper bounds this procedure may require some iteration since the component proportions that are raised could exceed their upper bounds.

15

2.2 Portland Cement Concrete Properties

2.2.1 Strength of Concrete

Strength of concrete is important to provide stability to structures during their service life. It is understood that concrete performs well when it is subjected to compressive loads and is weak when subjected to tensile loads. Thus by increasing the compressive strength concrete is assumed to perform well with increased compressive load carrying capacity. However, this is not true in all cases as equivalent durability of concrete is important for any given age of concrete. Even though we use high strength concrete the durability becomes an issue with age as the concrete deteriorate with surrounding environment conditions. Thus it is important to evaluate the residual strength in concrete when it under goes harsh environmental conditions.

The strength development in concrete or cementitious mortar is mainly due to the cement hydration reaction. With the use of SCMs as cement replacements, the pozzolanic reaction takes place by consuming excess calcium hydroxide (CH) produced during the cement hydration reaction. The consumption of CH, the acceleration of the hydration of C_3A and C_3S, the formation of carbo-aluminates, the change in the C-S-H and the formation of transition zone between the aggregate and cement paste demonstrate the reactivity of SCM [Ghrici et al., 2007]. Consequently, this reactivity improves the early strength for some SCMs, and for other SCMs the later age strength is improved. Strength of concrete in general terms is the compressive strength of concrete, for some applications the flexural strength of concrete is also important. Various researchers have compared the compressive strength and flexural strength of cementitious mixture and found out flexural strength is a tenth of compressive strength in magnitude [Ghrici et al., 2007]. The concept of statistical mixture design has also been used in concrete industry to blend supplementary cementitious materials with cement to achieve advantageous properties [Wang and Chen, 1997].

2.2.2 Durability of Concrete

Alkali Silica Reaction (ASR) is a complex phenomenon occurring in portland cement concrete that leads to distress and durability problems in concrete structures. This phenomenon was first discovered by Stanton [Stanton, 1940] in the late 1930's. ASR is a chemical reaction between reactive siliceous aggregates and the alkali hydroxides present in the pore solution of concrete and the hydrated cementitious paste. The reaction product results in a gel formation which is volumetrically unstable, called ASR gel [Mindess et al., 2003]. This gel is hygroscopic in nature [McKeen et al., 1998] i.e. with the absorption of surrounding moisture swelling of gel takes place and the volume of gel increases in the confined pores of aggregates. This increase in volume of gel exerts stresses on the aggregate and cementitious paste around it. When the stresses exerted overcome the tensile strength of aggregate or cementitious binder cracks are formed, which are eventually transferred to the surface of concrete with age, thus disrupting the concrete and decreasing the durability of concrete. This phenomenon is observed worldwide as map cracking pattern in concrete structures.

Soon after ASR was first identified as a dominant distress mechanism in concrete structures, several mitigation strategies were adopted to prevent/mitigate ASR distress in new construction activities. Some of the strategies include:

1. Screening potentially reactive aggregates using accelerated test methods

2. Limiting alkali content of concrete

3. Use of supplementary cementitious materials (SCMs)

4. Use of lithium admixtures and air entrainment in concrete

Among these strategies, the use of SCMs, particularly fly ash and ground granulated blast-furnace slag (GGBS or slag), to mitigate ASR has been widely employed. On a regional basis, other manufactured and natural SCMs have also been used to mitigate ASR. In some situations blended cements containing multiple SCMs are used to take advantage of

17

individual properties of each of the SCMs. Such blended cements commonly include combinations of slag and silica fume and fly ash, along with portland cement. Another strategy that is being increasingly used in dealing with ASR is the use of SCMs in combination with lithium admixtures. In order to reduce the cost of construction, it is important that reactive aggregate sources be used as effectively as possible. Hence it becomes important to use effective mitigation strategies for aggregates that are prone to ASR distress.

Fly ash is a finely divided coal combustion residue that contains aluminosiliceous glass with varying amount of lime (CaO) in it along with some crystallized mineral constituents. It is well recognized [S. and Chatterji, 1979] that fly ashes mitigate ASR distress in concrete through a combination of chemical and physical effects resulting from pozzolanic reaction. The pozzolanic reaction of fly ash is a strong function of its chemical, mineralogical and physical characteristics. Unlike fly ashes, the bulk chemical composition of slag from different sources is relatively similar. However, the mineralogy, glass content and fineness of different slags can vary from each other as these properties depend on the granulation and grinding process. Silica fume exclusively consists of SiO_2 of very fine particle size and a relatively high pozzolanic activity. Silica fume has proved to improve the early age strength requirements of cementitious mixture, but some researchers have reported concerns with silica fume mixes for their long term durability effects.

In general, ASR mechanism is a complex phenomenon, and to understand the cause and potential of this reaction, each individual parameter that affects the reaction has to be studied and solutions to mitigate the reaction should to be provided.

2.3   Role of SCMs in Modifying Concrete Properties

The use of SCMs has been studied in literature by various authors and the effectiveness of SCMs in improving concrete performance has been explained. SCMs are pozzolans that are rich in silica content and when mixed in concrete they react with calcium hydroxide, produced during cement hydration reaction, forming secondary CSH gel. This reaction

mechanism is known as pozzolanic reaction [S. and Chatterji, 1979]. Addition of supplementary materials can influence concrete mix proportions, rheological behavior of plastic concrete, degree of hydration of cement, strength and permeability of concrete, resistance to thermal cracking, alkali-silica expansion, and sulfate attack.

Various mechanisms are being proposed to explain the effectiveness of SCMs in modifying concrete properties, the most common of which are:

1. lower permeability and consequent lower ion mobility [Massazza, 1993];

2. strength improvement and higher resistance to the expansive stresses developed by ASR;

3. alkali dilution resulting from cement replacement, (at least for admixtures with a lower available alkali content), and

4. pozzolanic reaction producing secondary (pozzolanic) hydrates which entrap alkali ions and deplete portlandite in the cement paste, thus reducing the alkali ions and the pH in the pore solution [Duchesne and Brub, 1994, Chatterji, 1994].

Even though the chemical reaction mechanisms of supplementary cementitious materials in modifying concrete properties is not completely understood, the physical effect of replacing certain portion of cement with SCMs has yielded beneficial results and confidence among the users in concrete industry. The fresh properties of concrete such as workability, air content are greatly affected by using SCMs [Duval and Kadri, 1998]. Researchers have tried to improve the strength of concrete by replacing cement with fly ash [Poon et al., 2000] or by replacing sand with as fly ash [Rajamane et al., 2007]. Slag has also been used to improve the compressive strength of concrete at later ages, in some cases researchers [Altan and Erdogan, 2012] have tried to activate slag by adding alkalis (NaOH and KOH) in concrete to improve the early age properties.

Guneyisi et.al. [Guneyisi et al., 2012] used silica fume, metakaolin as SCMs to improve the strength and reduce the permeability and shrinkage of high strength concretes.

Metakaolin has also been by Al-Akhras et.al. [Al-Akhras, 2006] to address sulfate attack problems in concrete. Sulfate attack was also reduced in concrete by using fly ash and slag [Zuquan et al., 2007, Bakharev et al., 2002]. Rangaraju et.al. have used different SCMs [Rangaraju and Harish, 2011, Rangaraju and Math, 2012] such as fly ash(Class F and Class C), slag, silica fume, meta kaolin and other natural pozzolans for ASR mitigation studies. Some researchers [Moser et al., 2010, Shehata and Thomas, 2002] have also tried blending two different SCMs as ternary blends for achieving early age properties and ASR mitigation at later stages. Based on the extensive published literature, there is a general consensus that SCMs prove to enhance the mechanical and durability properties of cement concrete.

2.3.1   Slag

Slag is the general name for ground granulated blast furnace slag (GGBS) which has been widely employed in concrete mixtures as SCM. Slag is used in concrete by replacing with cement at dosages ranging from 0% to 70% [Rasheeduzzafar and Hussain, 1991]. The bulk chemical composition of slags from different sources is relatively similar having a chemical composition corresponding to melilite, a solid solution phase between gehlenite (C_2AS) and akermanite (C_2MS_2). However, the mineralogy, glass content and fineness of different slags can vary from each other as these properties depend on the granulation and grinding processes. ASTM C 989 recognizes three different grades of slag (Grades 80, 100 and 120) based on their strength activity index. Typically, only grade 100 and 120 slags are used as SCMs in replacing portland cement concrete.

The performance of slag, particularly in terms of its strength activity index, is influenced more by the granulation process and the degree to which it is ground, rather than on its chemical composition [Pal et al., 2003]. Slags cooled from a high temperature at a faster rate are likely to contain more reactive glass than those cooled slowly [Mostafa et al., 2001]. In slag-cement mixtures, hydration of cement provides alkali and sulfate for activating the glass. The reactivity of slag is important in terms of its ability to under go cementing

properties such as hydraulic reaction and pozzolanic reaction.

2.3.2 Fly ash

Fly ash is a finely divided coal combustion residue that mainly contains aluminosiliceous glass with varying amounts of lime (CaO) content. Existing specifications (ASTM C 618 and AASHTO M 295) broadly characterize fly ashes based only on their bulk chemical composition into two categorizes, namely, Class F and Class C fly ash. For Class F fly ash the selected oxide compositions of $SiO_2+Al_2O_3+Fe_2O_3$ ¿ 70% and for Class C fly ashes $SiO_2+Al_2O_3+Fe_2O_3$ oxide contents should be in between 50% - 70%. Canadian specification CSA A3001, categorizes fly ashes based on their lime content as low-lime or Type F ($\leq 8\% \pm 1\%$ CaO content), intermediate-lime content or Type CI (¿ 8% to $\leq 20\% \pm 2\%$ CaO content) and high-lime content or Type CH (¿ 20% CaO content).

Class F fly ash contains mainly alumino-silicate glass, sillimanite, and mullite. The glass content may be as high as 80%. Hematite, quartz, and magnetite are also found in Class F fly ashes. The glassy phase in the Class C fly ash is different from that in the Class F fly ash. The principal phase in the Class C fly ash is tricalcium aluminate (C_3A). The crystalline phases in Class C fly ash are much more reactive than those in Class F fly ash. In general, in both fly ashes the spherical sizes of the glassy phase vary between 1 μm and 100 μm, most of the material being under 20 μm. It is well recognized that fly ashes improve the properties of concrete through a combination of chemical and physical effects resulting from pozzolanic reaction.

2.3.3 Ternary Combination of SCMs in Concrete

Ternary blends in concrete usually consists of cement + two or more SCMs. Blending of two or more SCMs with cement in concrete has lead to many technical advantages. Using a conservative approach can require high replacement levels of fly ash or slag in binary systems. These high replacement levels produce concretes with very high electrical resistance, implying excellent overall durability, but at the cost of low early strength and

potential construction problems. A more liberal approach is to use ternary blends with lower dosages of SCMs that can provide adequate concrete resistance and ease of constructability.

The use of two types of SCMs as a ternary blend has the potential to synergistically optimize the contributions of each, considering factors such as early and late-age strength, workability and durability. Incorporating small amounts of silica fume with cement and fly ash or slag in ternary systems can be used to counterbalance the negative effect of high fly ash or slag replacement level on early age strength and low replacement level on durability [Bagheri et al., 2012, Lane and Ozyildirim, 1999]. Bagheri et. al. found that by addition of silica fume and slag in concrete the 28-day age strength of concrete was comparable to that of control concrete without any SCM. But the long term (180-day) durability performance such as chloride-ion permeability and chloride-ion migration was significantly reduced compared to control sample.

Another research conducted by Radlinski and Olek [Radlinski and Olek, 2012] using 20% fly ash (Class C) and 5% silica fume showed synergistic effect after 7-day age resulting in an increased compressive strength and resistance to chloride ion penetration as well as a reduced rate of water absorption (sorptivity) compared to predictions based on individual effects of FA and SF in respective binary systems. Radlinski found that the chemical effect of fly ash and silica fume manifested itself in the form of an increased amount of hydration products compared to predictions based on the individual effects of fly ash and silica fume in the binary systems. Based on these observations Radlinski concluded that fly ash and silica fume mutually compensate for each others deficiencies (noticeable when they are used alone in a binary system), incorporation of ternary cement + silica fume + fly ash cementitious systems is deemed to be benecial.

The combination of high lime fly ash and low lime fly ash was investigated by several researchers [Antiohos et al., 2005] and it was found that mixtures containing equal amounts of each fly ash were the most effective for moderate cement substitution, whilst for higher replacements the inter mixture possessing the highest active silica content shows supremacy at almost all hydration ages. Malvar and Lenke [Malvar and Lenke, 2003] investigated the

22

high lime and low lime combination for alkali-silica reaction mitigation studies. Malvar came up with chemical index to characterize fly ash and cement for asr mitigation, based on their chemical constituents. With the use of chemical index it was possible to estimate the minimum cement replacement required to reduce alkali-silica reaction expansion in ASTM C 1260 / C 1567 test below 0.08%.

Li and Zhao [Li and Zhao, 2003] did laboratory investigations on the inuence of combination of fly ash and slag on the properties of high-strength concrete. The results from this study showed that for a binary combination of 40% fly ash and 60% cement the compressive strengths were low up to 56-days compared to control specimen. But when the slag was added with a ternary blend of 15% slag, 25% fly ash and 60% cement, the early age compressive strength was found to be similar to the control specimen. For long term effects from 28-days to 360-days the binary combination of fly ash and cement had the highest compressive strength followed by the ternary combination and control specimen. Thus Li and Zhao concluded that the combination of fly ash and slag can improve both short-term and long-term properties of concrete.

2.4   Optimization of SCM Proportions in Ternary Concrete Mixtures

In design of experiments there are several mixture design techniques available that can be used to generate regression equations and predict mixture performance. In concrete industry the Simplex Centroid Design (Section 2.1.2) technique has been widely used to blend SCMs with cement to achieve advantageous properties such as:

- Optimum dosage levels to yield the most information from the fewest runs.

- Development of strength and durability prediction equation for ternary cementitious mixture.

- Comparative study of strength and durability response surfaces in a ternary triangle

for any given mixture within the design space.

The use of SCD for proportioning SCM dosage was first investigated by E.Douglas et.al. [Douglas and Pouskouleli, 1991] using cement, slag and fly ash (Class F & C) combination to predict compressive strength of mortars. However in this investigation the constraint on component proportions for slag and fly ash was not applied and 100% dosage was used. The problem of using 100% SCM dosage is SCMs do not undergo hydraulic reaction like cement and do not attain any strength at early ages. Some SCMs are believed to have slow hydraulic activity and they react with water to show cementing properties at later ages. Based on the results obtained Douglas concluded that the SCD technique can be used to predict compressive strength values within the design space with 95% or more accuracy.

Similar research was conducted by Wang et.al. [Wang and Chen, 1997] to predict compressive strength of mortars using SCD technique. In this investigation Wang applied the lower and upper bound constraints on component proportions and limited the dosages of fly ash to 40% max and slag to 70% max. The cement content had a minimum dosage of 30% for the mixture components to add up to 100%. Wang developed prediction equations and iso-contours for compressive strength and concluded that SCD can be used to predict compressive strengths of mortars with excellent accuracy.

2.5   Concluding Remarks on Literature

After reviewing the literature and examining how different researchers have perceived the strength and durability aspects of concrete, it is clear that there is little information in the literature that provides a comprehensive knowledge on optimizing the strength and durability of concrete for long run. Even though, the standard test procedures exist to evaluate the performance of concrete, there is lack of unified procedures and guidelines to compare multiple strength and durability properties of concrete for a optimum concrete mix. The increased use of SCMs in concrete has led to a need of extensive research required in evaluating SCMs for their effectiveness to use in concrete. The process of selecting ap-

propriate pozzolans and determining their dosage levels to effectively increase the durability of concrete has been rudimentary in nature. The use of design of experiments techniques is beneficial in designing ternary blend mixtures with fewer runs of experiments and generate a response surface to predict the performance along the response surface.

Chapter 3

Materials and Methods

This chapter describes various experimental materials and test methods used in this research study. Standard test procedures were used for studies related to cement paste, mortar and concrete specimens. Modifications done to the standard test are explained in their respective procedures. The commonly used analytical techniques for material characterization and cement paste studies are also discussed.

3.1   Materials

The materials used in the study include an ASTM C150 Type I cement (high alkali) from Lehigh Cement Company (Evansville Plant, PA), 1 slag Grade 100 from Holcim Skyway facility, 1 Class F fly ash from Proash Baltimore plant, and 5 reactive aggregates and 2 non reactive aggregates were used in this research study.

3.2   Aggregates

3.2.1   Reactive Aggregates

Seven aggregates were used in this study and were selected to represent various levels of alkali-silica reactivity. Five of the seven aggregates are characterized as reactive

aggregate, and the remaining two aggregates are non-reactive in nature. The details of the five reactive aggregates are as follows:

1. New Mexico Rhyolite- This aggregate is one of the most reactive aggregates found and it primarily consists of Rhyolite as the reactive component. This aggregate is gravel from Las Placitas Gravel pit in Bernalillo County in New Mexico. Figure 3.1 shows the thin section petrographic images of the aggregate.

2. Spratt Limestone - This aggregate has an established history of being alkali-silica reactive and has been used as a reference aggregate in numerous ASR research studies (Rangaraju et al. 2006). The source of this aggregate was from Ontario, Canada and is quarried from the Spratt quarry. It primarily consists of calcite with minor amounts of dolomite and about 10% insoluble residue. The alkali-silica reactive component of the rock is reported to be 3% - 4% microscopic chalcedony and black chert, which is finely dispersed in the matrix. Figure 3.2 shows the thin section petrographic images of the aggregate.

3. North Carolina Argillite - This aggregate primarily consists of reactive argillite / metatuff and its source is from Gold hill Quarry in North Carolina. This aggregate has an established field history of being alkali-silica reactive in several bridge structures across North Carolina. Figure 3.3 shows the thin section petrographic images of the aggregate.

4. South Dakota Quartzite - This aggregate primarily consists of strained quartz grains cemented with interstitial secondary quartz cement. The interstitial matrix also consists of micro crystalline quartz, hematite and kaolinite. This aggregate is quarried from L.G.Everist Quarry in Dell Rapids, South Dakota. This is a moderate-to-slow reactive aggregate and has an established history of being alkali-silica reactive in concrete pavements in Minnesota and South Dakota. Figure 3.4 shows the thin section petrographic images of the aggregate.

5. Stocker sand - This aggregate is a gravel from Tuscarawas County, Ohio. The common name of the aggregate Stocker Sand and Gravel. This is a moderate-to-slow reactive aggregate and has an established history of being alkali-silica reactive in concrete pavements in Pittsburgh and Ohio.

The details of the two non-reactive aggregates are as follows:

1. Adairsville Dolomite - This aggregate has an established field history of being non-reactive and it primarily consists of dolomite. It is quarried stone from Adairsville quarry in Georgia.

2. Glasscock Sand - This is non-reactive silica sand conforming to ASTM C778 and mainly consists of silicon dioxide SiO_2. This sand was provided by the local plant from Columbia, SC and its principal mineral is quartz. This sand is used as fine aggregate in the standard concrete tests.

Table 2 shows the basic properties of aggregates used.

3.3 Cement

High alkali cement (Type I) with a Na_2O equivalent of 0.86% (Na_2O_{eq}) and an autoclave expansion of 0.12% was used for this study. The source of the cement was from Lehigh plant in Evansville, PA. The chemical composition of this cement is provided in table 3.1. This cement was used for tests in this research study.

3.4 Supplementary Cementitious Materials

3.4.1 Fly ash

In this study, a low-lime fly ash ($CaO = 1\%$) was used as a supplementary cementitious material (SCM) for evaluation of a typical ASR mitigation measure in the test methods. The chemical composition of this fly ash is provided in Table 3.1. The fly ash
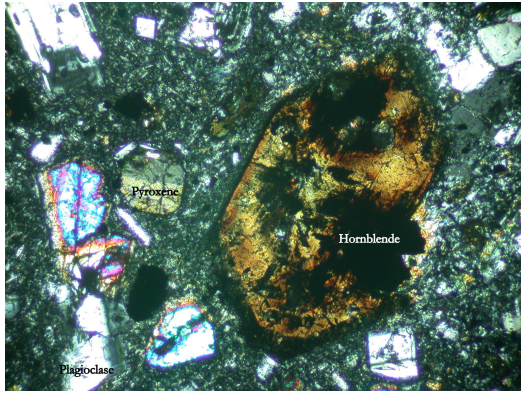
(a) NM1
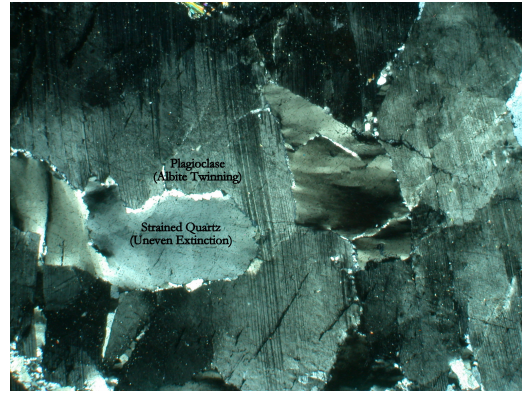
(b) NM2
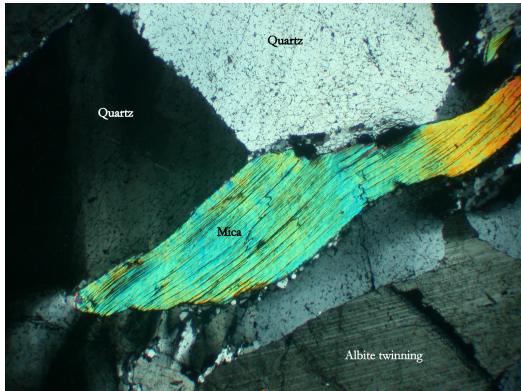
(c) NM3
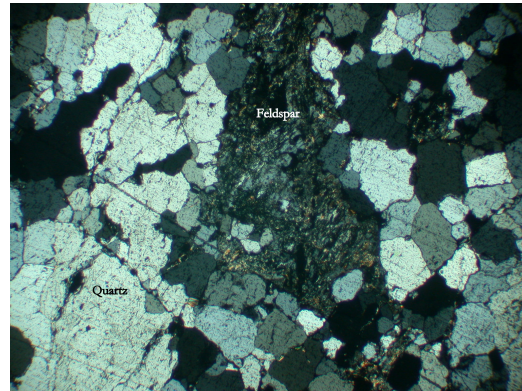
(d) NM4
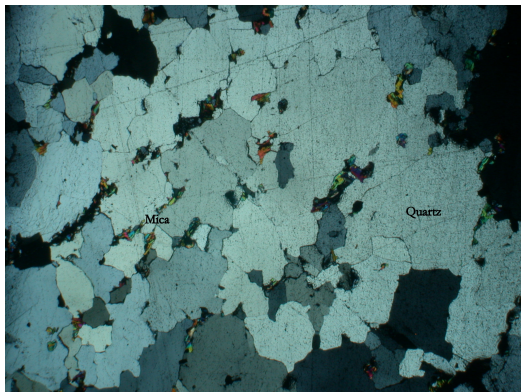
(e) NM5
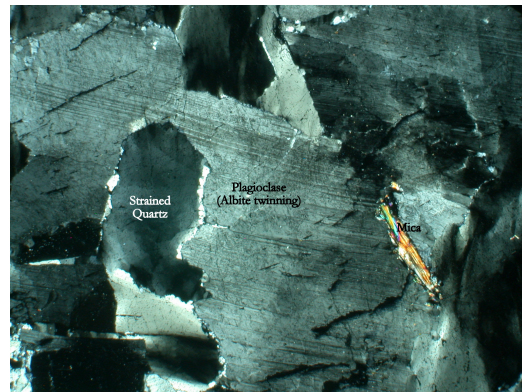
(f) NM6

Figure 3.1: Petrographic images of New Mexico aggregate grains

(a) SP1
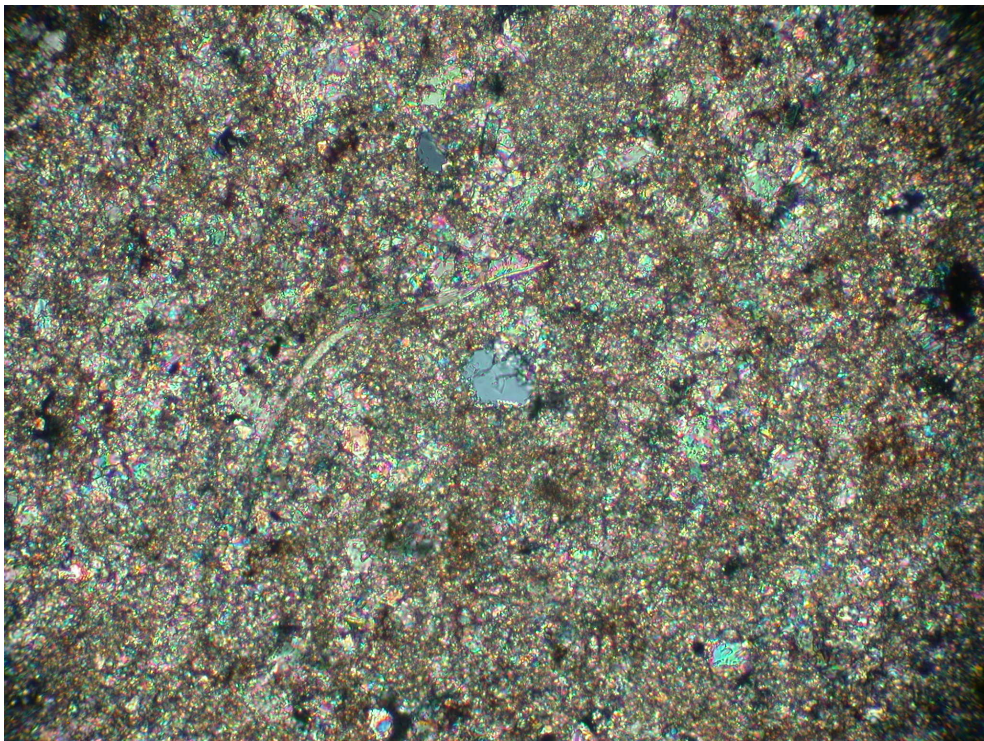
(b) SP2

Figure 3.2: Petrographic images of Spratt aggregate grains
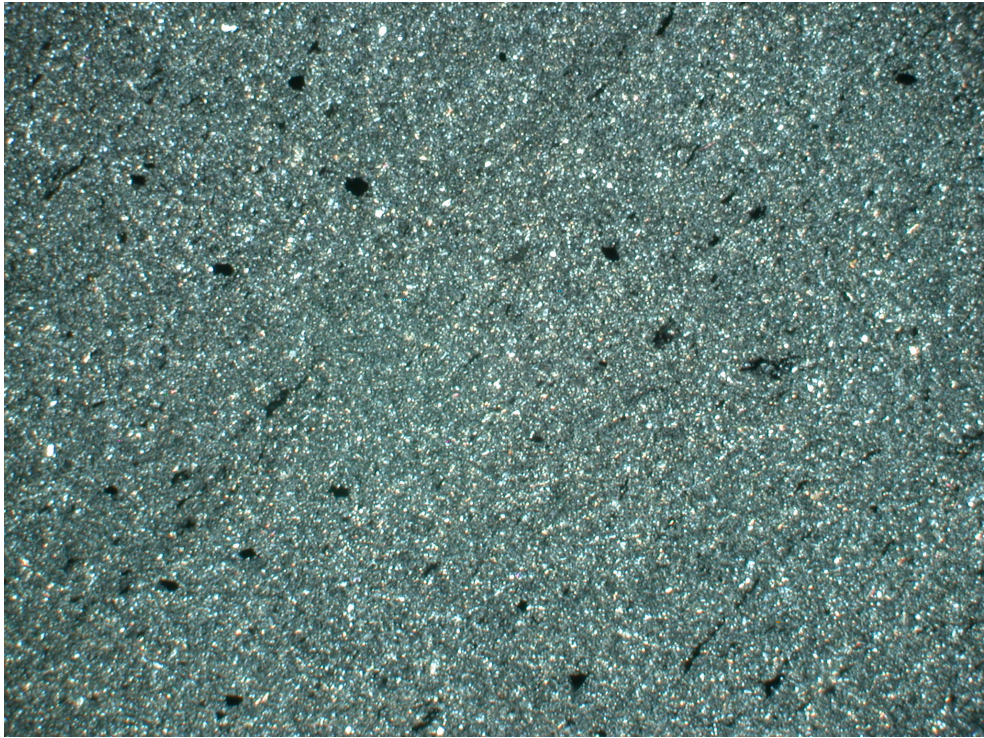
(a) NC1
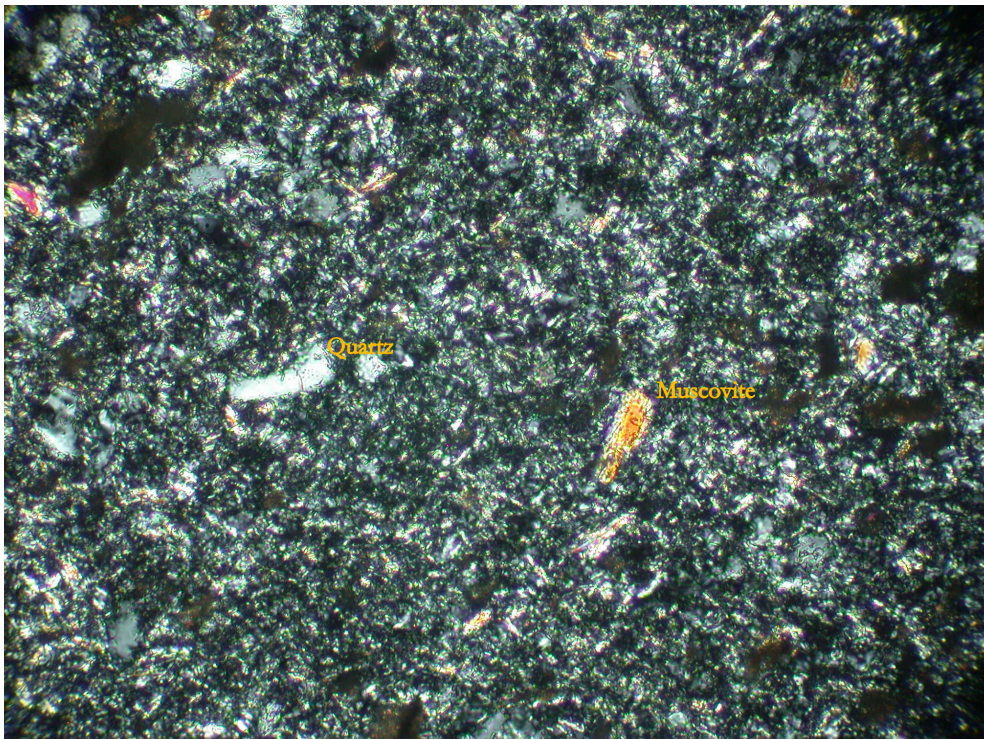
(b) NC2

Figure 3.3: Petrographic images of North Carolina aggregate grains
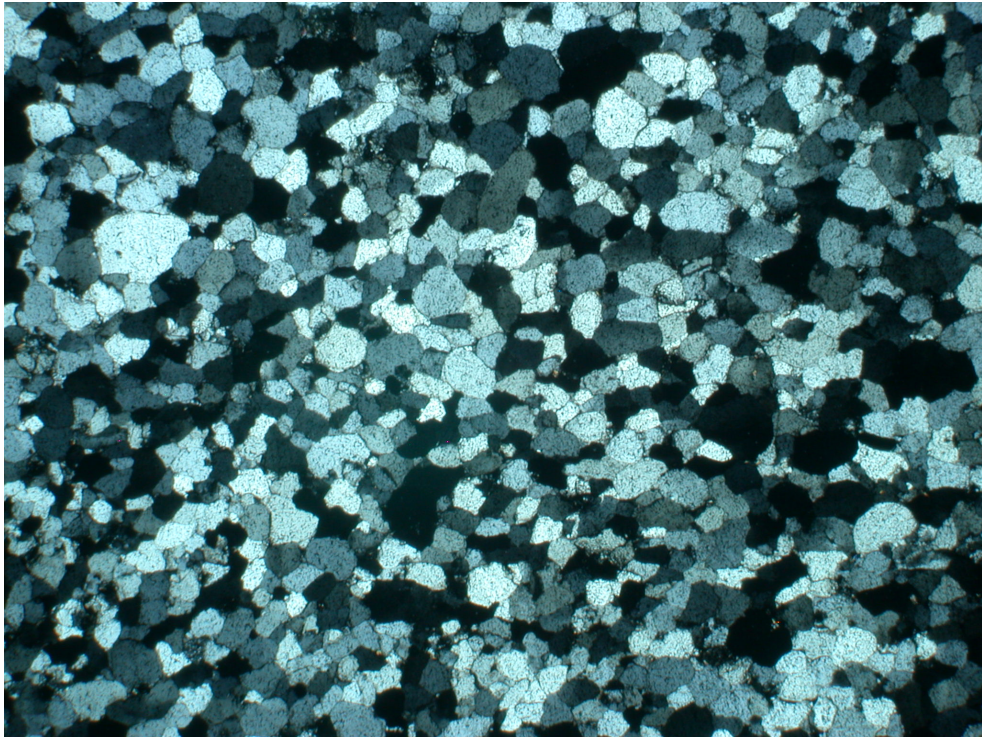
(a) SD1
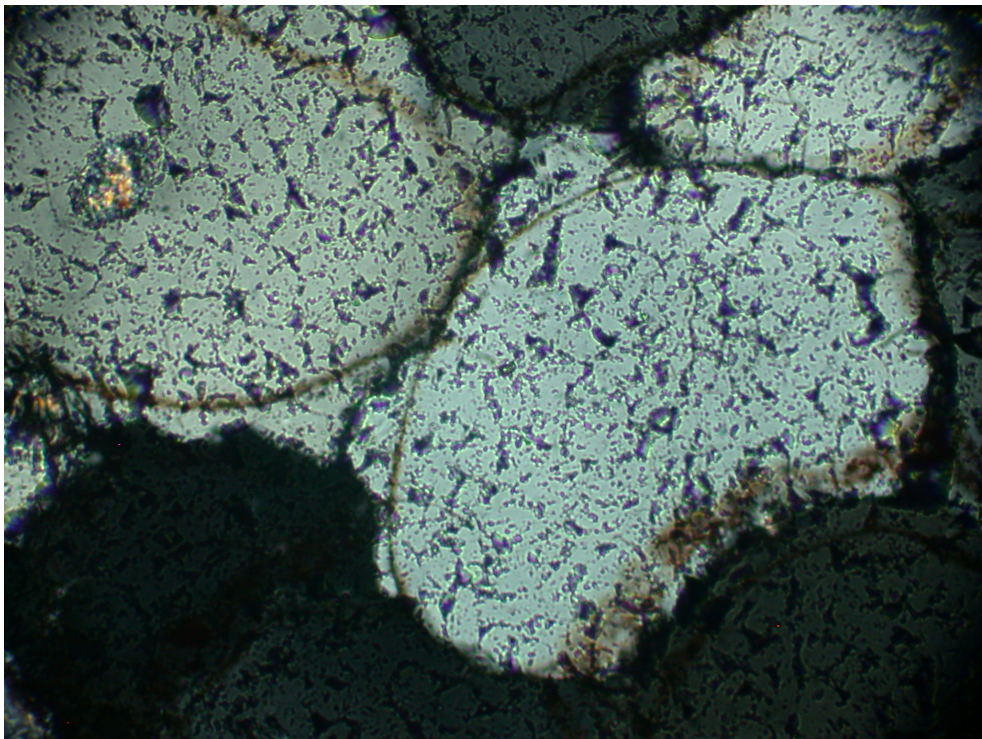
(b) SD2

Figure 3.4: Petrographic images of South Dakota aggregate grains

Table 3.1: Chemical Composition of Cementitious Material

Chemical Compositions	Oxide, %		
	Cement	Low-Lime Fly ash	Slag
SiO_2	19.74	59.5	38.17
Al_2O_3	4.98	28.69	7.31
Fe_2O_3	3.13	3.96	0.78
Total S+A+F	–	92.1	–
CaO	61.84	1.02	39.12
MgO	2.54	0.99	12.48
SO_3	4.15	0.14	2.56
Na_2O	–	0.35	–
$Na_2O_{eq} = Na_2O + 0.68K_2O$	0.82	2.13	–
K_2O	–	2.7	0.34
TiO_2	–	1.48	–
Loss on Ignition (LOI)	1.9	1.1	–
Insoluble Residue	0.25	–	–
C_3A	8	–	–
C_3S	52	–	–

had a specific gravity of 2.20 g/cc and an autoclave expansion of -0.04%. Based on the information provided in Table 3.1, the fly ash meets the requirements of ASTM C618-05 and AASHTO M295 specifications for a Class F fly ash.

3.4.2   Slag

In this study, a grade 100 ground granulated blast furnace slag (GGBFS) was used as a supplementary cementitious material (SCM) for evaluation of a typical ASR mitigation measure in the test methods. The chemical composition of this slags provided in Table 3.1. The slag had a specific gravity of 2.92 g/cc.

3.5   Reagents

The reagent grade sodium hydroxide (NaOH) salt was used for alkali-silica reactivity testing and rapid chloride ion permeability study. The reagent grade sodium hydroxide pellets were used to prepare a 1 normal (1N) solution. The concentration of 1N NaOH was

used as a soak solution for all the standard and modified ASTM test methods. The reagent grade sodium chloride (Na Cl) slat was used for rapid chloride ion permeability study. As per ASTM C1202 test requirements 3% Na Cl salt concentration and 0.3N NaOH solution were prepared.

3.6   Test Methods

The standard test method adopted in this study was accelerated mortar bar test method according to ASTM C 1260 specification. Several modifications are made to this test method to evaluate the aggregate size effects and deicers effects that can cause ASR. Two modified test methods of ASTM C 1260 and NRC - Concrete Micro bar Test are adopted to decrease the duration of laboratory test method on mortar and concrete samples. For the micro structure analysis of samples, scanning electron microscopy (SEM) and energy dispersive X-ray (EDX) analysis were conducted.

3.6.1   Specific Gravity and Absorption of Coarse Aggregates

The standard ASTM C127 test method was used to determine the specific gravity and absorption of coarse aggregate. In this method, a sample of coarse aggregate is immersed in water for approximately 24 ± 2 hours to essentially fill the pores. It is then removed from the water, the water is dried from the surface of the particles, and weighed. Subsequently the sample is weighed while submerged in water. Finally the sample is oven-dried and weighed a third time. Using the mass and weight measurements thus obtained and formulas in the method, it is possible to calculate three types of specific gravity and absorption of coarse aggregates.

3.6.2   Specific Gravity and Absorption of Fine Aggregates

The standard ASTM C128 test method was used to determine the specific gravity and absorption of fine aggregate. In this method, a sample of fine aggregate is immersed

in water for approximately 24 ± 2 hours to essentially fill the pores. It is then removed from the water, the water is dried from the surface of the particles using hair dryer and consistently checking for SSD condition using cone method, and weighed at SSD condition. A known quantity of SSD sample (500 ± 10 g) is placed inside the pycnometer and water is added to the mark on pycnometer ensuring all air bubbles are removed. The weights are taken for sample + water in pycnometer, and water filled to the mark in pycnometer. Using the mass and weight measurements thus obtained and formulas in the method, it is possible to calculate specific gravity and absorption of fine aggregates.

3.6.3 Bulk density and Voids in Coarse Aggregates

The standard ASTM C29 / C29M test method was used to determine the bulk density and voids in coarse aggregate, necessary for use for many methods of selecting proportions for concrete mixtures. In this method, a SSD sample of coarse aggregate is placed in known measure (container) in three equal layers and tamped 25 times after each layer with tamping rod. Once the container is full, the top of the container is leveled. Measurements are recorded for the mass of the measure plus contents, and the mass of the measure alone to the nearest 0.05 kg (0.1 lb). Using the mass and weight measurements thus obtained and formulas in the method, it is possible to calculate the bulk density and voids in coarse aggregate.

3.6.4 Petrographic analysis on Coarse Aggregates

The standard ASTM C295 test method was used to determine the potentially deleteriously reactive substance present in coarse aggregate. In this method, thin sections of coarse aggregate samples were prepared and examined under a petrographic microscope. The common reactive phases which include forms of silica such as opal, chalcedony, tridymite, and cristobalite; cryptocrystalline and microcrystalline quartz, strained quartz, or highly fractured quartz; and intermediate to acid (silica-rich) volcanic glass such as is likely to occur in rhyolite, andesite, or dacite were examined for their presence in aggregates.

3.6.5 Making and Curing Concrete Cylinders in the Laboratory

The standard ASTM C192 / C192M practice was used for making and curing concrete test specimens in the laboratory. Figures 3.5(a) to 3.5(h) shows the different steps involved in the process of making concrete cylinders:

1. Figure 3.5(a): A small quantity of cement is mixed with water in the drum mixer and is revolved till all the inner surface of drum gets coated with cement paste. This process is generally known as buttering the mixer.

2. Figure 3.5(b): Dry coarse aggregates are added with a small portion of total water.

3. Figure 3.5(c): Drum is revolved till all the coarse aggregates get coated with water.

4. Figure 3.5(d): Fine aggregates are added into the drum mixer with a small portion of total water.

5. Figure 3.5(e): Drum is revolved till all the coarse and fine aggregates get uniformly mixed.

6. Figure 3.5(f): Cementitious content is added into the drum mixer with a small portion of total water.

7. Figure 3.5(g): Drum is revolved till all the coarse and fine aggregates get uniformly coated with cementitious content.

8. Figure 3.5(h): Finally any remaining water is added and the drum is revolved till a consistent concrete mixture is obtained.

After the final step the fresh concrete was transferred to a tray and cylindrical concrete specimens of dimensions 4-inch diameter and 8-inch long were prepared. After 1-day of casting the hardened cylinders were demolded and cured by submerging in water bath kept in moist curing chamber (approx. $23\,^{\circ}\mathrm{C}$). The specimens were then taken out at 28-days and 56-days resp. and tested for strength and durability properties.

(a) 1

(b) 2

(c) 3

(d) 4

(e) 5

(f) 6

(g) 7

(h) 8

Figure 3.5: Concrete Mixing Procedure

(a) empty slump cone

(b) slump cone w/concrete

(c) slump cone w/concrete

(d) slump measurement
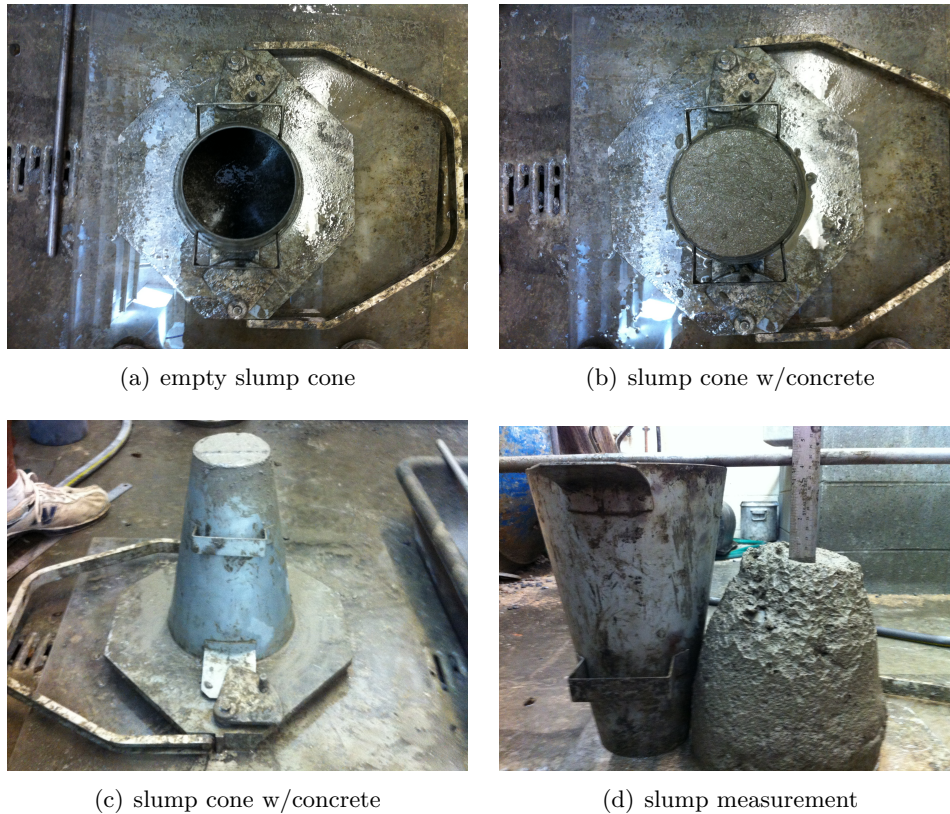
Figure 3.6: Slump cone test for concrete

3.6.6 Slump Test on Concrete

The standard ASTM C143 test method was used to evaluate the slump of cement concrete in laboratory. In this method, a sample of freshly mixed concrete is placed and compacted by rodding in a mold shaped as the frustum of a cone. The mold is raised, and the concrete is allowed to subside. The vertical distance between the original and displaced position of the center of the top surface of the concrete is measured and reported as the slump of the concrete. The process is shown in Figure 3.6.

3.6.7 Unit Weight of Concrete

The standard ASTM C138 / C138M test method was used to evaluate the unit weight (density, yield) of cement concrete. In this method, a freshly mixed concrete is

placed in known measure (container) in three equal layers and tamped 25 times after each layer with tamping rod. Once the container is full, the top of the container is leveled as shown in Figure 3.7(a). Measurements are recorded for the mass of the measure plus concrete, and the mass of the measure alone to the nearest 0.05 kg (0.1 lb). Using the mass and weight measurements thus obtained and formulas in the method, it is possible to calculate the unit weight of cement concrete.

3.6.8 Air Content of Concrete

The standard ASTM C231 / C231M test method was used to evaluate the air content of freshly mixed concrete by the pressure meter method. In this method, the pressure meter bowl of known measure is filled with freshly mixed concrete in 3 layers with tamping method and constantly hitting the outside of bowl with rubber mallet. Once the bowl is filled the top is leveled and closed with the pressure meter lid. Water is filled in the pressure meter through petcocks and complete fill is ensured without any air bubbles. The petcocks are closed and pressure is applied until the the zero mark is reached on the pressure meter dial. Release air into the meter by pressing down on the valve on the top of the meter; tap the meter while doing this to ensure pockets of air are removed. Figure 3.7(b) shows the gauge to the nearest 0.25% to determine the air content of concrete.

3.6.9 Compressive Strength of Concrete Cylinders

The standard ASTM C39 / C39M test method was used to evaluate the compressive strength of cylindrical concrete specimens. The concrete cylinders were prepared according to ASTM C C192 / C192M practice. The cured specimens after reaching the age of testing, were capped with neoprene pads and placed vertically in a compression testing methods. A uniform loading was applied till the concrete specimen failed. The maximum failure load applied was recorded and the compressive strength was calculated using the cross-sectional area of the concrete specimen. Figure 3.8(a) shows the failed concrete cylinder under compression.

(a) unit weight bowl   (b) pressure meter dial gauge
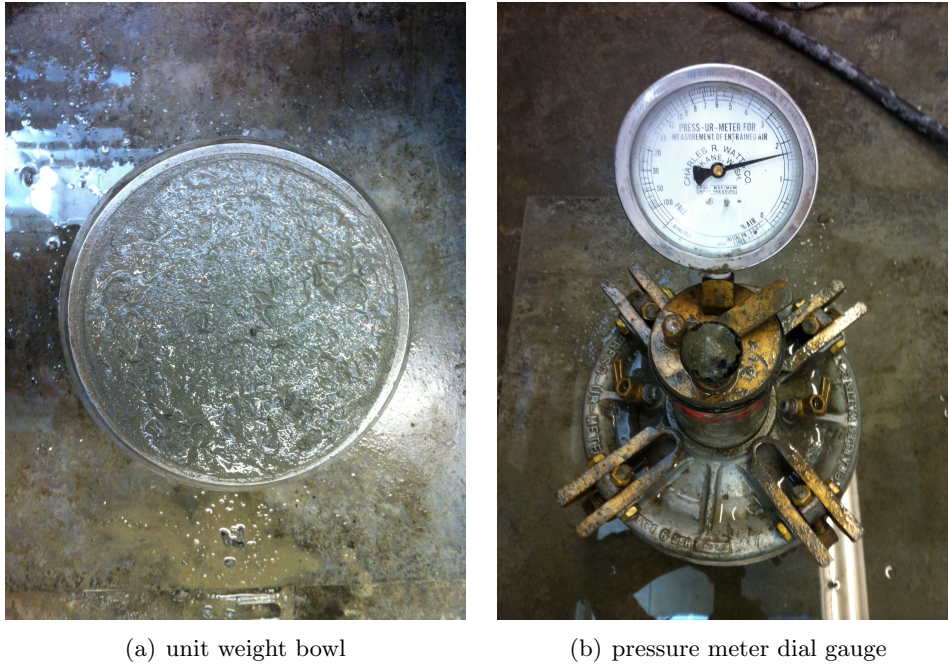
Figure 3.7: Air content test using pressure meter method

3.6.10 Split Tensile Strength of Concrete Cylinders

The standard ASTM C496 / C496M test method was used to evaluate the split tensile strength of concrete cylinders. The concrete cylinders were prepared according to ASTM C C192 / C192M practice. The cured specimens after reaching the age of testing were placed horizontally in the compression testing machine and load was applied along the length of specimen. A steel block was kept on the surface of concrete specimen to distribute the load uniformly along the length and to split the specimen into two halves. The maximum failure load applied was recorded and the split tensile strength was calculated using the formulas in the test method. Figure 3.8(b) shows the split tensile failure of concrete cylinder.

3.6.11 Rapid Chloride-Ion Permeability

The standard ASTM C1202 test method was used to evaluate the rapid chloride-ion permeability of concrete samples. In this method, a concrete cylinder sample with 4in

(a) Compression   (b) Split tensile
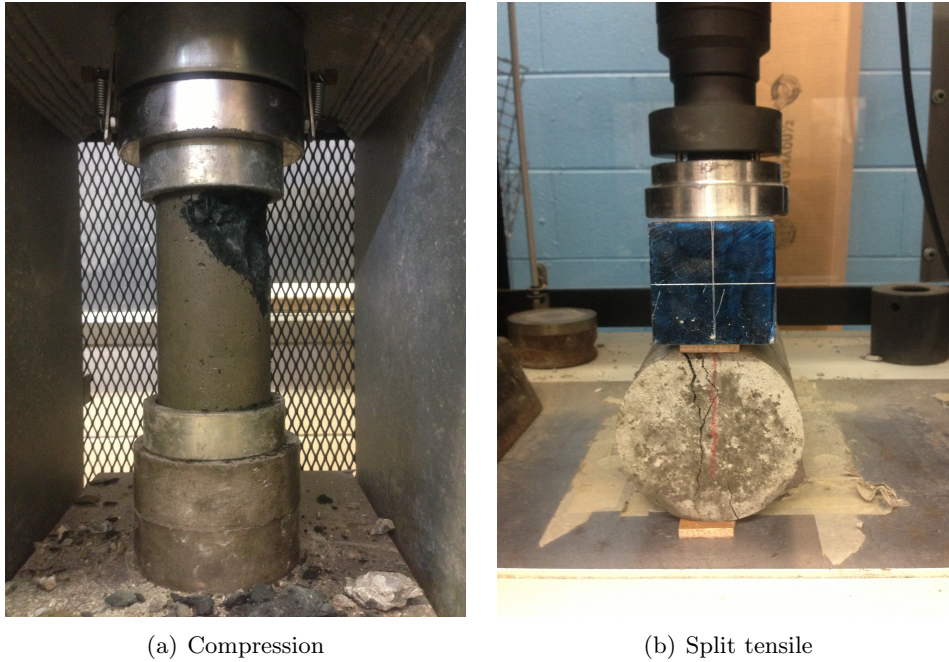
Figure 3.8: Strength tests on concrete

diameter and 8in long was cut into 2in long specimen. The side of the cylindrical specimen is coated with epoxy, and after the epoxy is dried, it is placed between the two cell chambers of test device. One side of the cell is filled with a 3% Na Cl solution and other side of the cell is filled with 0.3N NaOH solution. The system is then connected and a 60-volt potential is applied for 6 hours. Readings are taken every 30 minutes. At the end of 6 hours the sample is removed from the cell and the total charge (coulombs) passed through the specimen is recorded. Figure 3.9 shows the test setup for rapid chloride-ion permeability test.

3.6.12   Miniature Concrete Prism Test(MCPT) protocol

The Miniature Concrete Prism Test(MCPT) protocol is a test method developed to identify deleterious alkali-silica reaction mechanism distress in reactive aggregates. In this protocol, concrete prisms of dimensions 50mm x 50mm x 285mm (2in. x 2in. x 11.25in.) were used for evaluating the reactivity of both coarse and fine aggregates. The proportions of aggregate in the 12.5 mm 9.5 mm fraction and the 9.5 mm 4.75 mm fraction were
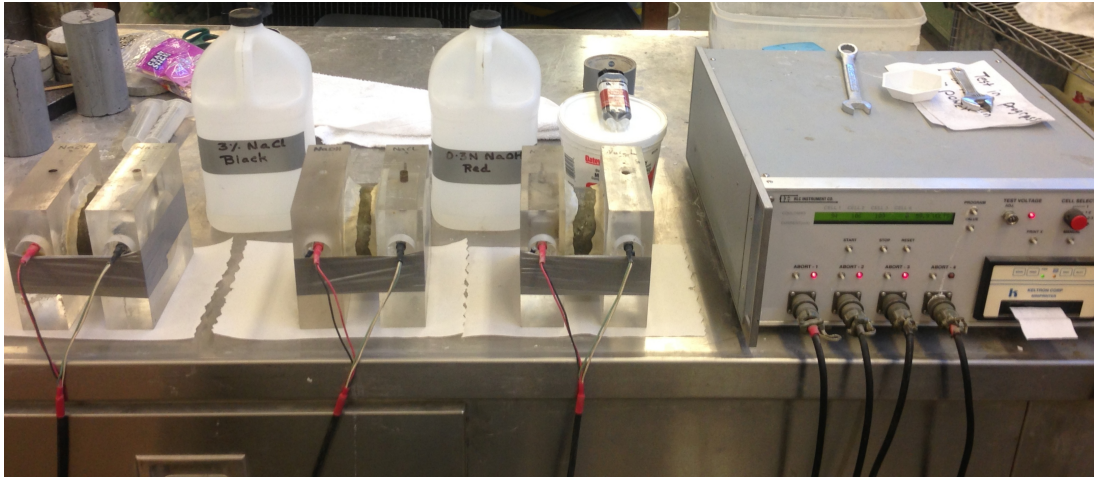
Figure 3.9: Rapid chloride-ion permeability test

selected, based on the assumption of maintaining a constant surface area across each of the two aggregate size fractions. To evaluate the coarse aggregate reactivity, a non-reactive fine aggregate is used in the concrete mixture to isolate the effects of the reactive aggregate. Similarly, when the reactivity of a fine aggregate is to be evaluated, a non-reactive coarse aggregate has to be used.

In this protocol, a cement having a high alkali content of $0.9 \pm 0.1\%$ Na_2O_eq. is required to be used. The alkali content of the concrete is boosted to 1.25% Na_2O_eq. by weight of cement similar to the procedure described in the standard ASTM C1293 test method. The test specimens are demolded after 24 hours of casting and submerged in water bath at $60\,^{\circ}$C for an additional 24 hours. At the end of 48 hours from the time of casting, the zero-day length change reading is taken and the prism specimens are transferred to 1N NaOH soak solution bath which is preconditioned to $60\,^{\circ}$C temperature. Subsequent length change readings are periodically taken at 3, 7, 10, 14, 21, 28, 42, and 56 days. Three prisms per test were used to calculate the average expansions and standard deviation of the test specimens. The expansions of prisms less than 0.04% at 56 days were considered to be non-reactive aggregates, and expansions of prisms above 0.04% at 56 days were considered as reactive aggregates.

For ASR mitigation studies the cement was replaced with SCMs at required dosages

(a) concrete prisms   (b) length comparator
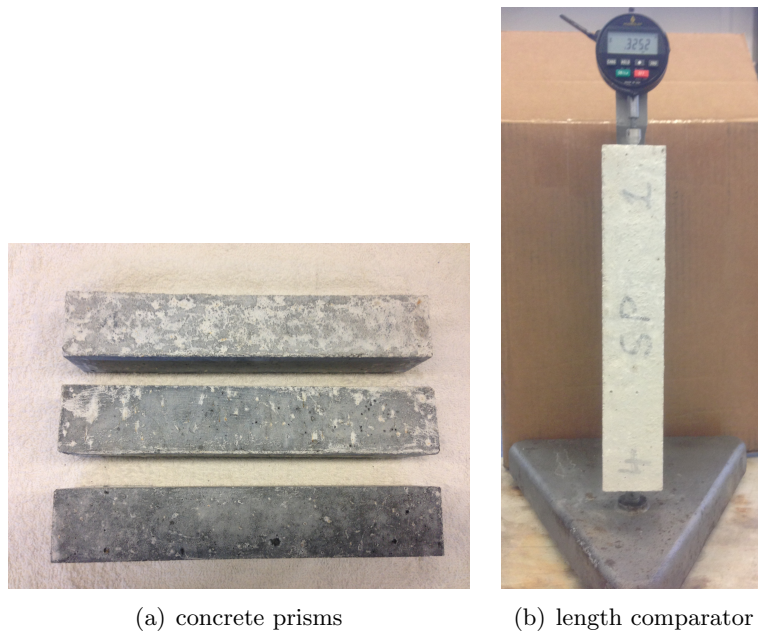
Figure 3.10: Miniature concrete prism test

and prisms were cast. The remaining process remains same as the regular test method.

3.6.13   Accelerated Mortar-bar Tests (AMBT)

In this test method, mortar bars 25mm X 25mm X 285mm (1in. x 1in. x 11.25in.) with gauge studs embedded at the ends were cast and moist cured for 24 hours in a curing room. After demolding, the bars were cured at 80 °C for 24 hours in a water bath. After curing in the water bath for 24 hours, the bars were kept in 1N NaOH soak solution, which was preheated to 80 °C for 24 hours. Periodic length change measurements were taken at regular intervals for 14 days, and percent expansions were calculated. The expansions of mortar bars less than 0.1% at 14 days were considered to be non-reactive aggregates, and expansions of mortar bars over 0.2% were considered as reactive aggregates. Mortar bar expansions between 0.1% and 0.2% were considered potentially reactive with additional confirmation required using petrographic examination, concrete prism tests (ASTM C1293) and/or past field performance. The standard ASTM C1567 test is similar to the ASTM C1260 test method, the difference being a portion of portland cement was replaced with

different SCMs at required dosages to cast the mortar bars.

3.6.14   X-Ray Diffraction (XRD)

The X-Ray Diffraction (XRD) technique was used as a qualitative tool to identify the crystalline phases of slag and Class F fly ash. All samples were characterized using a Rigaku Ultima IV multipurpose X-ray diffraction system. The cross beam optics technology allows the system to be permanently mounted and aligned. This system is designed for high level research performance standards and offers a variety of sample holders. The test parameters were set at 2Θ angle range from $5\,^{\circ}$ to $70\,^{\circ}$ (Cu $Kalpha$ radiation) with a scan rate of 0.1 steps per minute (i.e. 65 min scan per sample). The analysis of the peak intensities obtained from the XRD to identify the best possible match for a crystalline phase was done using the Inorganic Crystal Structure Database, NIST Crystal Data File and Powder Diffraction File electronic data base.

3.6.15   Laser Particle Size Distribution (PSD)

In this test method, particle size distribution and associated properties such as specific surface area of slag and Class F ash were determined using Malvern Mastersizer 2000. The results in this study are based on volume % passing and each value represents the average of four measurements. The particle size of slag and Class F ash represents the diameter of an equivalent sphere. Samples were prepared by dispersing a small amount of powder in 10 ml of deionized water and a drop of dispersing agent. The samples were then agitated for five minutes in an ultrasonic bath to disperse the material. The measurements were performed in deionized water using a refractive index of 1.55 and absorption of 0.1.

3.6.16   Thermogravimetric Analysis (TGA)

Thermogravimetric analysis is used to determine the calcium hydroxide(CH) depletion levels in ternary cementitious paste systems. In this method, paste samples were prepared in small cylindrical plastic molds with a w/c ratio of 0.45 and kept in the moist

curing room. At respective curing ages the samples were demolded and crushed using hammer and sieved through # 200 sieve. Thermogravimetric analysis was performed on about 30mg of the resulting powder by monitoring the weight while heating up from $30\,^{\circ}C$ to $900\,^{\circ}C$ at $20\,^{\circ}C/min$ and purging with N_2, in an AutoTGA 2950HR V5.4A TGA equipment. The amount of calcium hydroxide(CH) is expressed as % of the dry sample weight at $550\,^{\circ}C$ (W_{550}):

$$CH = \frac{W_{450} - W_{550}}{W_{550}} X \frac{74}{18} (*) \tag{3.1}$$

$(*)Ca(OH)_2$ (74g/mol) $\longrightarrow$ CaO + H_2O (18g/mol) weight difference determined using stepwise method

The exact boundaries for the temperature intervals were read from the derivative curve (DTG). The standard deviation on three independent measurements at all tested ages is not larger than 0.2% for CH.

3.6.17   Pore Solution Extraction

The pore solution extraction is a process in which the solution inside the harden cement paste samples is squeezed out with pressure and collected in nalgene containers. Pore solution expression was originally developed by Longuet et al. [Longuet et al., 1973] as a relatively simple method of removing pore solution from a cementitious material by using mechanical pressure. Barneyback and Diamond [Jr. and Diamond, 1981] improvised on the device suggested by Longuet. In this research, a device similar to one suggested by Barneyback is used. Figure 3.11 shows the pore solution expression device, the cement paste sample is compressed under high pressure inside the device chamber. A vacuum pump was connected to the pore solution drain system through a pore solution collection chamber. The pore solution obtained was then analyzed for ion concentrations using ICP technique and titration methods.

Figure 3.11: Pore solution expression device

3.6.18 Inductively Coupled Plasma (ICP)

In this test, the sample of pore solution obtained by extraction process was diluted with deionized water by 100 times (i.e. 1 ml of pore solution in 100 ml of deionized water). The diluted solution was then analyzed using ICP test for ion concentrations in the pore solution.

3.6.19 Potentiometric Titration

In this experiment titrations were conducted using a pH meter to follow the course of acid-base titrations as seen in Figure 3.12. In this test, the sample of pore solution obtained by extraction process was diluted with deionized water by 100 times. The resulting solution was then titrated against 0.1 N hydrochloric acid (H Cl) solution to complete the titration process. From the resulting titration curves, the equivalence point was identified and OH^- ion concentrations of the base solutions (cement pore solution) were determined.
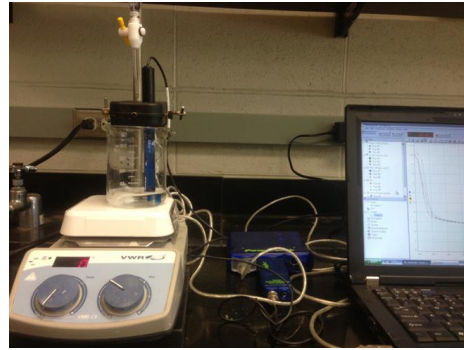
Figure 3.12: Potentiometric Titration setup

(a) sample holder

(b) EIS measurements

Figure 3.13: Electrical impedance spectroscopy test

3.6.20   Electrochemical Impedance Spectroscopy (EIS)

In this technique, the electrical resistance of the cementitious pastes were measured using two stainless steel electrodes connected to a potentio-stat. A small amplitude alternating potential signal at different frequencies (from 1Mhz to 100 mHz) were applied to cementitious paste systems and resistance was determined. For the impedance measurement of cementitious paste, an automated program was used that measured the electrical resistance of the cementitious pastes between two stainless steel electrodes. Figure 3.13 shows the cementitious paste sample holder with stainless steel electrodes and potentio-stat connections to the samples.

3.6.21 Scanning Electron Microscopy (SEM) and Energy Dispersive X-Ray (EDX) analysis

The micro structure analysis on aggregates and mortar bar samples was performed using SEM and EDX techniques. The analysis was performed at Clemson University's Advanced Materials Research Laboratories (AMRL) electron microscope facility, using a variable pressure Hitachi S-3400N scanning electron microscope. The techniques were performed on polished sample of mortar bars at a voltage of 20Kv. A portion of representative sample of approximately 5 cm width was cut from the mortar bars used for standard and modified ASTM C 1260 tests. The samples were then placed in circular molds and a combination of epoxy resin and hardener in a ratio of 100:12 was poured on top to completely submerge the samples within epoxy, any air bubbles present were removed using a vacuum suction pump and desiccators. The samples were then set to harden at room temperature.

Once hardened, the samples were polished to get a clean flat surface without defects. The polishing process was done on diamond embedded discs with grits numbered 80, 220, 600 and 1200 in the order of increasing fineness. To remove micro scratches the final polishing was done on finer discs by using diamond suspensions of 3 micron and 1/4 micron. The samples, once polished were then ready to be analyzed using the scanning electron microscope. The images were captured at 3 different magnification levels showing the general ASR affected structure and zooming in the ASR gel at higher magnification. The EDX technique was also performed on scanning electron microscope to verify the elements present in the cement based mortar bar structure, the presence of ASR gel in and around the aggregates was confirmed with EDX technique. To analyze the mineral composition structure of aggregates EDX mapping technique was used to identify the different elements present in the aggregates.

3.6.22 Mix Proportions

The mix proportions used were according to the Std. ASTM C 1260 / ASTM C 1567 requirements for a batch of 3 mortar bars. For concrete prism test to conduct

detailed investigations on slags Std. ASTM C 1293 mix proportions were adopted. The details of different test conducted is provided in the Experimental program chapter of this dissertation.

Chapter 4

Experimental Program

This chapter describes various experimental programs employed in this research study. The experimental program was developed based on the objectives listed in the research program. Different experimental matrix has been developed and adopted for the various different tests conducted on supplementary cementitious materials (SCM). The ASTM standard test procedures and modified versions of the standard test were used throughout the study.

4.1 Material Characterization

The various materials used in this study were characterized based on their physical, chemical and mineralogical properties.

4.1.1 Aggregates

The aggregates used in this study both fine and coarse were tested for their basic properties such as bulk unit weight, specific gravity and percent water absorption. Petrographic analysis was conducted on aggregates to determine their mineralogical composition.

4.1.2   SCMs

The SCMs used in this study were slag, class F fly ash and class C fly ash. The SCMs were characterized based on their physical properties and chemical composition.

Characterization of slag was carried out on one slag type (grade 100) as a preliminary step to determine the composition, fineness and pozzolanic reactivity. X-ray fluorescence (XRF) and particle size distribution (PSD) analysis was conducted to determine the bulk chemical composition and average particle size of slag grains. Thermogravimetric analysis (TGA) was conducted to determine the pozzolanic reactivity.

Characterization of fly ashes were carried out on two different fly ash types (Class F and Class C) as a preliminary step to determine the composition, fineness and pozzolanic reactivity of slags. In this study one class F ash and one class C ash was selected form each type for testing and analysis purpose. X-ray fluorescence (XRF) and particle size distribution (PSD) analysis were conducted to determine the bulk chemical composition and average particle size of fly ash grains.

4.2   Research Methodology

In this study concrete mixtures were designed according to ACI 211 mixture proportioning guidelines. Table   4.1 shows the mix design template for concrete materials proportioning. The aggregate gradation was selected according to standard ASTM C33 specification. For coarse aggregate gradation the total weight of coarse aggregate was divided in to three portions. Table 4.2 shows the aggregate gradations and quantities used for a typical batch of concrete. The volume fraction of dry rodded coarse aggregate used was 65% of the unit volume of concrete and the total cementitious content was limited to 420 kg/m^3. The water to cementitious material ratio used was 0.45 (w/cm = 0.45) for all concrete mixtures tested. The physical properties of coarse and fine aggregate were determined using ASTM specified methods.

The batch quantities were designed for 15 concrete cylinders considering the wastage

Table 4.1: Concrete mix design template

MIX DESIGN For $1m^3$ of Concrete				
Concrete Ingredients			Weight, kg	Volume, $/m^3$
Coarse aggregate	NC		1065.09	0.3698
Dry rodded Unit weight	1639 kg/m^3			
Specific gravity	2.88			
Absorption	0.58%			
Total cementitious content		420 kg/m^3		
Cement		Repl, (%)	420	0.1333
Specific gravity	3.15	100		
Slag		Repl, (%)	0	0.0000
Specific gravity	2.92	0		
fly ash		Repl, (%)	0	0.0000
Specific gravity	2.2	0		
W/Cm ratio	0.45			
Water			189	0.1890
Specific gravity	1			
Air content ,%	2.5		0	0.025
Fine aggregate	Glasscox		747	0.2828
Specific gravity	2.64			
Absorption	0.34%			

while mixing process. The total cylinders required for testing all concrete properties were
13. Table 4.2 shows the batch quantities for a typical concrete mixture.

Table 4.2: Batch quantities for a concrete mixture

Quantity Take off	Weight, gm
Coarse Aggregate (CA) Passing to Retained	
19 mm to 12.5 mm	8774
12.5 mm to 9.5 mm	8774
9.5 mm to 4.75 mm	8774
Fine Aggregate (FA)	
4.75 mm to 75 μm	18454
Cement	10380
Slag	0
Fly ash	0
Water adjusted for absorption of CA&FA	4886.3
Volume of Concrete (cft)	0.8585

For designing different mixtures the proportion of cement in the mix was varied by
replacing with SCMs. Table 4.3 shows the different SCM proportions and type of mix used
in this study. The material quantities for different mixture proportions can be found in
Appendix A and B. The detailed calculation of mixture components with lower and upper
bounds is discussed in the Appendix C.1 section.

Table 4.3: SCM proportions for Concrete Mixtures

Mix ID	Cement	Slag	F- Fly ash	Type
M1	1.00	0.00	0.00	Control
M2	0.30	0.70	0.00	Binary
M3	0.45	0.15	0.40	Ternary
M4	0.65	0.35	0.00	Binary
M5	0.65	0.00	0.35	Binary
M6	0.30	0.35	0.35	Ternary
M7	0.54	0.23	0.23	Ternary
M8	0.76	0.12	0.12	Ternary
M9	0.42	0.46	0.12	Ternary
M10	0.48	0.18	0.35	Ternary
M11	0.85	0.05	0.10	Ternary
M12	0.50	0.20	0.30	Ternary

4.2.1 Testing on Fresh Concrete

The fresh concrete properties such as slump, air content and unit weight were measured for all the different concrete mixtures. Standard ASTM C143 test method was used to measure the slump of concrete mixtures. Air content of fresh concrete was determined by pressure meter method.

4.2.2 Strength Tests on Concrete

Compressive strength and split tensile strength tests were performed on 4 x 8 inch concrete cylinders. The strength gain or loss was determined at two different ages 28-days and 56-days.

4.2.3 Durability Tests on Concrete

Rapid chloride-ion permeability and alkali-silica reaction tests were conducted on different concrete mixtures. The standard ASTM C1202 test was used to determine the permeation of chloride-ion through concrete specimen. To determine the alkali-silica reaction potential of aggregate in concrete mixture the modified version of standard ASTM C1293 known as Miniature Concrete Prism test (MCPT) was adopted. The alkali-silica reaction mitigation measures were also studied using different SCM proportions in the MCPT test method.

Table 4.4: Properties tested for concrete mixtures

Mix ID	Fresh Properties			Harden Properties			
	Slump	Unit weight	Air Content	Compressive Strength	Split Tensile	RCPT	ASR
	ASTM C143	ASTM C138	ASTM C231	ASTM C39	ASTM C496	ASTM C1202	MCPT
M1	x	x	x	x	x	x	x
M2	x	x	x	x	x	x	x
M3	x	x	x	x	x	x	x
M4	x	x	x	x	x	x	x
M5	x	x	x	x	x	x	x
M6	x	x	x	x	x	x	x
M7	x	x	x	x	x	x	x
M8	x	x	x	x	x	x	x
M9	x	x	x	x	x	x	x
M10	x	x	x	x	x	x	x
M11	x	x	x	x	x	x	x
M12	x	x	x	x	x	x	x

55

4.3 ASR Mitigation in Mortar-bar Tests Using SCMs

In order to investigate the effectiveness of SCM in mitigating alkali-silica reaction mechanism the standard ASTM C1260 / C1567 mortar bar tests were conducted. Different combinations of mortar mixtures made with cement, slag, Class F fly and Class C fly ash were studied. Three reactive aggregates and one non-reactive aggregate was used in this investigations.

4.3.1 Investigation on Combinations of Cement, Slag and Class F Fly Ash

In this investigation binary and ternary combinations of cement with slag and class F fly ash were studied. The two reactive aggregates used were from New Mexico and Spratt; and one non-reactive aggregate was from Adairsville. The aggregates were crushed and graded as per ASTM C1260 specifications. A series of standard ASTM C1260 / C1567 mortar bar tests were conducted with different proportions of SCMs. The total cementitious content was constant and water to cementitious materials ratio (w/cm = 0.47) was as per ASTM C1260 specification. The proportion of cement in the mix was varied by replacing with SCMs. Tables 4.5, 4.6, 4.7 show the different SCM proportions and type of mix used for New Mexico, Spratt and Adairsville aggregates respectively.

4.3.2 Investigation on Combinations of Cement, Class F and Class C Fly Ash

In this investigation binary and ternary combinations of cement with class C ash and class F fly ash were studied. One reactive aggregate, a gravel known as Stocker sand from Ohio was used for this study. The aggregate was graded as per ASTM C1260 specifications. The total cementitious content was constant and water to cementitious materials ratio (w/cm = 0.47) was as per ASTM C1260 specification. A series of standard ASTM C1260 / C1567 mortar bar tests were conducted with different proportions of SCMs. The proportion

Table 4.5: SCM proportions for New Mexico aggregate

Mix ID	Cement, %	Slag, %	Fly ash, %	Type
NM1	1.00	0.00	0.00	Control
NM2	0.30	0.70	0.00	Binary
NM3	0.45	0.15	0.40	Ternary
NM4	0.65	0.35	0.00	Binary
NM5	0.65	0.00	0.35	Binary
NM6	0.30	0.35	0.35	Ternary
NM7	0.54	0.23	0.23	Ternary
NM8	0.80	0.00	0.20	Binary
NM9	0.50	0.50	0.00	Binary
NM10	0.50	0.30	0.20	Ternary
NM11	0.70	0.15	0.15	Ternary
NM12	0.80	0.10	0.10	Ternary
NM13	0.75	0.13	0.13	Ternary
NM14	0.70	0.20	0.10	Ternary
NM15	0.60	0.25	0.15	Ternary

Table 4.6: SCM proportions for Spratt aggregate

Mix ID	Cement	Slag	Fly ash	Type
SP1	1.00	0.00	0.00	Control
SP2	0.30	0.70	0.00	Binary
SP3	0.45	0.15	0.40	Ternary
SP4	0.65	0.35	0.00	Binary
SP5	0.65	0.00	0.35	Binary
SP6	0.30	0.35	0.35	Ternary
SP7	0.54	0.23	0.23	Ternary
SP8	0.80	0.00	0.20	Binary
SP9	0.50	0.50	0.00	Binary
SP10	0.50	0.30	0.20	Ternary
SP11	0.70	0.15	0.15	Ternary
SP12	0.90	0.05	0.05	Ternary
SP13	0.80	0.10	0.10	Ternary
SP14	0.75	0.13	0.13	Ternary

Table 4.7: SCM proportions for Adairsville aggregate

Mix ID	Cement	Slag	Fly ash	Type
AD1	1.00	0.00	0.00	Control
AD2	0.30	0.70	0.00	Binary
AD3	0.45	0.15	0.40	Ternary
AD4	0.65	0.35	0.00	Binary
AD5	0.65	0.00	0.35	Binary
AD6	0.30	0.35	0.35	Ternary
AD7	0.54	0.23	0.23	Ternary
AD8	0.80	0.00	0.20	Binary
AD9	0.50	0.50	0.00	Binary
AD10	0.50	0.30	0.20	Ternary

of cement in the mix was varied by replacing with SCMs. Table 4.8 shows the different SCM proportions and type of mix used in this study.

Table 4.8: SCM proportions for Stocker sand

Mix ID	Cement	F- Fly ash	C- Fly ash	Type
ST1	1.00	0.00	0.00	Control
ST2	0.60	0.40	0.00	Binary
ST3	0.60	0.00	0.40	Binary
ST4	0.80	0.20	0.00	Binary
ST5	0.80	0.00	0.20	Binary
ST6	0.60	0.20	0.20	Ternary
ST7	0.73	0.13	0.13	Ternary
ST8	0.87	0.07	0.07	Ternary
ST9	0.67	0.27	0.07	Ternary
ST10	0.67	0.07	0.27	Ternary
ST11	0.85	0.05	0.10	Ternary
ST12	0.50	0.20	0.30	Ternary

4.4 Pore Solution Analysis on Cementitious Paste

In this investigation, various analytical techniques were used to analyze the pore solution chemistry of cementitious paste systems with combinations of cement, slag and Class F fly ash. Pore solution expression was originally developed by Longuet et al. [Longuet et al., 1973] as a relatively simple method of removing pore solution from a ce-

mentitious material by using mechanical pressure. The pore solution thus obtained was analyzed for ions present using ICP technique, the OH^- ion concentration was calculated using potentiometric titrations. Table 4.9 shows the test matrix for different SCM proportions used to make paste samples and analytical techniques used for analysis in this study. The cement alkali content was raised to 1.25% Na_2O_eq. by weight of cement for comparing the pore solution results with the ASR test results in MCPT test method.

Table 4.9: Test matrix for pore solution analysis

Mix ID	Cement	Slag	Flyash	w/cm	Titration	ICP
M1	1.00	0.00	0.00	0.45	x	x
M2	0.30	0.70	0.00	0.45	x	x
M3	0.45	0.15	0.40	0.45	x	x
M4	0.65	0.35	0.00	0.45	x	x
M5	0.65	0.00	0.35	0.45	x	x
M6	0.30	0.35	0.35	0.45	x	x
M7	0.54	0.23	0.23	0.45	x	x

4.5 Electrochemical Impedance Spectroscopy Analysis on Cementitious Paste

Electrochemical Impedance Spectroscopy analysis technique was performed on cementitious paste systems to measure the resistivity of hardened cementitious paste systems with age. The cement alkali content was raised to 1.25% Na_2O_eq. by weight of cement for comparing the resistivity results with the ASR test results in MCPT test method. The EIS technique gives an indication of change in electrical resistivity of cementitious paste systems due to hydration process. Table 4.10 shows the test matrix for different SCM proportions used to make paste samples and analytical techniques used for analysis in this study

Table 4.10: Test matrix for EIS analysis

Mix ID	Cement	Slag	Flyash	w/cm	EIS
M1	1.00	0.00	0.00	0.45	x
M2	0.30	0.70	0.00	0.45	x
M3	0.45	0.15	0.40	0.45	x
M4	0.65	0.35	0.00	0.45	x
M5	0.65	0.00	0.35	0.45	x
M6	0.30	0.35	0.35	0.45	x
M7	0.54	0.23	0.23	0.45	x

Chapter 5

Results and Discussions

This chapter reports the findings of the research investigations as described in experimental program. The SCMs used were characterized for their particle size and mineralogical composition. For concrete studies the fresh properties such as slump, air content and unit weight are reported; and for hardened properties compressive strength, split tensile strength, rapid chloride-ion permeability and alkali-silica reactivity are reported. For mortar studies only alkali-silica reactivity is reported. For cementitious paste studies, pore solution composition and electrical resistivity were reported.

The results obtained from mortar and concrete studies were analyzed using simplex-centroid design technique and the analysis results were discussed. The fundamental investigations conducted on cementitious paste studies were also discussed.

5.1 Characterization of SCMs

The supplementary cementitious materials used in this study were slag and class F fly ash. The physical properties such as fineness and chemical properties such as chemical composition and mineralogical composition were investigated. The effectiveness of SCMs in improving cement concrete properties were analyzed by testing.
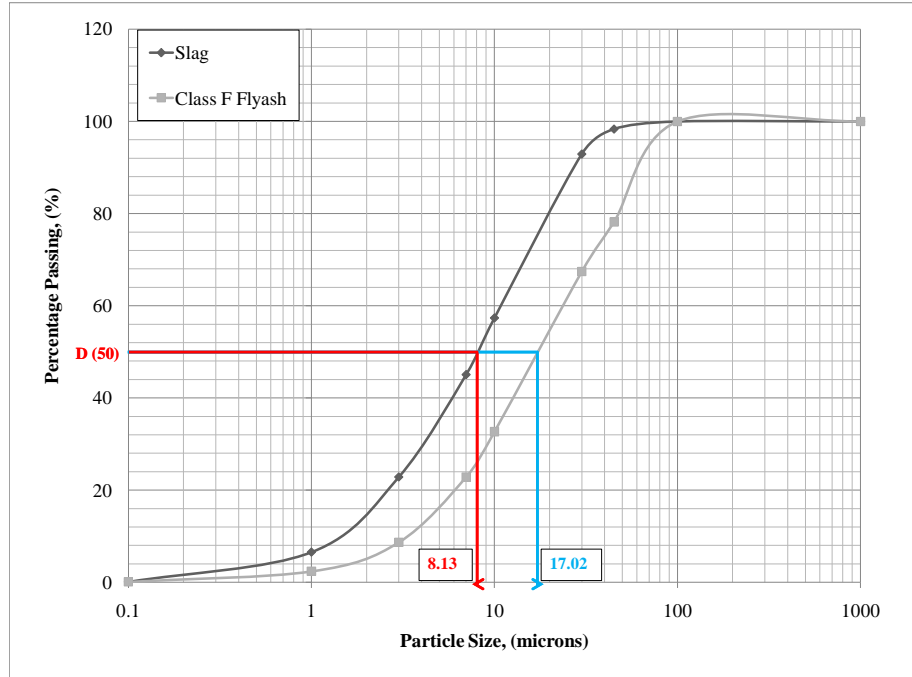
Figure 5.1: Particle size distribution and D_{50} size of slag and class F fly ash

5.1.1 Particle Size Distribution of SCMs

Figure 5.1 shows the particle size distribution curve of slag and class F ash. As the figure shows, the average particle size (D50) for slag was $8.13\mu m$ and for class F fly ash was $17.02\mu m$, these results indicate that SCMs (as-obtained or virgin) were well-graded in their particle size distribution. In addition, additional information on the average specific surface area and corresponding particle size finer than 10%, 50% and 90% for slag and class F fly ash are shown in Table 5.1.

Table 5.1: Particle size and specific surface area of SCMs

SCMs	Size, μm			Sp. Surface area (m^2/g)
	D_{10}	D_{50}	D_{90}	
Slag	1.384	8.13	26.19	1.84
Class F fly ash	3.379	17.023	76.11	0.887

5.1.2 Mineralogical Composition of SCMs

The XRD analysis performed on slag and class F fly ash yielded the mineralogical data and the nature of the glass present in slag and class F fly ash as shown in Figure 5.2. The characteristic broad hump seen in class F fly ash XRD pattern contained Mullite, Quartz and Hematite as the predominant crystalline phases representing the aluminosiliceous glass and having a maximum intensity at representative 2Θ angle. The slag sample was amorphous in nature and did not have any major crystalline peaks.

5.2 Properties of Fresh Concrete

5.2.1 Slump of Concrete

The results in Table 5.2 and Figure 5.3 show the slump values of concrete mixtures measured using standard ASTM C143 test method, as these results suggest, the replacement of cement with slag and fly ash increases the slump of concrete for certain dosages as compared to pure cement. For slag mixtures, the minimum dosage of 5% and maximum dosage of 70% yield lower slump values compared to pure cement. For fly ash mixtures it is observed that the slump values increase in most cases, the reason being because fly ash particles are spherical they have a ball bearing effect on cement grains which will increase the flow of concrete yielding higher slump values. The ternary mixtures have an improved effect on slump values as compared to pure cement mixtures due to this potential ball bearing effect.

5.2.2 Percent Air Content of Concrete

The results in Table 5.2 and Figure 5.4 show the percent air content values of concrete mixtures measured using standard ASTM C231 test method, as these results suggest, the replacement of cement with slag and fly ash significantly changes the air content of concrete at certain dosages. The pure cement concrete mixture was designed at 2.5% air content and the value obtained after testing was 2.6%. The average particle size of slag
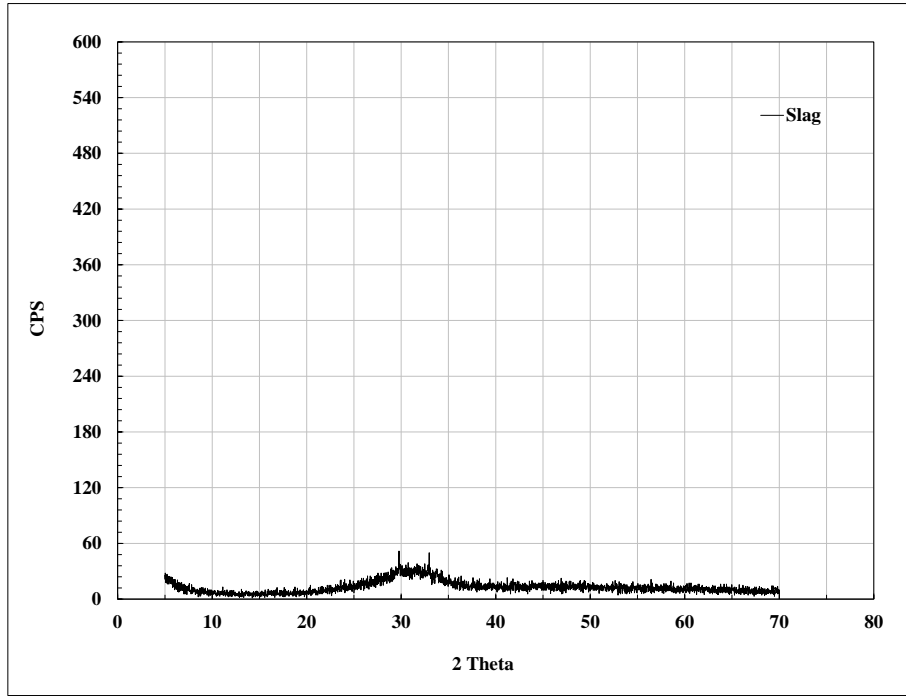
(a) Slag
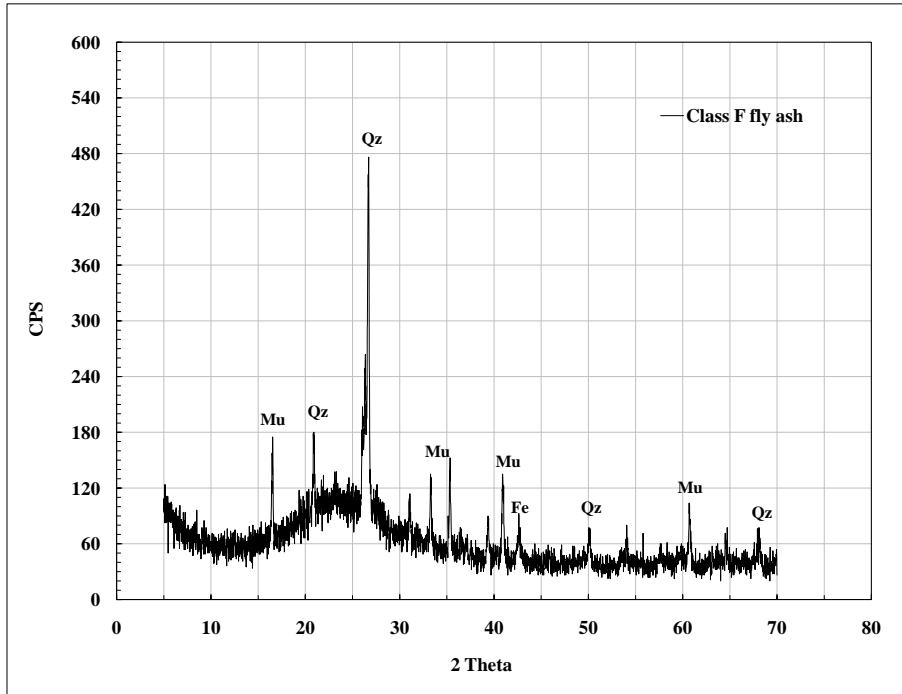
(b) Class F fly ash

Figure 5.2: X-Ray Diffraction pattern of SCMs

64

Table 5.2: Fresh properties of concrete mixtures

Cement	Slag	fly ash	Mix ID's	Slump, in	Unit Wt , pcf	Air , %
1	0	0	1	5	139.23	2.6
0.3	0.7	0	2	4.5	136.01	1.9
0.45	0.15	0.4	3	5.5	139.70	1.3
0.65	0.35	0	4	6.5	135.25	3.3
0.65	0	0.35	5	5.5	138.21	1.2
0.3	0.35	0.35	6	7	135.71	2
0.54	0.23	0.23	7	5.5	137.29	2.1
0.76	0.12	0.12	8	7.3	137.42	1.9
0.42	0.46	0.12	9	6.2	129.85	3.1
0.475	0.175	0.35	10	5.5	133.52	1.4
0.85	0.05	0.1	11	4	137.58	1.8
0.5	0.2	0.3	12	7.1	135.40	2

grains is smaller than cement grains and fly ash grains particle size is larger than that of cement grains, thus when cement is replaced with slag and fly ash the smaller particles will act as filler material between the void structure of cement grains and reduce the air content. However, from Table 5.2 it was observed that mixtures #4 and #9 had higher air content than pure cement concrete.

5.2.3 Unit Weight of Concrete

The results in Table 5.2 and Figure 5.5 show the unit weight values of concrete mixtures measured using standard ASTM C138 test method, as these results suggest, the replacement of cement with slag and fly ash does not significantly changes the unit weight of concrete as compared to pure cement concrete mixture. The unit weight depends on the specific gravity of individual materials that go into the concrete mixture, with all other materials being the same the unit weight changes depending on the specific gravity of slag and fly ash when replaced at certain dosage with cement. The specific gravity of slag (2.9) is close to cement (3.15) whereas fly ash has a specific gravity of 2.2, thus as results indicate the unit weight does not change significantly. However, with higher fly ash dosages there is possibility that the unit weight of concrete could be reduced to some extent.
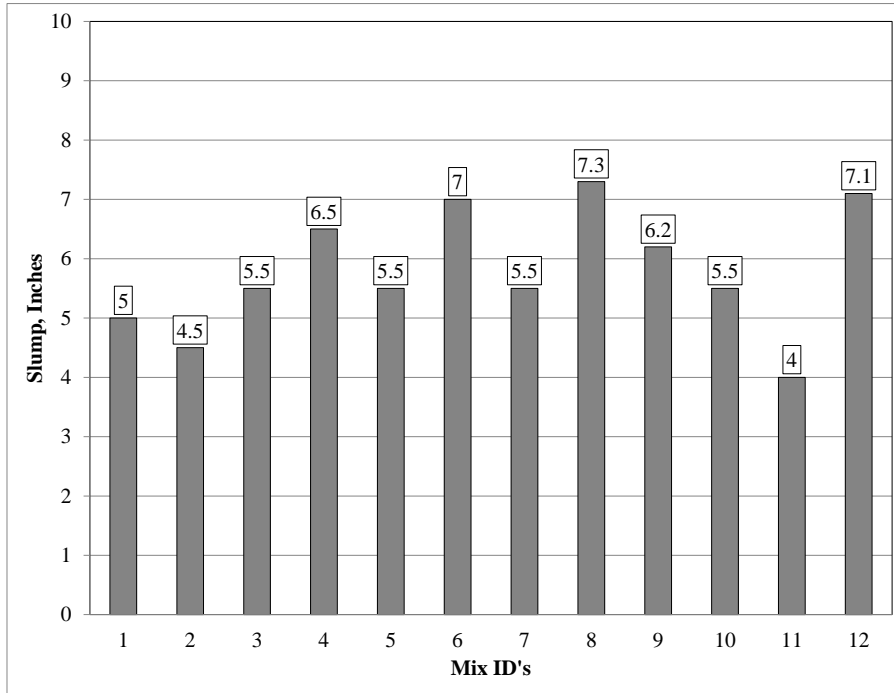
Figure 5.3: Slump of concrete mixtures

5.3 Properties of Hardened Concrete

5.3.1 Compressive Strength

The results in Table 5.3 and Figure 5.6 show the compressive strength values of concrete mixtures measured using standard ASTM C39 test method, as these results suggest, the replacement of cement with slag and fly ash significantly effects the strength of concrete as compared to pure cement mixture. The compressive strength is reduced in most cases up to 28-days of testing, however at 56-days, the compressive strength increases compared to the pure cement concrete specimen. This increase in strength is due to the pozzolanic reaction of slag and fly ash occurring at later ages. The results also suggest that the ternary blends of slag and fly ash with cement has improved strength effects compared to their binary mixtures.

66
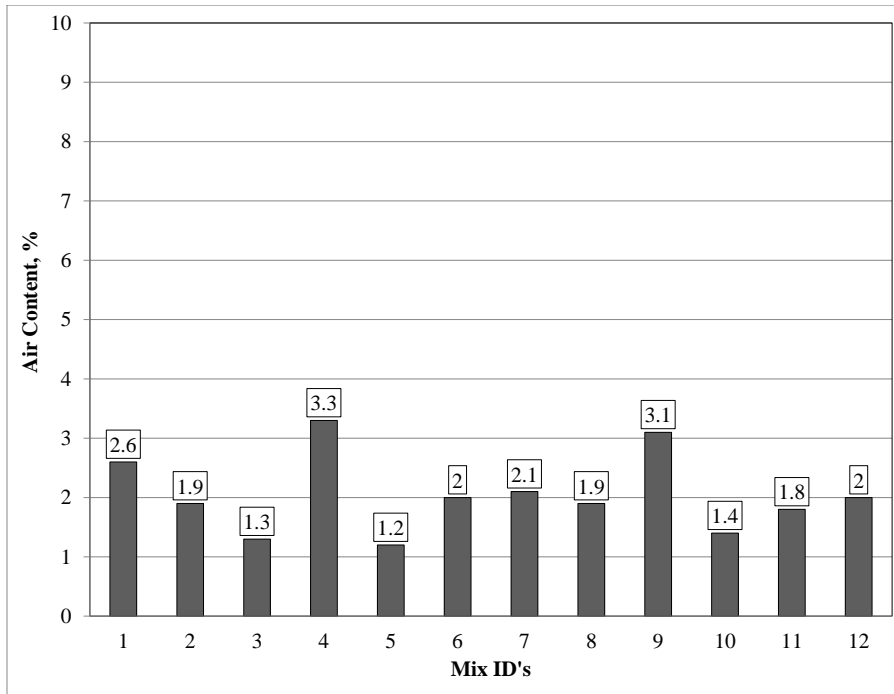
Figure 5.4: Percent air content of concrete mixtures
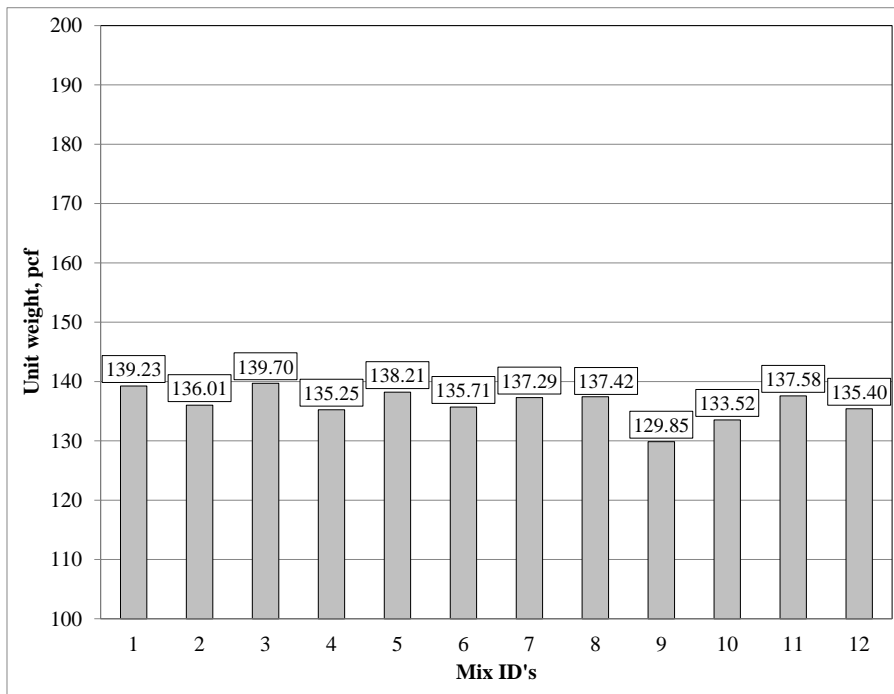
Figure 5.5: Unit weight of concrete mixtures

Table 5.3: Hardened properties of concrete mixtures at 56-days

Mix ID	Cement	Slag	F- Fly ash	Comp Stg, psi	Split Tensile, psi	RCPT, Coulomb	MCPT, %expn
M1	1.00	0.00	0.00	6285	680	3002	0.186
M2	0.30	0.70	0.00	5739	621	455	-0.008
M3	0.45	0.15	0.40	5999	593	929	-0.003
M4	0.65	0.35	0.00	7621	729	1220	0.010
M5	0.65	0.00	0.35	5620	525	1624	0.004
M6	0.30	0.35	0.35	5336	652	459	-0.008
M7	0.54	0.23	0.23	7190	742	946	-0.001
M8	0.76	0.12	0.12	7123	678	2456	0.019
M9	0.42	0.46	0.12	6853	690	726	0.024
M10	0.475	0.175	0.35	6042	605	1206	0.018
M11	0.85	0.05	0.10	6788	687	2378	0.033
M12	0.50	0.20	0.30	6501	714	1135	0.022
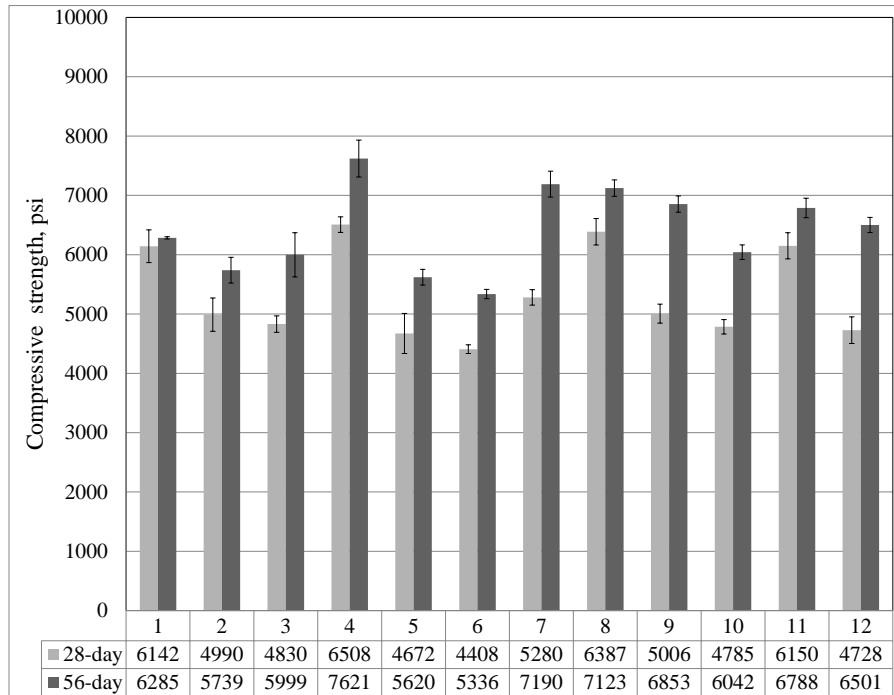
Figure 5.6: Compressive strength of concrete mixtures

5.3.2 Split Tensile Strength

The results in Table 5.3 and Figure 5.7 show the split tensile strength values of concrete mixtures measured using standard ASTM C496 test method, as these results suggest, the replacement of cement with slag and fly ash significantly effects the split tensile strength of concrete as compared to pure cement mixture. As a rule of thumb, the tensile strength of concrete is around 10% of its compressive strength, the ACI 318 specification suggests an empirical equation to determine the tensile strength of concrete by using its compressive strength. These assumptions are only true for pure cement concrete and when SCMs are used the results widely varies as seen in Figure 5.7.

5.3.3 Rapid Chloride-Ion Permeability

The results in Table 5.3 and Figure 5.8 show the rapid chloride-ion permeability coulomb values of concrete mixtures measured using standard ASTM C1202 test method,

	1	2	3	4	5	6	7	8	9	10	11	12
■ 28-day	718	635	612	672	490	493	543	642	523	434	711	563
■ 56-day	680	621	593	729	525	652	742	678	690	605	687	714
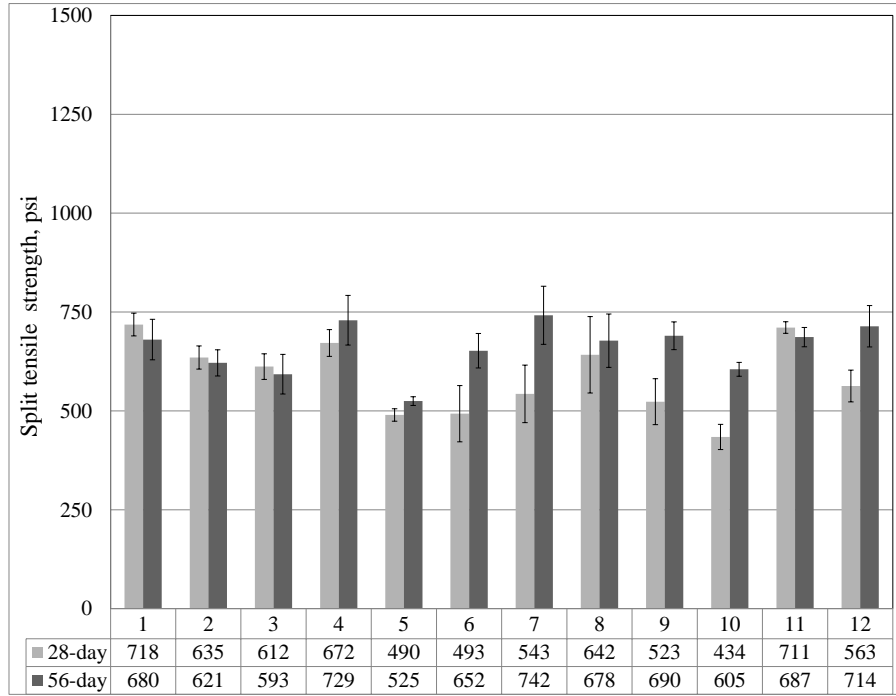
Figure 5.7: Split Tensile strength of concrete mixtures

as these results suggest, the chloride-ion permeability decreases with decrease in cement content when replaced with SCMs. Binary mixtures of slag performed better as compared to fly ash mixtures, the ternary mixtures showed a wide range of permeability values primarily depending on the cement content and SCM dosages. The mixtures #2 and #6 both have 30% cement with mixture #2 having 70% slag and mixture #6 having 35% slag and 35% fly ash, the results suggest that both these mixtures have similar coulomb values. While mixtures #4 and #5 both have 65% cement, the dosage levels of slag in mixture #4 is 35% and fly ash in mixture #5 is 35%. As seen in Figure 5.8 the coulomb values are different for mixtures #4 and #5, these results suggest that slag and fly ash can influence the chloride-ion permeability of concrete mixtures with slag performing better than fly ash at same replacement levels.
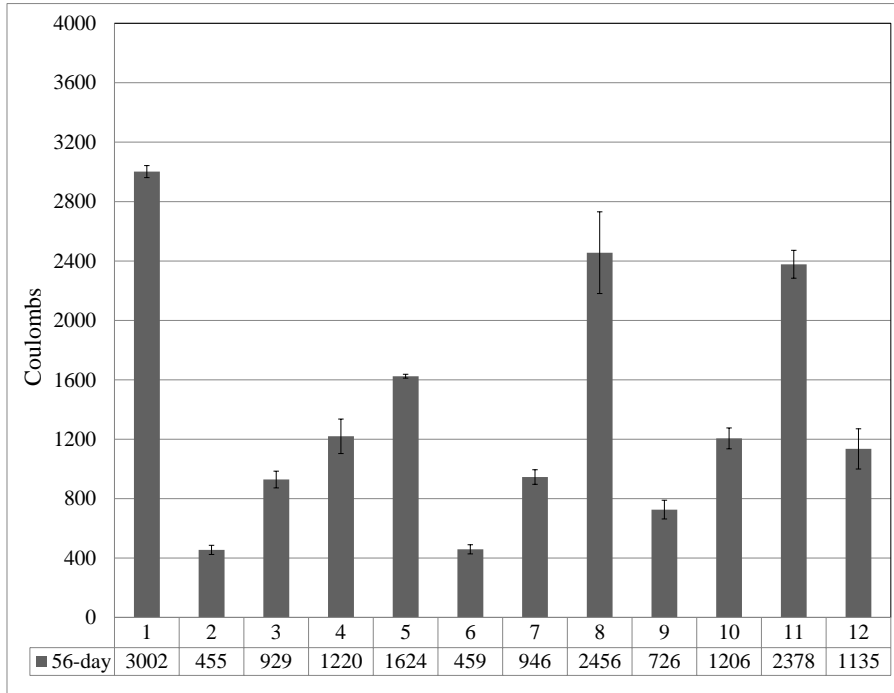
Figure 5.8: Rapid Chloride-ion permeability of concrete mixtures

5.3.4 Alkali-Silica Reaction

The results in Table 5.3 and Figure 5.9(a) show the concrete prism expansion values in percentage measured using standard Miniature Concrete Prism Test method, as these results suggest, the replacement of cement with slag and fly ash is effective in mitigating alkali-silica reaction expansions in concrete. The threshold for expansion limit in miniature concrete prism test is 0.04% at @ 56 days. The reactive aggregate tested had the control mixture expansion without any SCMs $\bar{0}.186\%$ at 56-days, whereas for mixtures with binary and ternary combinations of SCMs the expansions were well below the threshold, as seen in Figure 5.9(b).
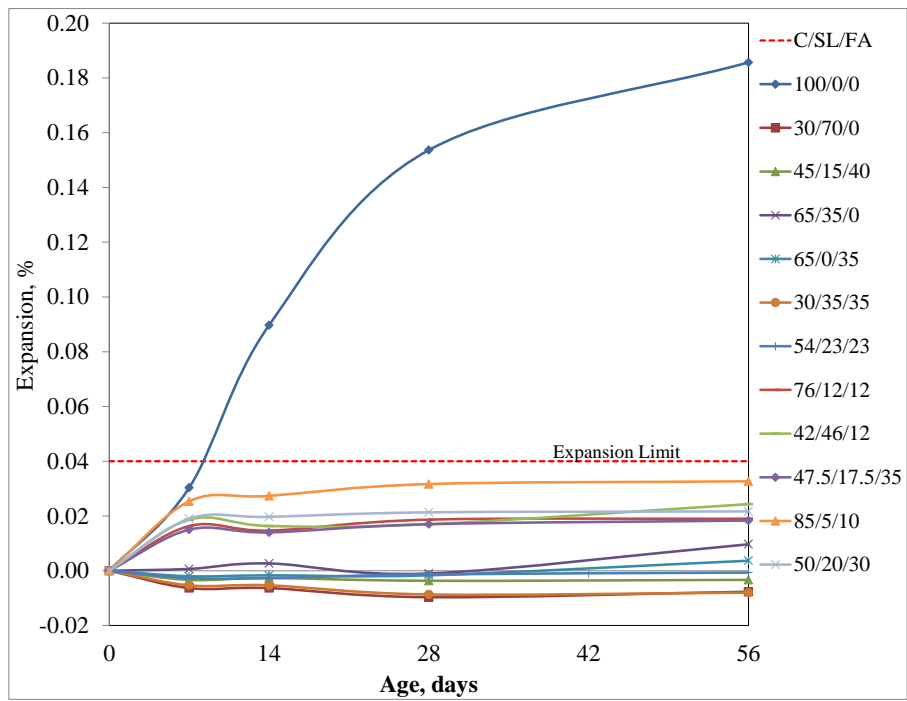
(a) MCPT expansions with age
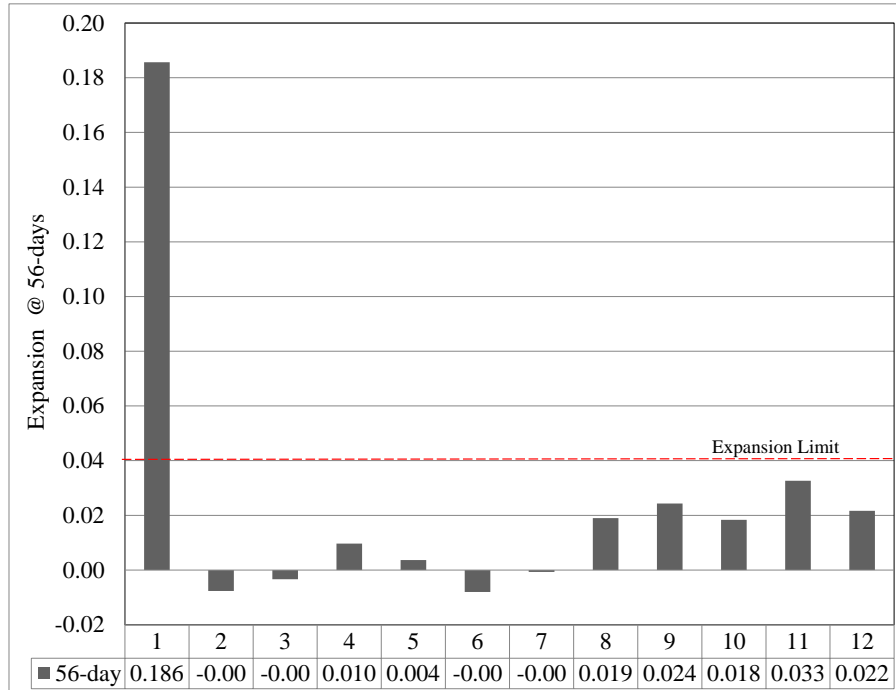
(b) 56-day expansions

Figure 5.9: Miniature Concrete Prism test expansions for concrete mixtures

5.4 Evaluation of Alkali-Silica Reaction Mitigation in Mortars

Standard ASTM C1260 / C1567 accelerated mortar bar tests were conducted with combinations of cement, slag, class F fly and class C fly ash mixtures to evaluate the effectiveness of SCMs in mitigating the alkali-silica reaction. The expansion limit for the standard ASTM C1260 / C1567 mortar bar test is 0.1% at 14 days, expansions of mortar bar specimens after that time period fail the test because of the potential for the alkali-silica reaction.

5.4.1 Investigation of Combinations of Cement, Slag and Class F Fly Ash

Binary combinations of cement + slag, cement + class F ash and ternary combinations of cement + slag + class F fly ash mixtures were studied using two reactive aggregates, one from New Mexico and one from Spratt and one non-reactive aggregate from Adairsville.
New Mexico aggregate:

Table 4.5 shows the proportions of SCMs used in the accelerated mortar bar tests for the New Mexico reactive aggregate. Mixtures #2, #9 and #4 are binary mixtures of cement + slag combination with slag dosage levels of 70%, 50% and 35%, respectively. Mixtures #5 and #8 are binary mixtures of cement + class F fly ash combination with class F fly ash dosage levels of 35% and 20%, respectively. Mixture #1 is the control sample containing no SCMs and all other mixtures are ternary mixtures of cement + slag + class F fly ash.

Figure 5.10 shows the 14-day mortar bar expansions of these New Mexico aggregate mixtures with different SCMs, as this figure shows, the control sample prepared with New Mexico aggregate has a 14-day mortar bar expansion of 0.89%, suggesting it is a highly reactive aggregate. The cement replaced by 70% and 50% of slag tend to have expansions below 0.1% at 14 days and, thus, these appear to be effective dosages to mitigate ASR in mortars. The 35% slag dosage has a 14-day mortar bar expansion above 0.1% and is not an effective dosage in mitigating ASR in mortars. These results suggest the cost effective
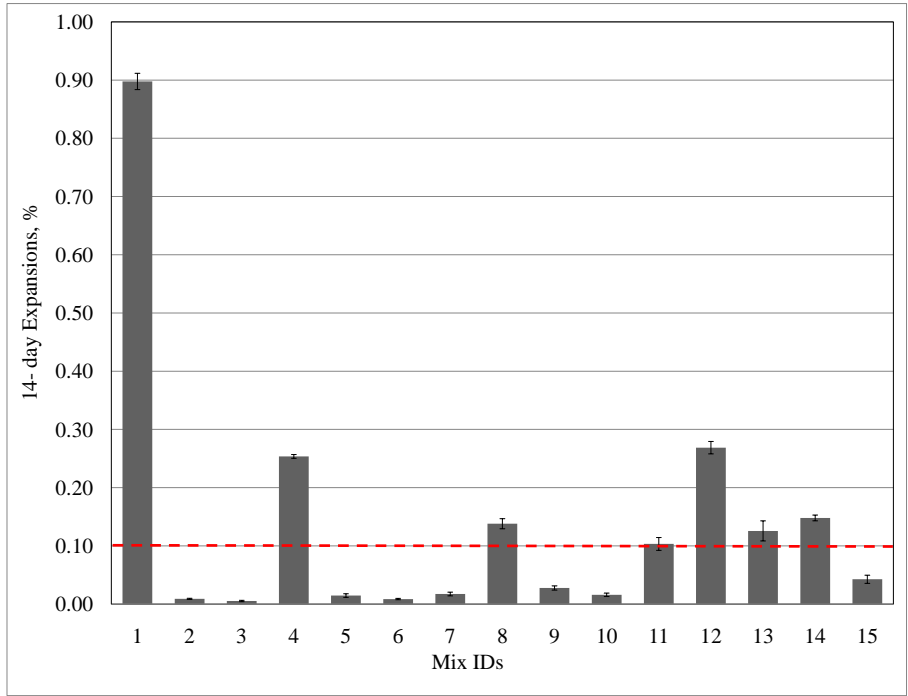
Figure 5.10: 14-day mortar bar expansions for New Mexico aggregate

dosage level of slag ranges between 50% and 35% to reduce the expansions below 0.1% at 14 days for the New Mexico aggregate.

For class F fly ash dosage levels cement replaced with 35% of the SCM is an effective dosage while 20% is not an effective dosage mitigating the ASR in mortars. The cost effective dosage level of class F fly ash appears to be between 35% and 20% to reduce the expansion below 0.1% at 14 days. For ternary mixtures with different combinations of cement + slag + class F fly ash, the expansions vary above and below 0.1% at 14 days. Because these results are widely varying, another method is needed to determine a cost-effective dosage for ternary mixtures of the New Mexico aggregate.

Spratt aggregate:

Table 4.6 shows the proportions of SCMs used in the accelerated mortar bar tests for the Spratt reactive aggregate. Mixtures #2, #9 and #4 are binary mixtures of cement + slag combination with slag dosage levels of 70%, 50% and 35%, respectively. Mixtures

74
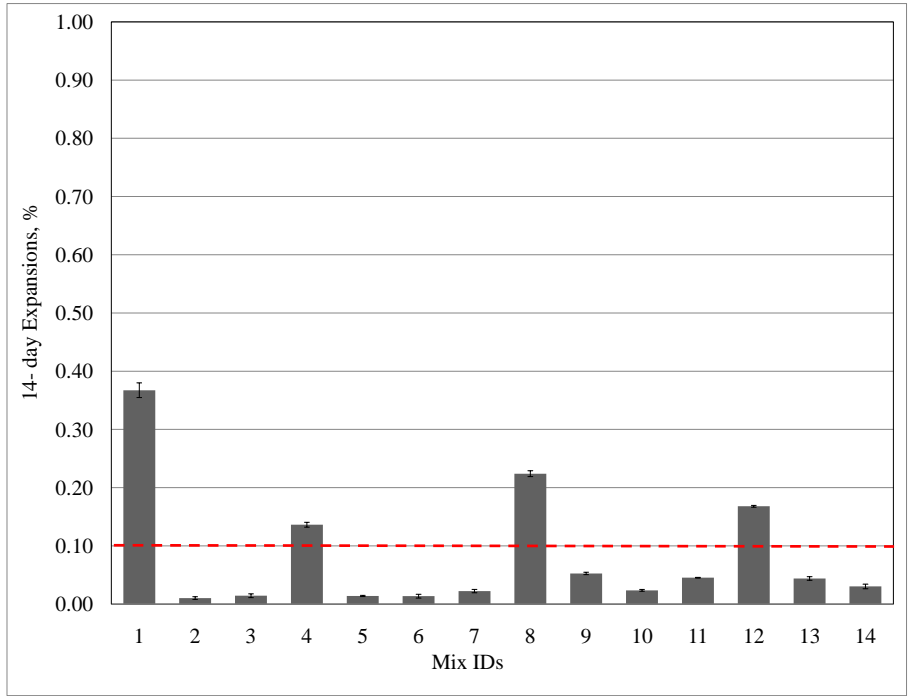
Figure 5.11: 14-day mortar bar expansions for Spratt aggregate

#5 and #8 are binary mixtures of cement + class F fly ash combination with class F fly ash dosage levels of 35% and 20%, respectively. Mixture #1 is the control sample containing no SCMs and all other mixtures are ternary mixtures of cement + slag + class F fly ash.

Figure 5.11 shows the 14-day mortar bar expansions of these Spratt aggregate mixtures with different SCMs, as this figure shows, the control sample prepared with Spratt aggregate has a 14-day mortar bar expansion of 0.37%, suggesting it is a highly reactive aggregate. The cement replaced by 70% and 50% of slag tend to have expansions below 0.1% at 14 days and, thus, appear to be effective dosages to mitigate ASR in mortars. The 35% slag dosage has 14-day mortar bar expansion above 0.1% and is not an effective dosage in mitigating ASR in mortars. These results suggest the cost effective dosage level of slag ranges between 50% and 35% to reduce the expansions below 0.1% at 14 days for the Spratt aggregate.

For class F fly ash dosage levels cement replaced with 35% of the SCM is an effective
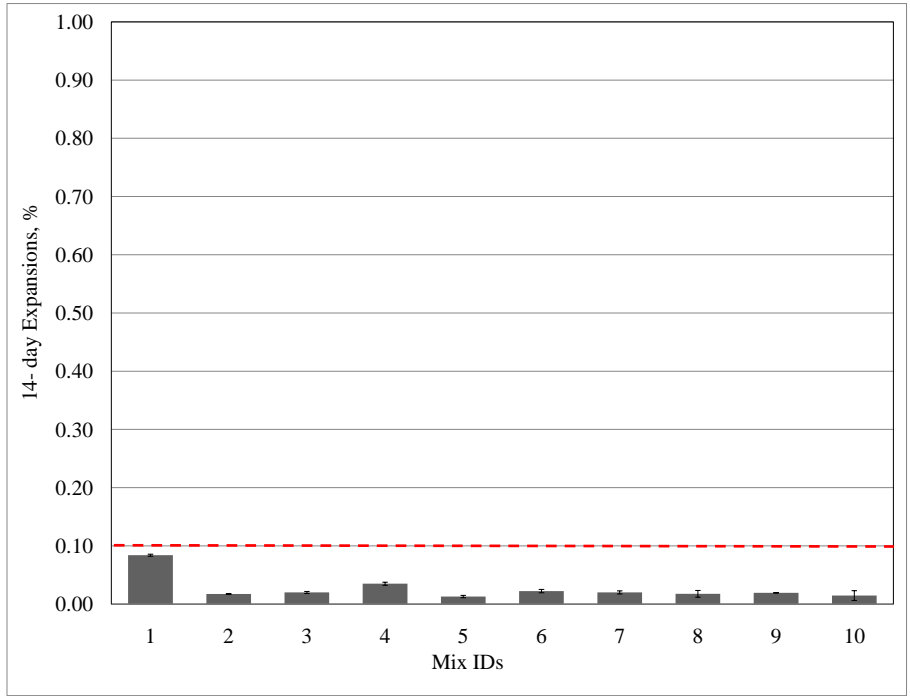
Figure 5.12: 14-day mortar bar expansions for Adairsville aggregate

dosage while 20% is not an effective dosage mitigating the ASR in mortars. The cost effective dosage level of class F fly ash appears to be between 35% and 20% to reduce the expansion below 0.1% at 14 days. For ternary mixtures with different combinations of cement + slag + class F fly ash, the expansions vary above and below 0.1% at 14 days. Because these results are widely varying, another method is needed to determine a cost-effective dosage for ternary mixtures of the Spratt aggregate.

Adairsville aggregate

Table 4.7 shows the proportions of SCMs used in the accelerated mortar bar tests for Adairsville aggregate. From figure 5.12 the control sample prepared with Adairsville aggregate has a 14-day mortar bar expansion of 0.08% which is less than 0.1%, these results suggest that, Adairsville aggregate is a non-reactive in nature. Figure 5.12 shows the 14-day mortar bar expansions of Adairsville aggregate mixtures with different SCMs. As seen in the figure, all the mixtures tend to have expansions below 0.1% at 14-days of testing.
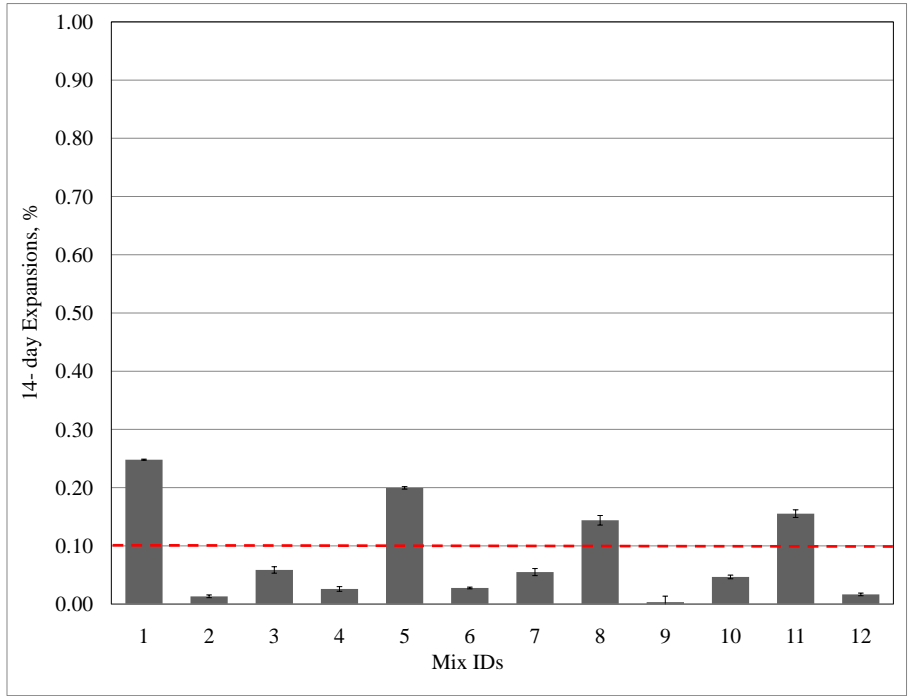
Figure 5.13: 14-day mortar bar expansions for Stocker sand

5.4.2 Investigation on Combinations of Cement, Class F and Class C Fly Ash

Binary combinations of cement + class F ash, cement + class C ash and ternary combinations of cement + class F ash + class C fly ash mixtures were studied using Stocker sand, a reactive gravel from Pittsburgh. Table 4.8 shows the proportions of SCMs used in the accelerated mortar bar tests for the Stocker reactive aggregate. Mixtures #2 and #4 are binary mixtures of cement + class F fly ash combination with fly ash dosage levels of 40% and 20%, respectively. Mixtures #3 and #5 are binary mixtures of cement + class C fly ash combination with class C fly ash dosage levels of 40% and 20%, respectively. The mixture #1 is the control sample containing no SCMs and all other mixtures are ternary mixtures of cement + class F fly ash + class C fly ash.

Figure 5.13 shows the 14-day mortar bar expansions of these Stocker sand mixtures with different SCMs, as this figure shows, the control sample prepared with Stocker sand has

77

a 14-day mortar bar expansion of 0.25%, suggesting it is a moderately reactive aggregate. The cement replaced by 20% class F fly ash tend to have expansions below 0.1% at 14 days and, thus, appear to be effective dosages to mitigate ASR in mortars. For class C fly ash, the cement replaced by 20% ash was not effective in mitigating ASR, whereas the 40% fly ash dosage appeared to be effective dosage to mitigate ASR in mortars.

5.5 Simplex-Centroid Design (SCD)

Henry Scheffe's simplex-centroid design model with seven design points was used to develop prediction equations and response surfaces for the test parameters of the concrete mixtures. Equation 5.1 is shown below:

$$y = \beta 1 x_1 + \beta 2 x_2 + \beta 3 x_3 + \beta 4 x_1 x_2 + \beta 5 x_2 x_3 + \beta 6 x_1 x_3 + \beta 7 x_1 x_2 x_3 \tag{5.1}$$

where, x_1, x_2, x_3 are the mixtures components cement, slag and fly Ash, respectively; and β is the coefficient that generates the response surface for any given performance parameter "y". Once the model was generated its predictability power was validated. Five additional points were chosen in the simplex region and tested experimentally with the actual test values comparing them with the values predicted from the simplex-centroid design model to validate the model.

5.5.1 Model Validation

To validate the simplex-centroid design model five data points within the simplex region were tested. Three approaches were adopted to measure how well the model predicted the new data points:

1. The first approach estimated the squared correlation (R^2) of the actual and predicted values bivariate fit, with the R^2 close to 1 being more accurate.

2. The second approach estimated the slope ($\Delta Actual$ / unit $\Delta Predicted$), with the slope close to 1 being more accurate. An interval estimate of slope was used to determine if the slope was significantly different from 1.

3. The third approach involves a visual assessment comparing these fitted actual vs. their predicted line to the line of equality (slope = 1). This assessment shows the prediction ability (either under or over) of the fitted actual vs. the predicted line with respect to the line of equality.

The prediction equation models and response surfaces were developed using the simplex-centroid design Equation 5.1 for different fresh and harden properties of concrete mixtures. Seven design points were used to develop prediction equations for test parameters of the concrete mixtures and five additional points were used to validate the prediction power of the models. Iso-contour response surfaces were created using the prediction models for various concrete properties. The JMP statistical software was used for analysis and validation purpose in this study.

5.6 The Model of Fresh Concrete Properties

The Fresh properties of concrete, slump, percent air content and unit weight, were determined based on ASTM C143, C231 and C138, respectively. Using these standard test results, the prediction models of fresh concrete properties were developed. Equation 5.2 shows the concrete slump model, Equation 5.3 the concrete percent air content model and equation 5.4 the concrete unit weight model.

$$y = 5x_1^* + 4.5x_2^* + 4.23x_3^* + 7x_1^*x_2^* + 3.54x_2^*x_3^* + 10.54x_1^*x_3^* - 38.04x_1^*x_2^*x_3^* \qquad (5.2)$$

$$y = 2.6x_1^* + 1.9x_2^* - 0.69x_3^* + 4.2x_1^*x_2^* + 0.98x_2^*x_3^* + 5.58x_1^*x_3^* - 10.13x_1^*x_2^*x_3^* \qquad (5.3)$$

$$y = 139.23x_1^* + 136.01x_2^* + 151.54x_3^* - 9.48x_1^*x_2^* - 28.7x_2^*x_3^* - 32.2x_1^*x_3^* + 77.19x_1^*x_2^*x_3^* \quad (5.4)$$

where,

$$x_1^* = \frac{x_1 - 0.3}{0.7}, \quad x_2^* = \frac{x_2}{0.7}, \quad x_3^* = \frac{x_3}{0.7} \qquad (5.5)$$
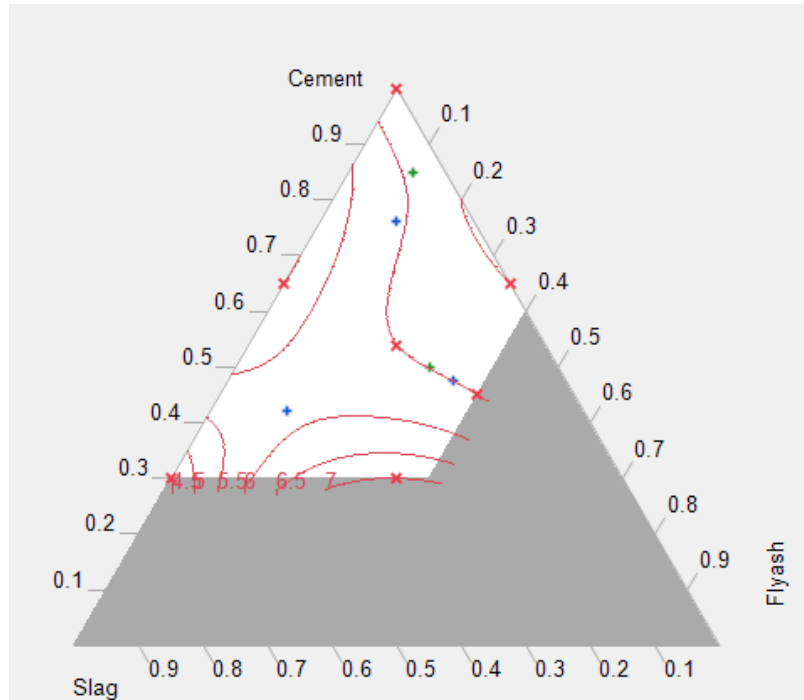
Figure 5.14: Iso-contour response surface for concrete slump (in.)

5.7 The Model of Hardened Concrete Properties

5.7.1 Compressive Strength Model

The compressive strength model was developed using the results obtained from ASTM C39 test. Equations 5.6 and 5.7 show the compression strength prediction models for concrete cylinders at 28-day and 56-day age respectively.

$$y = 6142x_1^* + 4989.6x_2^* + 5330.7x_3^* + 3768.6x_1^*x_2^* - 4257.4x_2^*x_3^* - 3010.1x_1^*x_3^* + 4409.5x_1^*x_2^*x_3^*$$

$$(5.6)$$

$$y = 6285x_1^* + 5739x_2^* + 3301.4x_3^* + 6436x_1^*x_2^* + 3307.2x_2^*x_3^* + 3263.2x_1^*x_3^* + 16610.5x_1^*x_2^*x_3^* \quad (5.7)$$

These equations were subsequently used to predict the compressive strength values for the 5 additional concrete mixtures chosen from the simplex region. The actual test result values

81
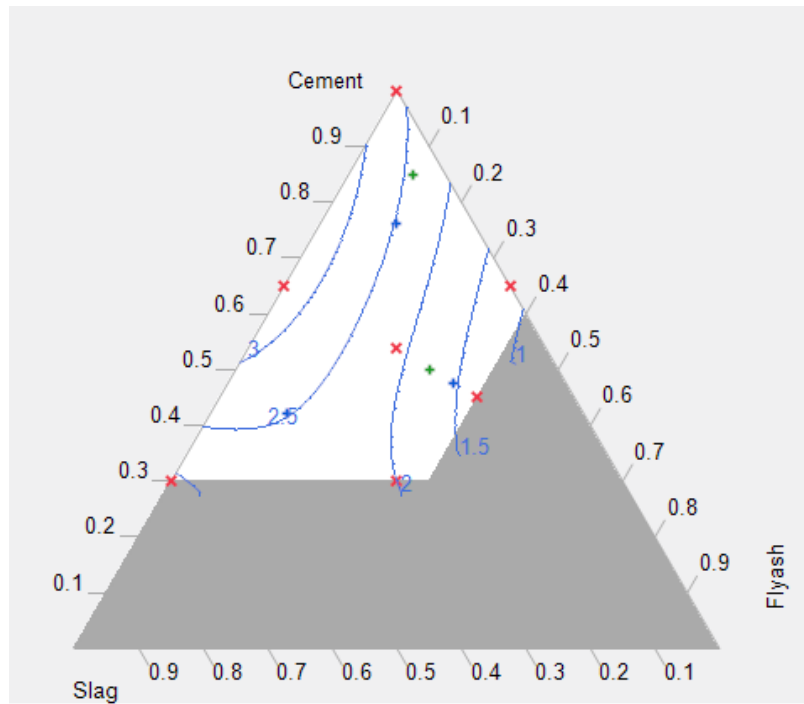
Figure 5.15: Iso-contour response surface for percent air content of concrete
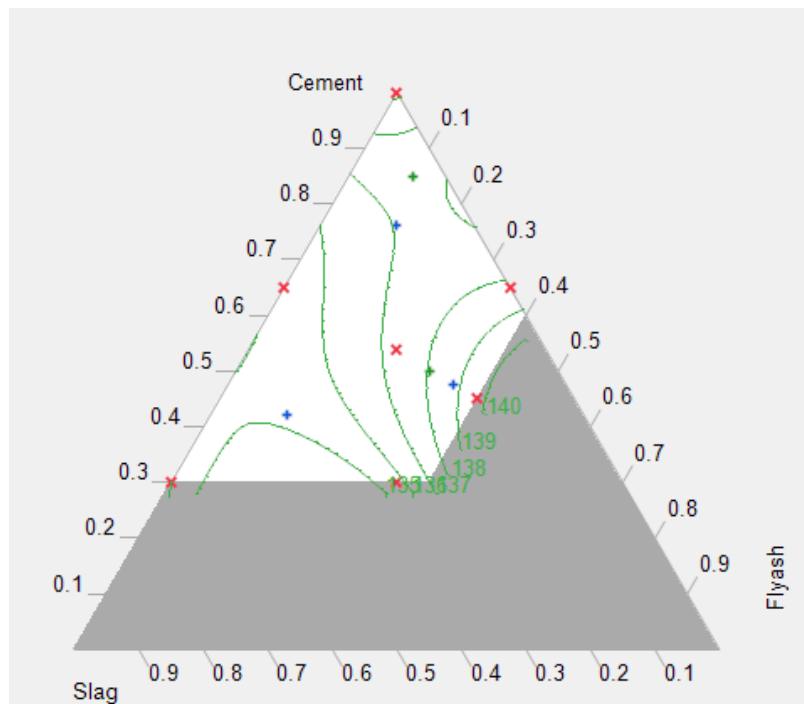
Figure 5.16: Iso-contour response surface for unit weight of concrete (pcf)

were compared with the predicted values to validate the model. Figure 5.17 shows the bi-variate fit plot of actual vs. predicted compressive strength values for the 5 concrete mixtures. For the 28-day age of concrete, the bi-variate fit is good as $R^2 = 0.93$ and the interval estimate of slope has 1 within the interval range. The visual inspection of the bi-variate fit w.r.t. the line of equality shows that the compressive strength model under predicts the strength values to 5300 psi and over predicts the values above that strength. For 56-day age compressive strength model of concrete, the bi-variate fit is good as the $R^2 = 0.88$ and the interval estimate slope = 1, the visual inspection shows that the model under predicts the values to 7100 psi.

Based on these observations the compressive strength model can be used to predict compressive strength values within the simplex region for different proportions of cement, slag and Class F fly ash.

The compressive strength design model was used to develop response surfaces within the simplex design region, the iso-contour compressive strength response surfaces created being shown in Figure 5.18. These iso-contours indicates the change in compressive strength values for the mixtures along the contour lines.

5.7.2 Split Tensile Strength Model

The split tensile strength model was developed using the results obtained from ASTM C496 test. Equation 5.8 shows the split tensile strength prediction model for concrete cylinders at 56-day age of testing:

$$y = 680x_1^* + 621x_2^* + 90.1x_3^* + 314x_1^*x_2^* + 559.78x_2^*x_3^* + 1185.78x_1^*x_3^* + 1317.22x_1^*x_2^*x_3^* \tag{5.8}$$

This equation was used to predict the split tensile strength values for 5 additional concrete mixtures chosen from within the simplex region. The actual test result values were subsequently compared with the predicted values to validate the model. Figure 5.19 shows the bi-variate fit plot of actual vs. predicted split tensile strength values for the 5 concrete
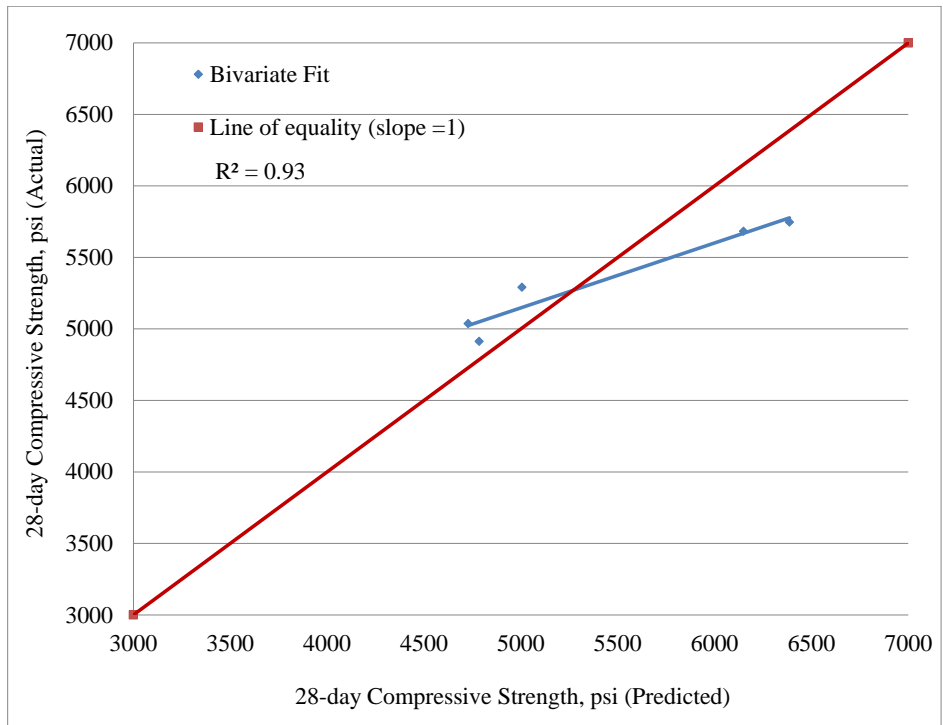
(a) 28-day
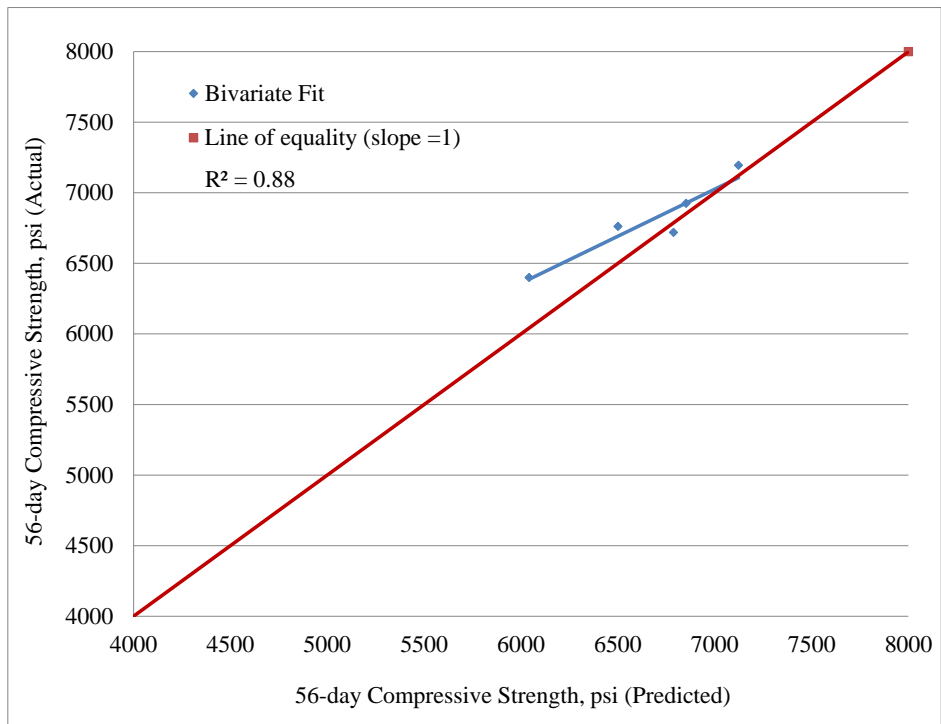
(b) 56-day

Figure 5.17: Actual vs. Predicted fit for compressive strength
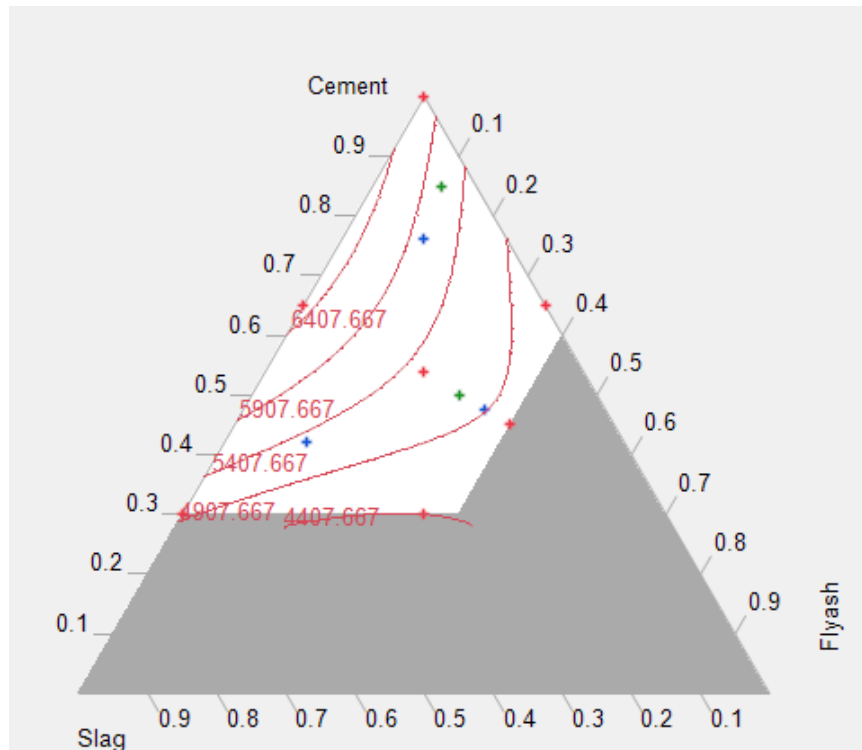
(a) 28-day
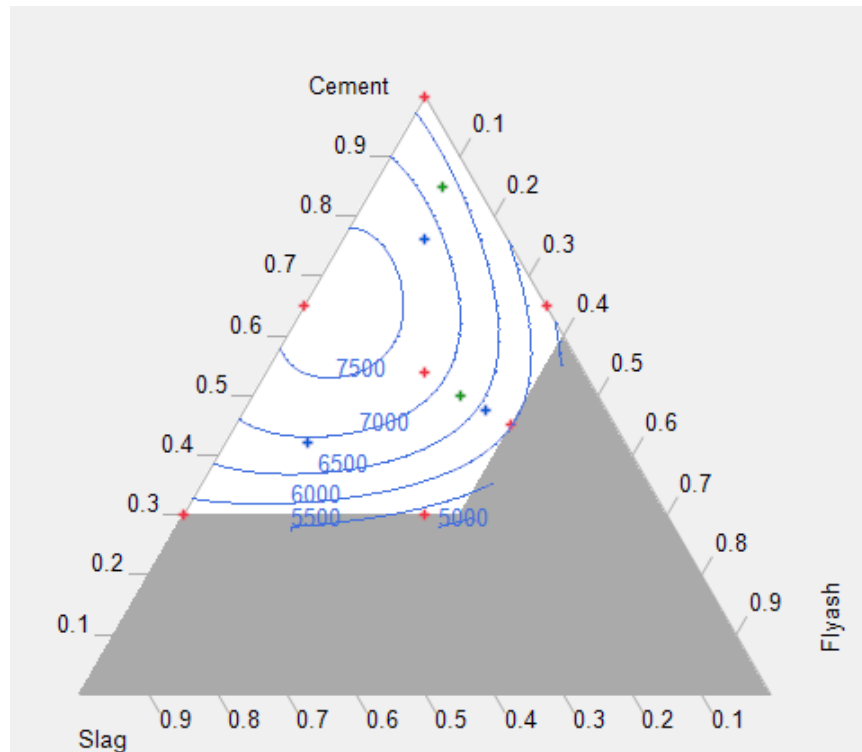
(b) 56-day

Figure 5.18: Iso-contour response surface for compressive strengths (psi)

85
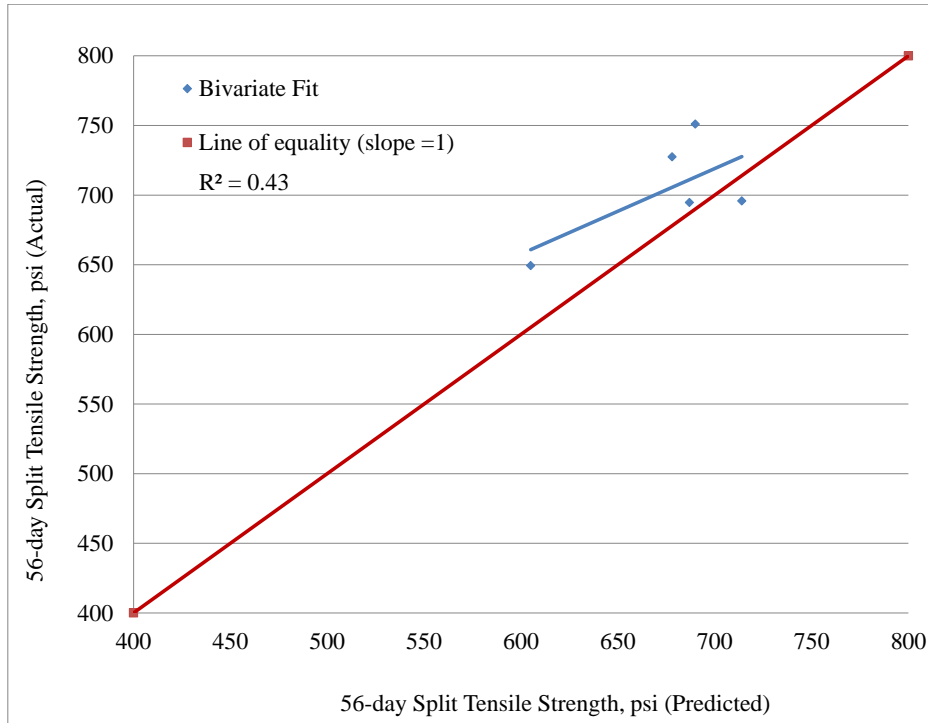
Figure 5.19: Actual vs Predicted fit for 56-day split tensile strength

mixtures in the simplex region. The visual inspection of the bi-variate fit w.r.t. the line of equality shows that the split tensile strength model under predicts the split tensile strength values. As the results suggest, the bi-variate fit is not good because of the $R^2 = 0.43$, whereas the interval estimate of slope has 1 in its range.

Based on these observations, the split tensile strength model cannot be used to predict tensile strength values within the simplex region because the sensitivity of the test procedure for yielding tensile strength values is not consistent. The values obtained from actual testing are low in magnitude and the difference in tensile strength values is not high as evidenced by the low R^2 from bi-variate fit.

5.7.3 Rapid Chloride-Ion Permeability Model

The rapid chloride ion permeability model was developed using the results obtained from ASTM C1202 test. Equation 5.9 shows the rapid chloride ion permeability prediction
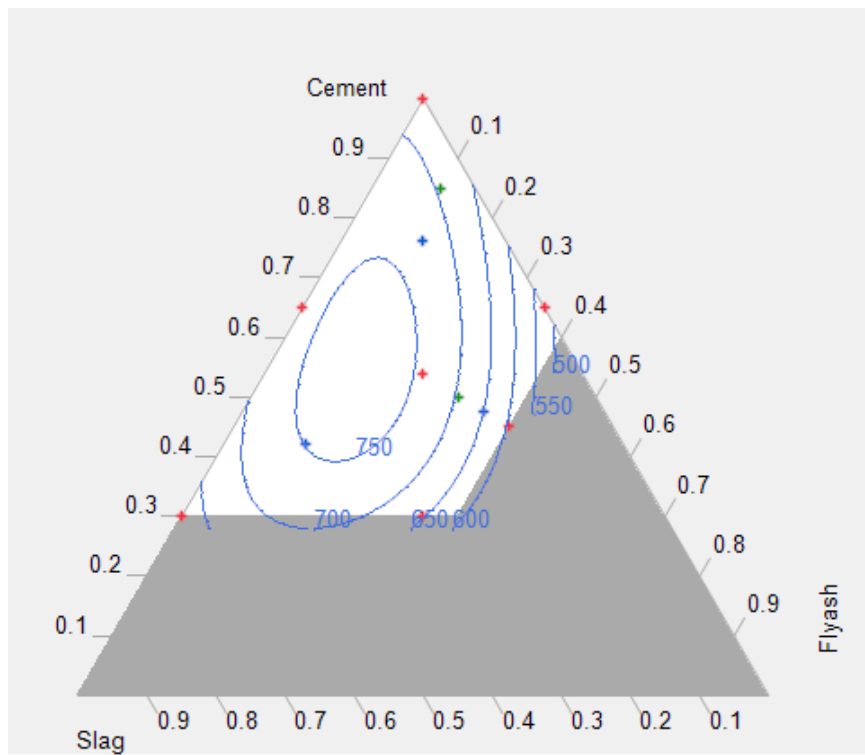
Figure 5.20: Iso-contour response surface for split tensile strengths (psi)
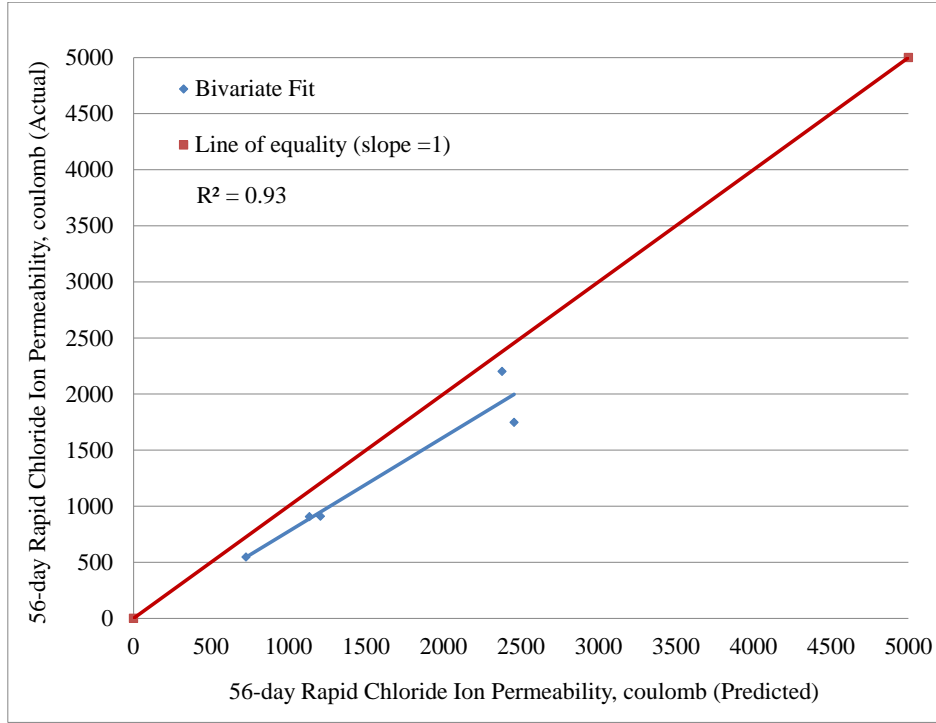
Figure 5.21: Actual vs Predicted fit for rapid chloride ion permeability at 56-day

model for concrete cylinders at 56-day age of testing.

$$y = 3002x_1^* + 455x_2^* + 1366.67x_3^* - 2034x_1^*x_2^* - 2241.33x_2^*x_3^* - 1807.33x_1^*x_3^* - 136.63x_1^*x_2^*x_3^*$$

(5.9)

This equation was used to predict the rapid chloride ion permeability values for the 5 additional concrete mixtures chosen from the simplex region. The actual test result values were compared with the predicted values to validate the model. Figure 5.21 shows the bi-variate fit plot of actual vs. predicted split tensile strength values for the 5 concrete mixtures in the simplex region. At 56-day age of testing, the bi-variate fit is good as the $R^2 = 0.93$ and the interval estimate of slope has 1 within the interval range. The visual inspection of the bi-variate fit w.r.t. the line of equality shows that the rapid chloride ion permeability model consistently over predicts the chloride-ion permeability values.

Based on these observations, the rapid chloride ion permeability model can be used to predict chloride ion permeability values within the simplex region for different proportions
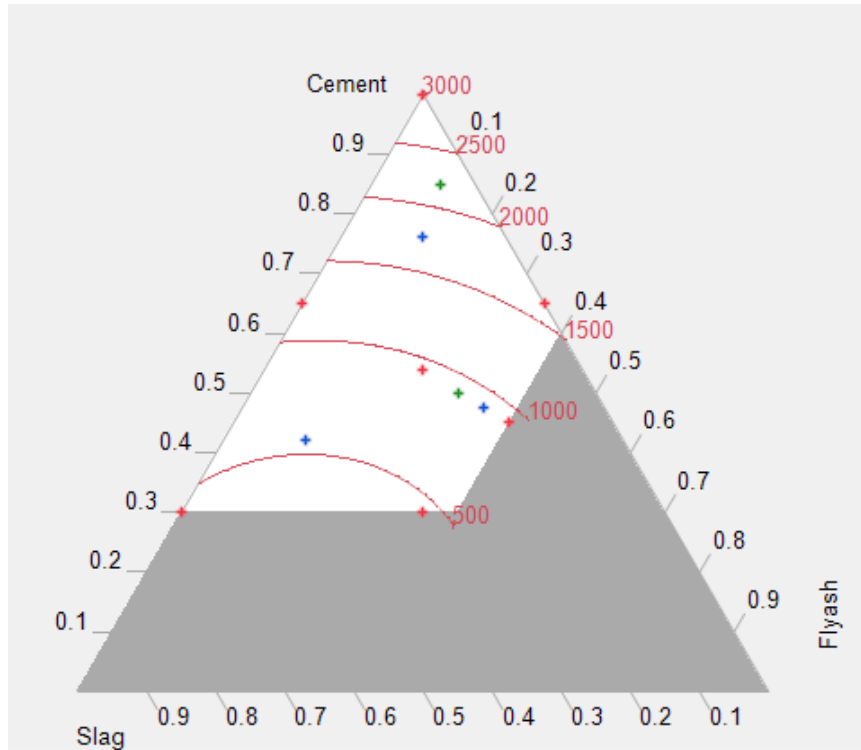
Figure 5.22: Iso-contour response surface for rapid chloride ion permeability (coulombs)

of cement, slag and Class F fly ash. However, care should be taken while using these values for designing concrete mixtures because of its over prediction. Once the mix design proportions are chosen, the ASTM C1202 test should be conducted to verify the chloride-ion permeability values of concrete mixtures to meet the requirements.

The rapid chloride ion permeability design model was used to develop response surfaces within the simplex design region with the resulting iso-contour coulomb response surfaces being shown in Figure 5.22. These iso-contours indicate the change in the rapid chloride ion permeability values for the mixtures along the contour lines.

5.7.4 Miniature Concrete Prism Test ASR Expansions Model

The ASR expansion model was developed using the results obtained from the Miniature Concrete Prism Test. Equation 5.10 shows the ASR expansion prediction model for
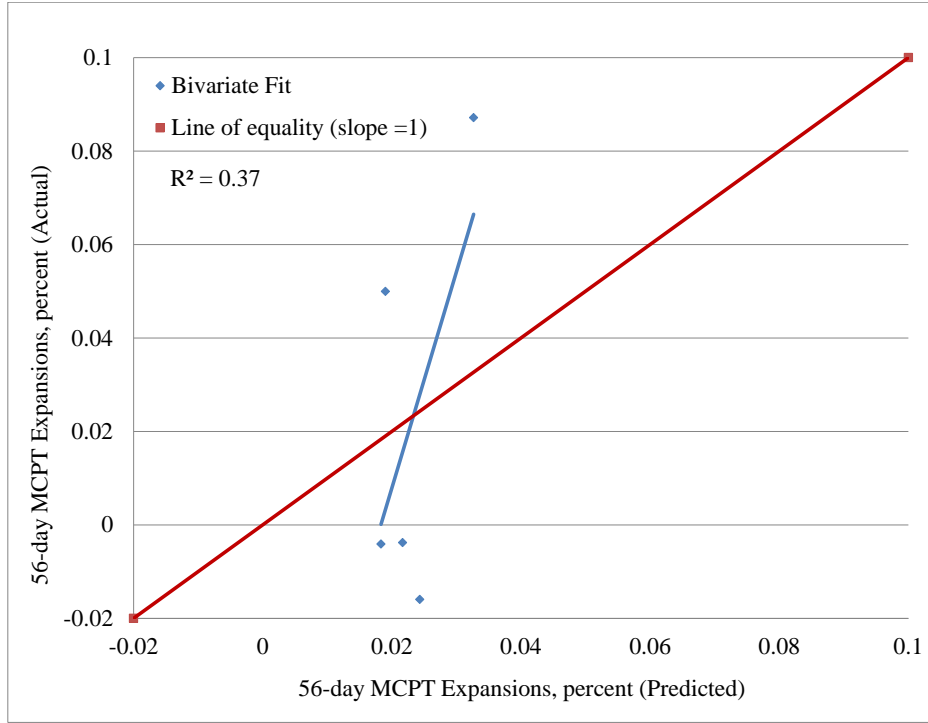
Figure 5.23: Actual vs Predicted fit for MCPT expansions at 56-day

the concrete cylinders at 56-day age of testing.

$$y = 0.186x_1^* - 0.008x_2^* + 0.05x_3^* - 0.316x_1^*x_2^* - 0.456x_2^*x_3^* - 0.116x_1^*x_3^* + 0.565x_1^*x_2^*x_3^* \quad (5.10)$$

This equation was used to predict the ASR expansion values for the 5 additional concrete mixtures chosen from the simplex region. The actual test result values were compared with the predicted values to validate the model. Figure 5.23 shows the bi-variate fit plot of the actual vs. predicted ASR expansion values for the 5 concrete mixtures in the simplex region. While the interval estimate of slope has 1 within the interval range, the bi-variate fit is not good because the $R^2 = 0.37$. This model cannot be validated by comparing the actual test result values with the predicted values because the expansion values obtained from the MCPT test are low.

The deleterious effects of alkali-silica reaction in concrete were evaluated using a threshold expansion limit of 0.04% at 56-day of testing. As Figure 5.9(b) indicates, all the
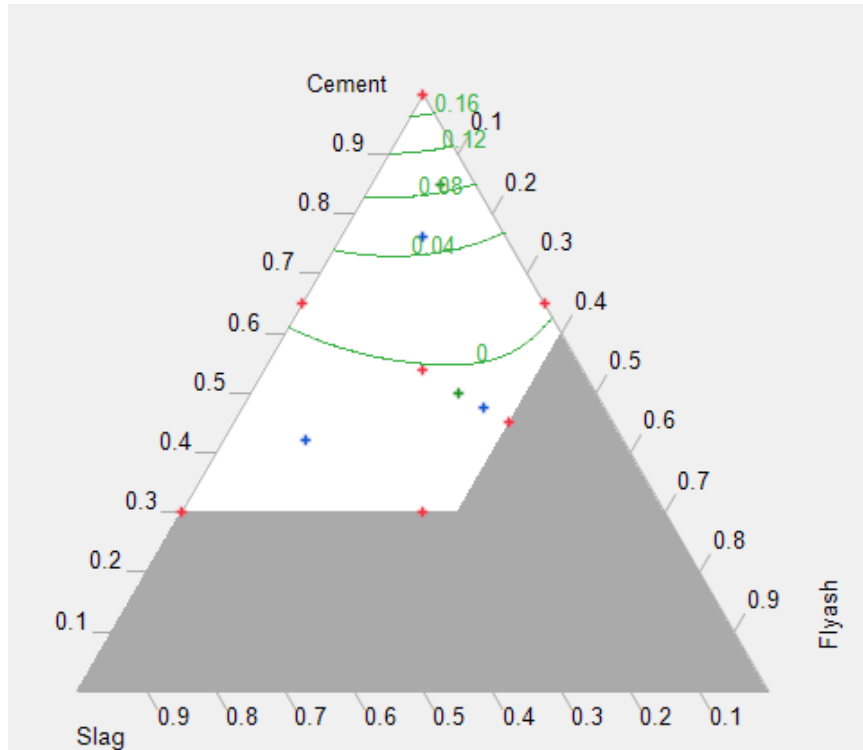
Figure 5.24: Iso-contour response surface for MCPT expansions (percent)

mixtures are within this expansion limit, however, they should be verified by testing in lab to check for possible expansion of the concrete mix to meet the requirements.

The ASR expansion model was used to develop response surfaces within the simplex design region with the iso-contour expansion response surfaces being shown in Figure 5.24. The iso-contours give an indicate the change in ASR expansion values for mixtures along the contour lines. These evaluations indicated that the mixtures below the threshold expansion contour in the simplex region did not show any alkali-silica reaction distress.

5.7.5   Mortar Bar ASR Expansions Model

The deleterious effects of alkali-silica reaction in mortar were evaluated using a threshold expansion limit of 0.1% at 14-day of testing in the ASTM C1567 test method as shown in Figure 5.25. These evaluations indicated that the mixtures below the threshold expansion contour in the simplex region did not show any alkali-silica reaction distress. As
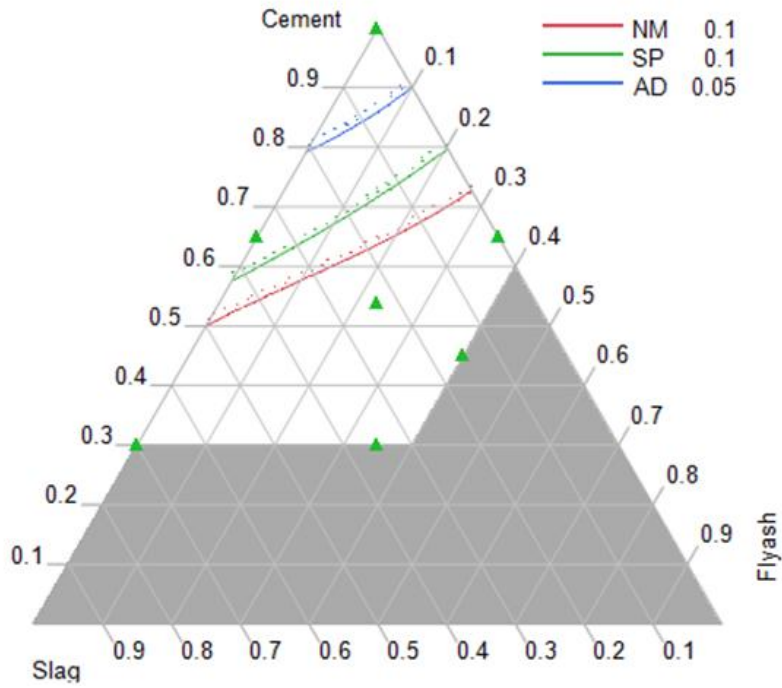
Figure 5.25: Iso-contour response surface for mortar bar expansions with different aggregates (percent)

seen in figure, the proportions of SCMs vary with the reactivity of aggregates. For highly reactive aggregates, higher SCM dosages are required to suppress the mortar bar expansions below 0.1% threshold.

5.8 Studies on Cementitious Paste Systems

5.8.1 Pore Solution Analysis

The pore solution obtained from different cementitious paste systems were analyzed for ionic concentrations. The pore solution was extracted from cementitious paste samples at different ages. The 0-day sample represents the pore solution of fresh cement paste extracted at 45±10 minutes after casting. The 7-day and 56-day samples represents their respective ages kept at room temperature. The 56T-day samples represents the 56-day age of sample cured at elevated temperature 60 °C. The ion concentrations were determined using ICP method and major cations (Na^+, K^+, Ca^{++}) and anions (S^{--}, OH^-) that dominate the pore solution composition were reported. The OH^- ion concentration was determined using potentio-metric titrations, by titrating the pore solution against H Cl solution. Figure 5.26 shows an example titration curve of 100% cement sample kept in room temperature for 56-days. From the titration curve the volume of H Cl required to neutralize the pore solution at pH = 7 is used to calculate the OH^- ion concentration. It is also observed that the titration curve at the starting point of reaction has pH $\approx$ 11.5, this is due to the dilution effect of pore solution by 100 times. Thus when the diluted solution values were back calculate to their original concentrations the pH $\approx$ 13.8, this confirms the known fact that the pH of pure cement samples is close to 14.

Table 5.4 shows the molar concentrations of ions present in cementitious paste systems kept at 60 °C for 56-days.

Table 5.4: Molar concentrations of ions present in cementitious paste systems

Cement	Slag	Fly ash	Na^+	K^+	Ca^{++}	S^{--}	OH^-
1	0	0	0.537926	0.463534	0.004292	0.275927	0.3584168
0.3	0.7	0	0.04515	4.25E-05	8.66E-05	0.000695	0.08828
0.45	0.15	0.4	0.101784	0.109679	0.000393	0.06879	0.050761
0.65	0.35	0	0.021314	0.02394	0.010055	0.011383	0.2207
0.65	0	0.35	0.26042	0.273733	0.00121	0.053485	0.300152
0.3	0.35	0.35	0.102432	0.103079	0.001325	0.063873	0.070624
0.54	0.23	0.23	0.182494	0.174386	0.00134	0.081244	0.167732
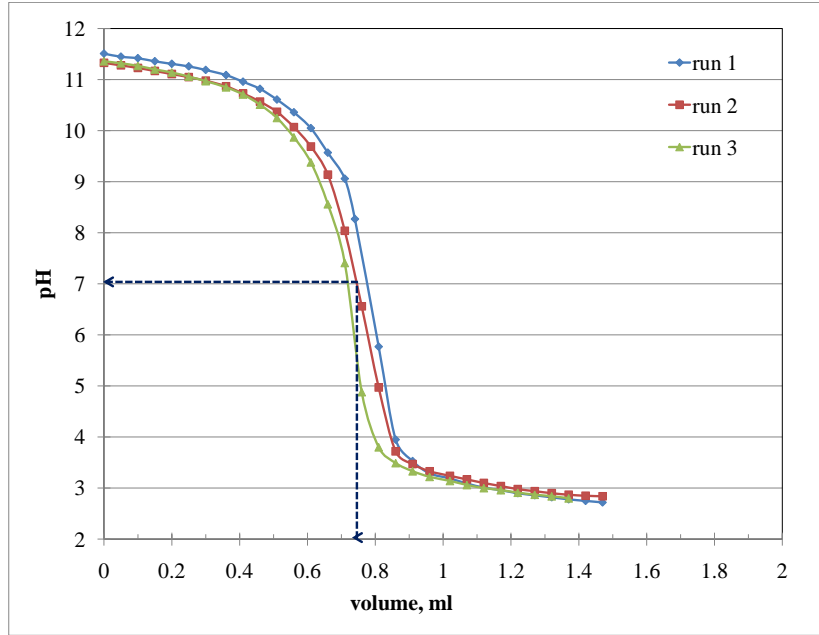
Figure 5.26: Potentiometric titration of pore solution from pure cement paste sample at 56 days

Figure 5.27 shows the ion concentrations of 100% cement paste sample at different ages. At 0-days, in the initial 45 minutes when the cement paste is mixed with water the alkalis (Na^+, K^+) present on the cement grains dissolve into the water. The gypsum ($CaSO_4.2(H_2O)$) also dissolves into the water and dissipates sulfate (SO_4^{-2}) ions into the system. After this initial reaction all the cations and anions are suspended in a hydrous solution and are at equilibrium forming the pore solution. As the hydration reaction continues the sulfate ions gets trapped in the cement hydration products forming the calcium sulfoaluminate (ettringite, monosulfate) phases. In order to maintain the equilibrium in pore solution composition, the hydroxyl (OH^-) ions comes into the solution forming NaOH and KOH solution.

In Figure 5.27 the phenomenon of forming NaOH and KOH solution is observed at 7-days and 56-days respectively, the Na^+, K^+ ions are neutralized mainly by OH^- ions and very less amount of SO_4^{-2} ions are present in the pore solution system. At elevated temperatures for cement paste samples kept in 60 °C up to 56-days, the (SO_4^{-2}) ions come
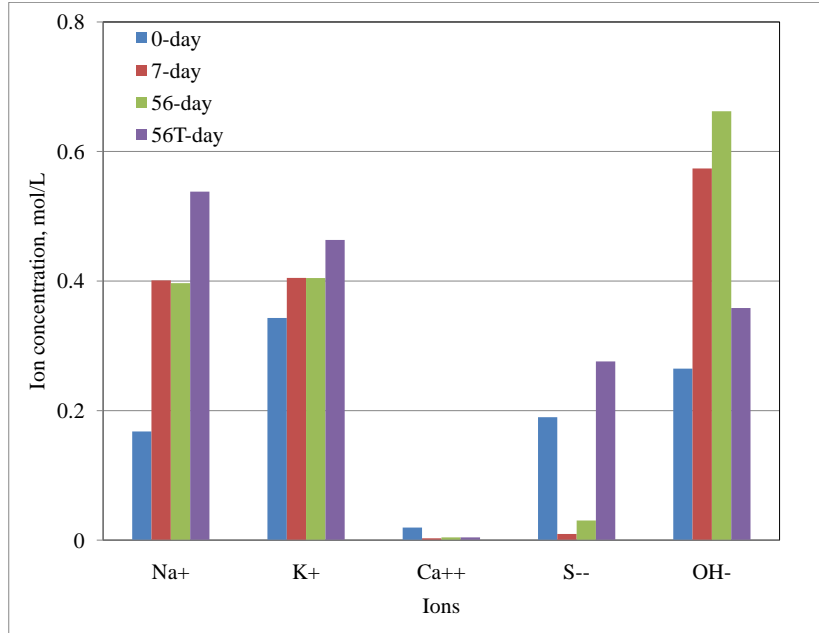
Figure 5.27: Ion concentrations for 100% cement sample

back into the pore solution. At elevated temperatures the instability of calcium sulfoaluminate phases takes place and SO_4^{-2} ions dissolve back into the pore solution system. The OH^- ion concentration is also reduced as the SO_4^{-2} ions provide the negative charge to neutralize the cations. This observation is an important out come of this research study.

Figures 5.28 to 5.33 show the ion concentrations for cementitious paste systems with binary and ternary combinations of cement, slag and class F fly ash. The ionic concentrations decrease with the increase in cement replacements levels with SCMs, thus it is evident that SCMs do not contribute towards the composition of pore solution. From Figures 5.28 to 5.33 it is also observed that in most cases when cement is replaced with SCMs the alkalinity of pore solution also reduces, this is due to the pozzolanic reactivity of SCMs. At 7-day and 56-day age the Na^+, K^+ ions concentration is decreasing and simultaneously the OH^- ion concentration required to neutralize the Na^+, K^+ ions is also decreasing. This phenomenon is not observed in 100% cement paste sample (Figure 5.27), with pozzolanic reaction the alkali ions get trapped in to the secondary C-S-H gel and the pore solution
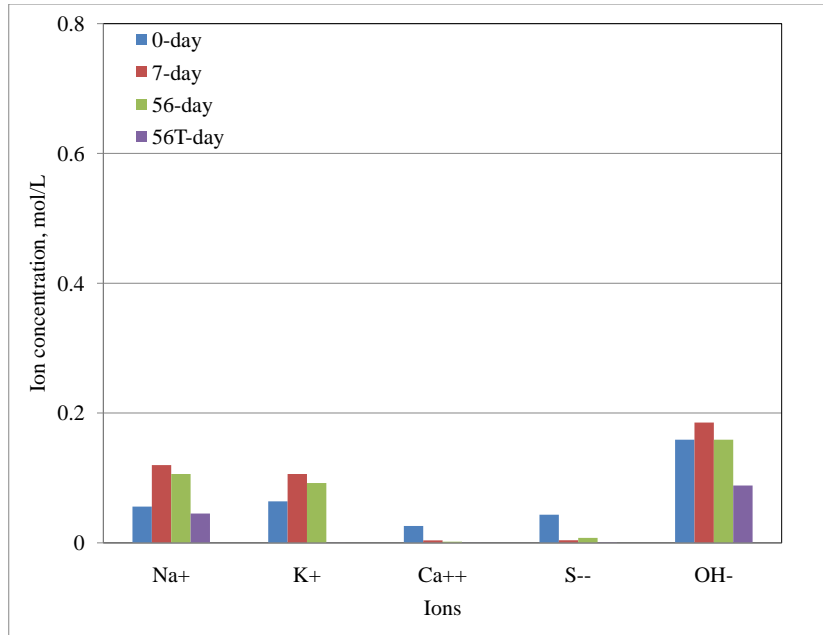
Figure 5.28: Ion concentrations for 30% cement + 70% slag sample
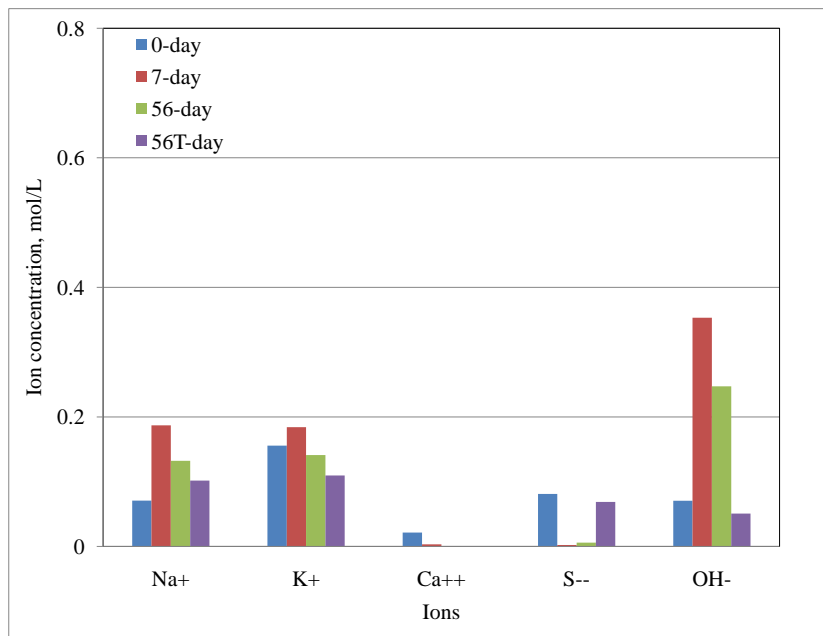
Figure 5.29: Ion concentrations for 45% cement + 15% slag + 40% fly ash sample

96
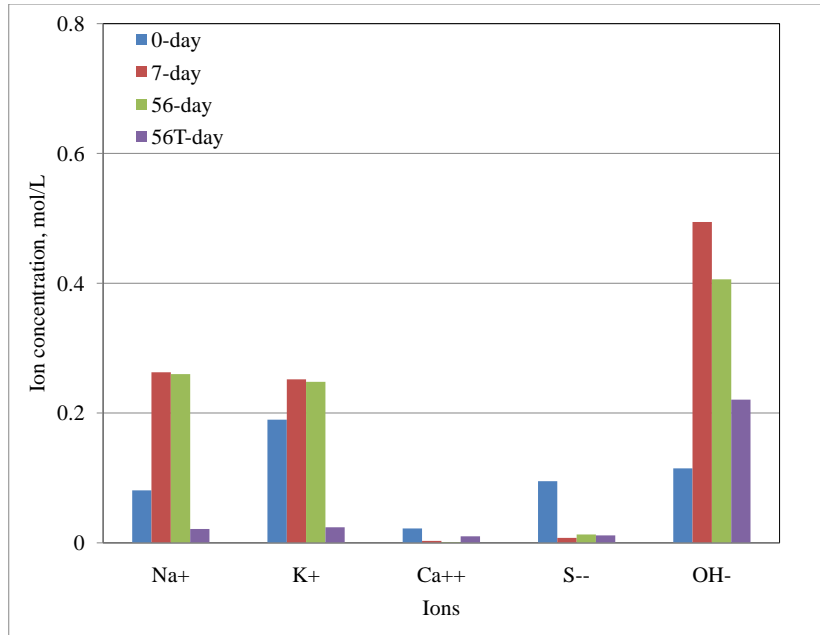
Figure 5.30: Ion concentrations for 65% cement + 35% slag sample
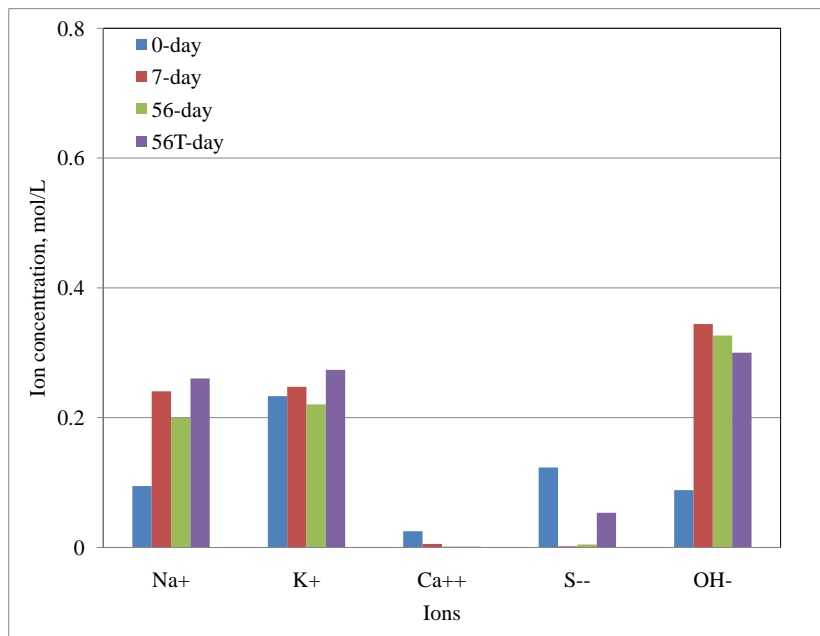
Figure 5.31: Ion concentrations for 65% cement + 35% fly ash sample
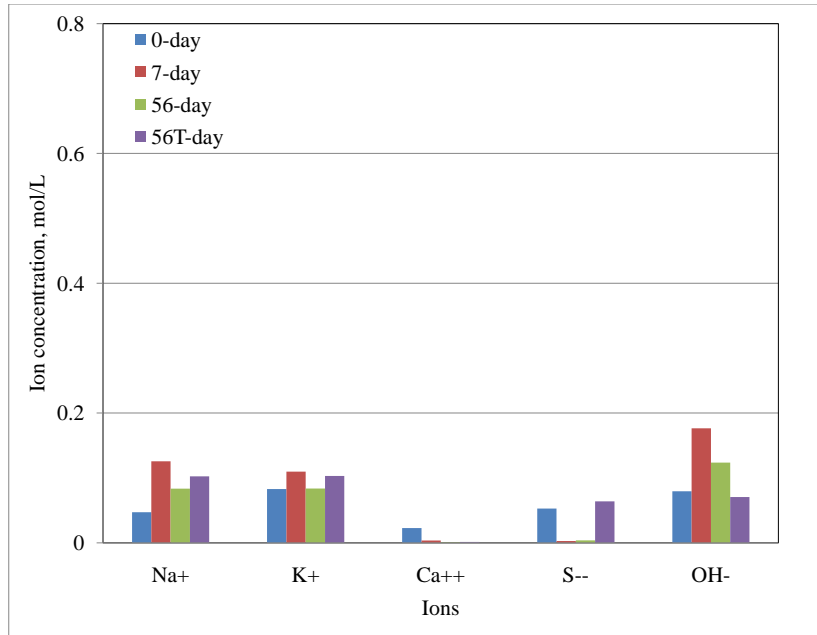
Figure 5.32: Ion concentrations for 30% cement + 35% slag + 35% fly ash sample
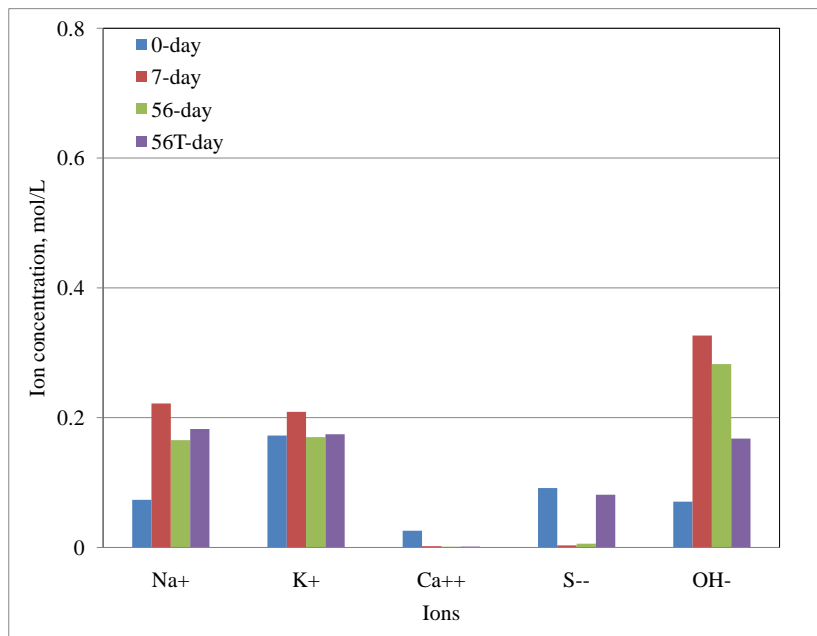
Figure 5.33: Ion concentrations for 54% cement + 23% slag + 23% fly ash sample

alkalinity is reduced. At elevated temperatures (56T-day) due to the instability of calcium sulfoaluminate phases the SO_4^{-2} ions dissolve back into the pore solution. Due to increased negative charge in pore solution there is a possibility that the loosely held Na^+, K^+ ions in secondary C-S-H gel can dissolve back into the pore solution to maintain the equilibrium.

Figure 5.34 shows the change in ionic concentrations for different cementitious paste systems compared to the MCPT expansions at 56-day of testing. From the Figure 5.34 it is evident that as the sodium (Na^+) and hydroxyl (OH^-) ion concentrations increase, the MCPT expansions also increases.

5.8.2 Electrical Resistivity of Cementitious Paste Systems

The EIS technique was used to measure the electrical resistivity of the cementitious paste systems, the results being shown as see in Figure 5.35 indicate that SCMs increase the resistivity of cementitious paste. While the resistivity of pure cement remains constant after 28-days of testing, in increases with age for the binary mixtures of cement + slag and for cement + fly ash. However, after 90 days, the resistivity of slag mixtures stabilize while the resistivity of fly ash ones continue to increase. The ternary blend combination of cement + slag + fly ash, shows the highest resistivity at 120-days of testing. In these ternary combinations, the negative effects of binary mixtures are compensated by further decreasing the conductivity of cementitious paste systems.

From the observations made in pore solution studies, it is evident that SCMs reduce the pore solution ionic concentrations. The reason for this increase in the resistivity is due to the reduction of the ionic concentration of pore solution caused by the SCMs as supported by in pore solution studies.
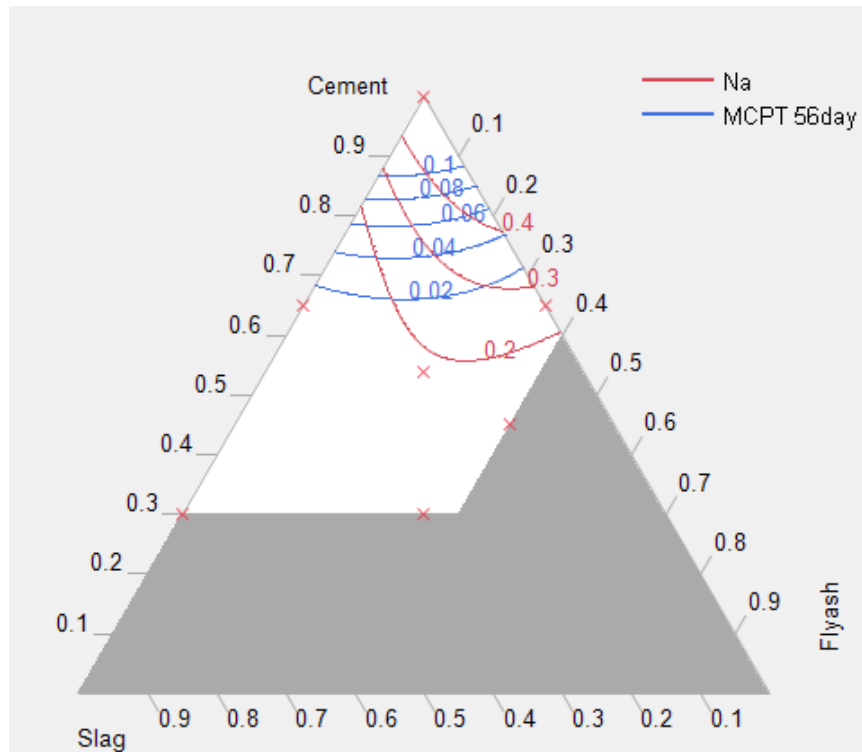
(a) Na^+ ion (mol/L)
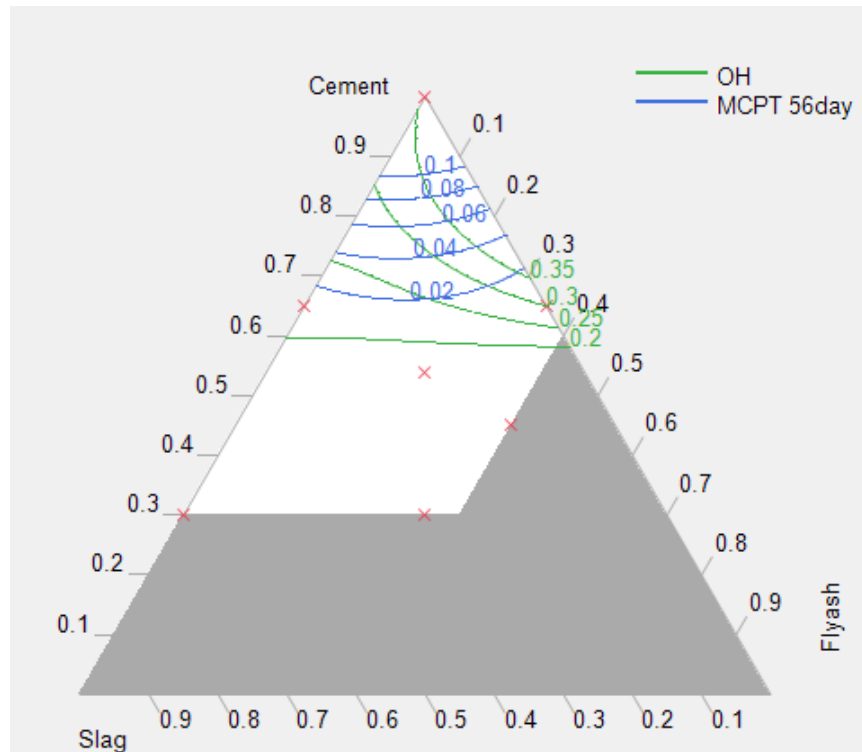
(b) OH^- ion (mol/L)

Figure 5.34: Iso-contours for Ionic concentrations vs. 56-day MCPT expansions
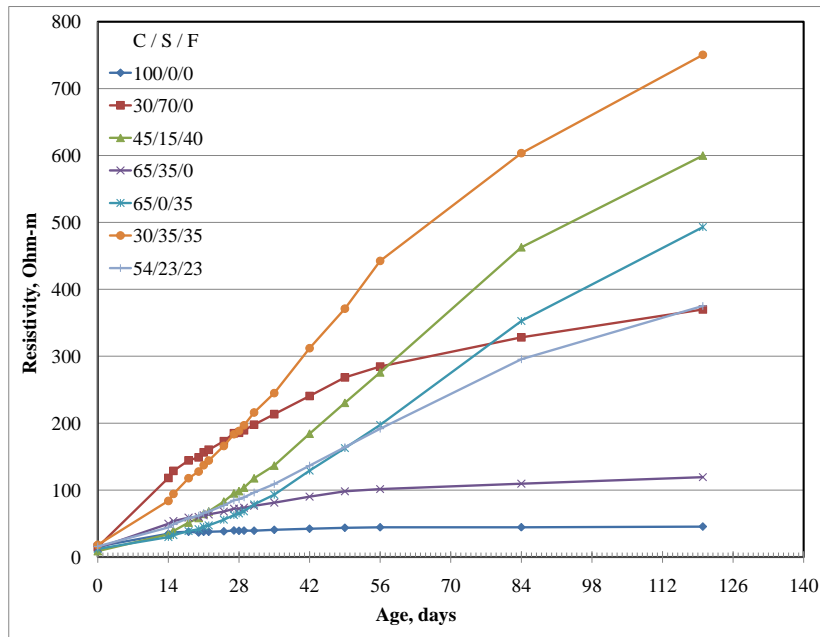
Figure 5.35: Electrical resistivity of cementitious paste systems (ohm-m)

5.9 Response Surface Methodology for Optimizing SCM Proportions of Concrete Mixtures

Response surfaces were generated using JMP statistical software for concrete properties using the performance prediction models. To optimize the SCM proportions in concrete, various response surfaces were selected and overlapped on the simplex triangle. Threshold contour curves were plotted to meet the desired concrete properties within this simplex triangle and an optimum region was found. The SCM proportions falling within this region would meet the specification requirements for desired concrete mixture properties.

The results of the response surface methodology to optimize SCM proportions are illustrated below using examples of concrete as used in concrete industry:

EXAMPLE 1: Driveway Concrete

The requirements of driveway concrete are low cost and adequate strength to withstand the load of vehicles. Typical driveway concrete requirements are listed below:

- Compressive Strength: 3000 psi

- Slump: 4 inches

- Air Content: 2.5% (6% for F-T conditions)

- Cost: Lower the better

Figure 5.36 shows the response surface methodology of optimum SCM proportions for driveway concrete in unshaded area of the simplex triangle.

EXAMPLE 2: Highway Pavements

The requirements of a highway pavement concrete is low slump and adequate strength to withstand the load of vehicles moving. Durability is a major concern for such pavement

Response		Contour	Current Y	Lo Limit	Hi Limit
Slump		4	6.4816597	4	.
Air %		1	2.2317907	2	.
56-day Comp		.	6071.1333	3000	.
RCPT 56day		3500	429.30096	.	.
ASR 56day		0.2	-0.013783	.	.
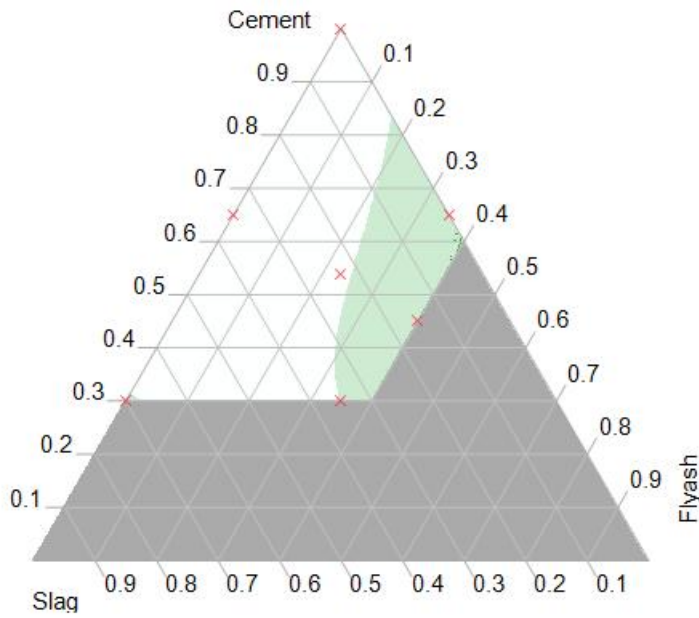
Figure 5.36: Unshaded Area Showing Optimum Mixture Proportions for Driveway Concrete

because it is subjected to both physical and chemical deterioration with moving traffic and adverse environmental conditions:

- Compressive Strength: 4000 psi

- Slump: 0.5 to 1 inch

- Air Content: 2.5% (6% for F-T conditions)

- ASR: expansions less than 0.04% in concrete prism test

Figure 5.37 shows the response surface methodology of optimum SCM proportions for highway pavement concrete in unshaded area of the simplex triangle.

Example 3: Bridge Decks

The requirements of bridge deck concrete is high strength to withstand the load of vehicles moving. The slump should be also high so that the concrete can flow through the steel reinforcement cage. The electrical resistivity of concrete should be low to protect the reinforced steel from chlorides and to reduce corrosion:

- Compressive Strength: 5000 psi to 6000 psi

- Slump:4 inches

- Air Content: 2.5% (6% for F-T conditions)

- RCPT: less than 1000 coulombs

Figure 5.37: Unshaded Area Showing Optimum Mixture Proportions for Highway Pavement Concrete

Response	Contour	Current Y	Lo Limit	Hi Limit
— Slump	4	6.4816597	5.5	.
— Air %	1	2.2317907	2.5	.
— 56-day Comp	.	6071.1333	5500	.
— RCPT 56day	3500	429.30096	.	1000
— ASR 56day	0.2	-0.013783	.	.
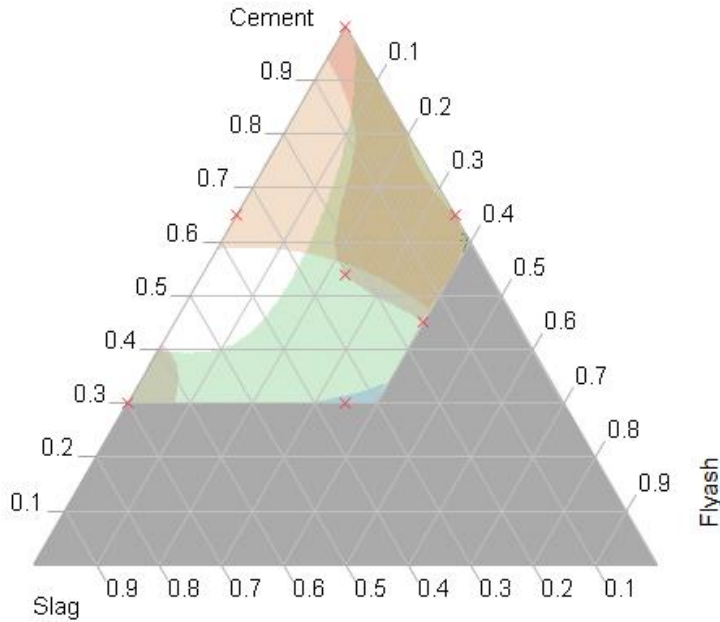
Figure 5.38: Unshaded Area Showing Optimum Mixture Proportions for Bridge Deck Concrete

Figure 5.38 shows the response surface methodology of optimum SCM proportions for bridge deck concrete in unshaded area of the simplex triangle.

106

5.10 Guidelines for Developing SCD Model

1. Determine the Concrete Application

2. Determine the desired properties, which will become the Y-parameter in the equation in Step 6

3. Decide the SCMs to be used and their range of proportions, which will act as upper and lower bound constraints in mixture design.

4. Calculate the 7 design points of simplex-centroid mixture design.

5. Conduct laboratory experiments on these 7 mixtures to obtain the results (Y-values) of desired properties.

6. Use these Y-values to generate prediction equations

7. For validation, choose points within the region and test for actual vs. predicted bi-variate fit.

8. Generate iso-contours for Y-parameters and select a region for trial optimum mixtures.

9. Conduct experiments on selected trial mixtures and use the optimum mixture proportions for concrete construction.

Chapter 6

Conclusions

This chapter reports the conclusions for the concrete, mortar and paste specimens. In addition, recommendations for further research are presented at the end of this chapter.

6.1   Concrete

The following conclusions can be drawn from this study on optimizing SCM proportions to meet multiple performance requirements of ternary concrete mixtures:

1. The compressive strength of concrete for the binary combination of cement + slag is higher than for the binary combination of cement + class F fly ash compared to the control sample at 56 days of testing. However, an optimum dosage of binary combinations exists for each of these combinations at which the compressive strength is at its maximum.

2. The ternary combination of cement + slag + Class F fly ash has higher compressive strength compared to the control sample at 56 days of testing.

3. The split tensile strength of concrete follows the same trend as the compressive strength in terms of binder combinations but at lower magnitudes.

4. The binary and ternary combinations of cement + slag + Class F fly ash in concrete reduce the rapid chloride-ion permeability of concrete.

5. The ternary mixtures of cement + slag + Class F fly ash improve the overall performance of concrete.

6. The mixture design technique is effective in reducing the number of test runs needed to generate predictive surfaces.

7. The application of the simplex-centroid design technique is helpful in optimizing concrete mixtures while maintaining their strength and durability.

8. The iso-contours generated using strength and durability models can be used to design concrete mixtures based on the properties desired.

9. The optimum concrete mixtures found within the simplex region reduce the total cement usage, which in turn decreases the embodied energy and carbon footprint of concrete structures.

6.2 Mortar

1. The ASR expansions in the accelerated mortar bar tests change with respect to the reactivity of the aggregates. Thus, the optimum dosages of SCMs for reducing the expansions below 0.1% differ with the aggregate.

2. The simplex-centroid design model can be used to determine the optimum dosages of SCMs to mitigate ASR expansions below 0.1% at 14-days in the ASTM C1567 test method.

6.3 Cementitious paste systems

1. The electrical resistivity of cementitious paste systems increases with SCMs when compared to the pure cement sample.

2. The cementitious paste samples with cement + slag combination have higher electrical resistivity at early ages but stabilize after 56 days. The combination of cement + class F fly ash samples have lower electrical resistivity at early ages but tend to increase beyond 56 days up to 120 days of testing. The pure cement paste exhibits stable electrical resistivity after 28 days of testing.

3. The pore solution analysis indicates that because of the pozzolanic reaction of SCMs, the alkali ions become trapped in the secondary C-S-H gel, reducing the pore solution alkalinity with age.

4. Because of the instability of calcium sulfoaluminate phases at elevated temperatures, the sulfate (SO_4^{-2}) ions dissolve back into the pore solution of cementitious paste systems.

5. The OH^- ion concentration in the pore solution is reduced for two reasons: (i) the decrease in the ionic concentrations of Na^+, K^+ ions because of the secondary pozzolanic reaction (ii) the increase in SO_4^{-2} ion concentration due to dissolution of AFt and AFm phases at elevated temperatures.

6. The electrical resistivity of cementitious paste systems increases due to the reduction of the ionic concentration of pore solution caused by the SCMs.

Appendices

Appendix A   Concrete properties data

Table 1: Concrete Mixture Proportions for NC Aggregate, gms

Cement	Slag	Flyash	ID's	Coarse Aggte	Fine aggte	Cement	Slag	Flyash	Adj. water
1.00	0.00	0.00	Mix 1	315867	18454	10380	0.0	0.0	4886.3
0.30	0.70	0.00	Mix 2	315867	17974	3114	7266.0	0.0	4884.7
0.45	0.15	0.40	Mix 3	315867	16848	4671	1557.0	4152.0	4880.8
0.65	0.35	0.00	Mix 4	315867	18214	6747	3633.0	0.0	4885.5
0.65	0.00	0.35	Mix 5	315867	17139	6747	0.0	3633.0	4881.8
0.30	0.35	0.35	Mix 6	315867	16899	3114	3633.0	3633.0	4881.0
0.54	0.23	0.23	Mix 7	315867	17432	5605	2387.0	2387.0	4882.8
0.76	0.12	0.12	Mix 8	315867	17921	7889	1246	1246	4884.5
0.42	0.46	0.12	Mix 9	315867	17688	4359	4775	1246	4883.7
0.48	0.18	0.35	Mix 10	315867	18105	4930	1297	3633	4651.6
0.85	0.05	0.10	Mix 11	315867	18044	8823	519	1038	4884.9
0.50	0.20	0.30	Mix 12	315867	17190	5190	2076	3114	4882.0

Table 2: Concrete Fresh Properties

Mix ID's	Slump, in	Unit Wt , pcf	Air , %
1	5	139.23	2.6
2	4.5	136.01	1.9
3	5.5	139.70	1.3
4	6.5	135.25	3.3
5	5.5	138.21	1.2
6	7	135.71	2
7	5.5	137.29	2.1
8	7.3	137.42	1.9
9	6.2	129.85	3.1
10	5.5	133.52	1.4
11	4	137.58	1.8
12	7.1	135.40	2

Table 3: Concrete Cylinder Compressive Strength Values at 28 days

Mix #	1	2	3	Avg	Std. Dev
1	6399	5850	6177	6142	276
2	5140	4665	5164	4990	281
3	4743	4990	4758	4830	138
4	6571	6596	6357	6508	131
5	4981	4724	4311	4672	338
6	4491	4379	4353	4408	73
7	5130	5360	5350	5280	130
8	6516	6516	6128	6387	224
9	5012	5163	4842	5006	161
10	4756	4681	4919	4785	122
11	6126	5942	6381	6150	220
12	4942	4495	4747	4728	224

Table 4: Concrete Cylinder Compressive Strength Values at 56 days

Mix #	1	2	3	Avg	Std. Dev
1	6298	6293	6263	6285	19
2	5973	5701	5544	5739	217
3	5570	6183	6244	5999	373
4	7921	7641	7300	7621	311
5	5621	5752	5488	5620	132
6	5318	5269	5422	5336	78
7	6938	7298	7334	7190	219
8	6992	7109	7268	7123	139
9	6839	6724	6997	6853	137
10	6169	6033	5924	6042	123
11	6835	6605	6923	6788	164
12	6523	6617	6364	6501	128

Table 5: Concrete Cylinder Split Tensile Strength Values at 28 days

Mix #	1	2	3	Avg	Std. Dev
1	703.56	751.41	699.92	718	29
2	618.57	668.91	617.45	635	29
3	636.91	575.18	623.88	612	33
4	641.76	708.45	664.96	672	34
5	501.58	471.91	495.68	490	16
6	574.48	461.55	443	493	71
7	568.93	460.99	599.5	543	73
8	740.41	638.2	546.89	642	97
9	507.97	587.4	474.16	523	58
10	399.47	440.83	461.93	434	32
11	727.03	706.18	698.74	711	15
12	597.37	572.84	518.87	563	40

Table 6: Concrete Cylinder Split Tensile Strength Values at 56 days

Mix #	1	2	3	Avg	Std. Dev
1	733	678	630	680	51
2	656.23	590.31	617.94	621	33
3	589.3	644.37	544.42	593	50
4	671.59	719.94	796.02	729	63
5	512.48	528.1	533.62	525	11
6	695.8	652.35	608.27	652	44
7	725.6	821.98	677.64	742	74
8	620.49	659.84	752.22	678	68
9	664.21	730.06	675.58	690	35
10	624.37	590.34	600.72	605	17
11	696.92	658.8	704.19	687	24
12	732.66	754.42	654.83	714	52

Table 7: Concrete Cylinder RCPT Coulomb Values at 56 days

Mix #	1	2	3	Avg	Std. Dev
1	3022	3028	2955	3002	41
2	475	419	470	455	31
3	905	888	993	929	56
4	1324	1241	1094	1220	116
5	1627	1636	1610	1624	13
6	424	484	468	459	31
7	928	908	1001	946	49
8	2140	2587	2641	2456	275
9	669	715	794	726	63
10	1144	1282	1191	1206	70
11	2399	2275	2459	2378	94
12	980	1228	1197	1135	135

Table 8: Miniature Concrete Prism Test Expansions

Cement	Slag	Flyash	28-day Expn		56-day Expn	
			Avg.	Std.dev	Avg.	Std.dev
1.00	0.00	0.00	0.154	0.030	0.186	0.017
0.30	0.70	0.00	-0.010	0.006	-0.008	0.005
0.45	0.15	0.40	-0.004	0.003	-0.003	0.003
0.65	0.35	0.00	-0.001	0.003	0.010	0.003
0.65	0.00	0.35	-0.002	0.003	0.004	0.002
0.30	0.35	0.35	-0.009	0.006	-0.008	0.006
0.54	0.23	0.23	-0.001	0.006	-0.001	0.006
0.76	0.12	0.12	0.019	0.003	0.019	0.003
0.42	0.46	0.12	0.017	0.004	0.024	0.003
0.48	0.18	0.35	0.017	0.003	0.018	0.003
0.85	0.05	0.10	0.032	0.001	0.033	0.001
0.50	0.20	0.30	0.021	0.008	0.022	0.007

Appendix B   Mortar data

Table 9: Mortar Bar Expansions for New Mexico Aggregate

ID	14 days		28 days	
	Avg	std dev	Avg	std dev
NM 1	0.898	0.014	1.091	0.018
NM 2	0.009	0.001	0.043	0.005
NM 3	0.005	0.001	0.023	0.002
NM 4	0.254	0.003	0.518	0.005
NM 5	0.015	0.003	0.058	0.009
NM 6	0.009	0.001	0.027	0.002
NM 7	0.017	0.003	0.065	0.006
NM 8	0.138	0.009	0.342	0.019
NM 9	0.028	0.004	0.175	0.011
NM 10	0.016	0.003	0.053	0.008
NM 11	0.103	0.011	0.308	0.013
NM 12	0.269	0.011	0.044	0.028
NM 13	0.126	0.017	0.546	0.047
NM 14	0.148	0.005	0.332	0.142
NM 15	0.043	0.007	0.345	0.375

Table 10: Mortar Bar Expansions for Spratt Aggregate

ID	14 days		28 days	
	Avg	std dev	Avg	std dev
SP 1	0.367333	0.012583	0.73	0.022
SP 2	0.010333	0.002309	0.07	0.007
SP 3	0.014333	0.003215	0.03	0.003
SP 4	0.136333	0.004163	0.33	0.013
SP 5	0.014	0.001	0.05	0.001
SP 6	0.013667	0.003215	0.03	0.005
SP 7	0.022333	0.002887	0.07	0.011
SP 8	0.224	0.005	0.52	0.018
SP 9	0.052667	0.002082	0.18	0.009
SP 10	0.023667	0.001528	0.08	0.008
SP 11	0.045333	0.000577	0.16	0.003
SP 12	0.168	0.001528	0.41	0.031
SP 13	0.044	0.003055	0.15	0.003
SP 14	0.030333	0.004	0.11	0.033

Table 11: Mortar Bar Expansions for Adairsville Aggregate

ID	14 days		28 days	
	Avg	std dev	Avg	std dev
AD 1	0.084	0.002	0.120	0.001
AD 2	0.017	0.001	0.025	0.002
AD 3	0.020	0.002	0.025	0.002
AD 4	0.035	0.003	0.056	0.001
AD 5	0.013	0.002	0.025	0.003
AD 6	0.022	0.003	0.027	0.002
AD 7	0.020	0.003	0.029	0.002
AD 8	0.018	0.006	0.025	0.005
AD 9	0.019	0.001	0.030	0.001
AD 10	0.015	0.008	0.044	0.022

Table 12: Mortar Bar Expansions for Stocker Aggregate

ID	14 days		28 days	
	Avg	std dev	Avg	std dev
ST 1	0.248	0.001	0.429	0.003
ST 2	0.013	0.002	0.010	0.002
ST 3	0.059	0.006	0.089	0.009
ST 4	0.026	0.004	0.039	0.003
ST 5	0.200	0.002	0.289	0.007
ST 6	0.028	0.002	0.033	0.003
ST 7	0.055	0.006	0.072	0.008
ST 8	0.144	0.008	0.243	0.012
ST 9	0.003	0.010	0.012	0.011
ST 10	0.047	0.003	0.074	0.008
ST 11	0.155	0.007	0.255	0.004
ST 12	0.017	0.002	0.026	0.006

Appendix C   Simplex Centroid Design

C.1   Lower bound constraint calculation

The minimum and maximum dosages of Cement, Slag and Fly ash are the constraints on component proportions:

$0.3 \leq Cement \leq 1$ $0 \leq Slag \leq 0.7$ $0 \leq Flyash \leq 0.4$

Sum of all lower bounds is: $\sum L_i = 0.3 + 0 + 0 = 0.3$

Table 13: Pseudocomponent calculation for upper and lower bound constraints

Design points	Pseudo components (x_i^*)		
	X1	X2	X3
1	1	0	0
2	0	1	0
3	0	0	1
4	0.5	0.5	0
5	0.5	0	0.5
6	0	0.5	0.5
7	0.33	0.33	0.33
	Transformation $[x_i = L_i + (1 - L)x_i^*]$		
1	1.00	0.00	0.00
2	0.30	0.70	0.00
	0.30	0.00	0.70
X3 max is 0.4, hence 0.7-0.4 = 0.3, 0.3 is equally divided to other components			
3	0.3+0.15= 0.45	0+0.15= 0.15	0.40
4	0.65	0.35	0.00
5	0.65	0.00	0.35
6	0.30	0.35	0.35
7	0.53	0.23	0.23
	Original components (x_i)		
1	1.00	0.00	0.00
2	0.30	0.70	0.00
3	0.45	0.15	0.40
4	0.65	0.35	0.00
5	0.65	0.00	0.35
6	0.30	0.35	0.35
7	0.54	0.23	0.23

Table 14: Actual vs. Predicted values for Concrete Slump, inches

Mix #	Actual	Predicted
1	5	5
2	5	4
3	6	5
4	7	7
5	6	6
6	7	7
7	6	6
8	7	6
9	6	6
10	6	5
11	4	5
12	7	5

Table 15: Actual vs. Predicted values for Concrete Air, %

Mix #	Actual	Predicted
1	2.60	2.60
2	1.90	1.90
3	1.30	1.30
4	3.30	3.30
5	1.20	1.20
6	2.00	2.00
7	2.10	2.10
8	1.90	2.47
9	3.10	2.51
10	1.40	1.55
11	1.80	2.40
12	2.00	1.78

Table 16: Actual vs. Predicted values for Concrete Unit Weight, kg/m^3

Mix #	Actual	Predicted
1	139.23	139.23
2	136.01	136.01
3	139.70	139.70
4	135.25	135.25
5	138.21	138.21
6	135.71	135.71
7	137.29	137.29
8	137.42	137.03
9	129.85	135.17
10	133.52	138.78
11	137.58	137.29
12	135.40	138.05

Table 17: Actual vs. Predicted values for Concrete Compressive Strength, psi

Mix #	28 day		56 day	
	Actual	Predicted	Actual	Predicted
1	6142.00	6142.00	6285.00	6285.00
2	4989.67	4989.67	5739.00	5739.00
3	4830.33	4830.33	5999.00	5999.00
4	6508.00	6508.00	7621.00	7621.00
5	4672.00	4672.00	5620.00	5620.00
6	4407.67	4407.67	5336.00	5336.00
7	5280.00	5280.00	7190.00	7190.00
8	6386.67	5747.02	7123.00	7194.21
9	5005.67	5291.17	6853.00	6925.34
10	4785.33	4913.17	6042.00	6399.33
11	6149.67	5682.06	6788.00	6718.66
12	4728.00	5037.08	6501.00	6761.37

Table 18: Actual vs. Predicted values for Concrete Split Tensile Strength, psi

Mix #	28 day		56 day	
	Actual	Predicted	Actual	Predicted
1	718.30	757.91	680.00	680.00
2	634.98	620.37	621.00	621.00
3	611.99	535.33	593.00	593.00
4	671.72	676.37	729.00	729.00
5	489.72	526.47	525.00	525.00
6	493.01	481.83	652.00	652.00
7	543.14	550.00	742.00	742.00
8	641.83	619.81	678.00	727.48
9	523.18	561.04	690.00	750.95
10	434.08	530.90	605.00	649.29
11	710.65	641.78	687.00	694.63
12	563.03	533.82	714.00	695.79

Table 19: Actual vs. Predicted values for Concrete RCPT, coulombs

Mix #	56 day	
	Actual	Predicted
1	3002	3002
2	455	455
3	929	929
4	1220	1220
5	1624	1624
6	459	459
7	946	946
8	2456	1747.65
9	726	546.67
10	1206	910.11
11	2378	2201.18
12	1135	906.85

Table 20: Actual vs. Predicted values for MCPT, %

Mix #	56 day	
	Actual	Predicted
1	0.186	0.186
2	-0.008	-0.008
3	-0.003	-0.003
4	0.010	0.010
5	0.004	0.004
6	-0.008	-0.008
7	-0.001	-0.001
8	0.020	0.050
9	0.020	-0.016
10	0.020	-0.004
11	0.030	0.087
12	0.020	-0.004

Table 21: Actual vs. Predicted values for New Mexico mortar bars, %

Mix #	Actual	Predicted
1	5	5
2	0.898	0.898
3	0.009	0.009
4	0.005	0.005
5	0.254	0.254
6	0.015	0.015
7	0.009	0.009
8	0.017	0.017
9	0.270	0.280
10	0.043	-0.006
11	0.033	0.040
12	0.138	0.237

Table 22: Actual vs. Predicted values for Spratt mortar bars, %

Mix #	Actual	Predicted
1	0.370	0.370
2	0.010	0.010
3	0.014	0.014
4	0.136	0.136
5	0.014	0.014
6	0.014	0.014
7	0.022	0.022
8	0.224	0.129
9	0.053	0.014
10	0.024	0.029
11	0.045	0.102
12	0.019	0.069

Table 23: Actual vs. Predicted values for Adairsville mortar bars, %

Mix #	Actual	Predicted
1	0.080	0.080
2	0.017	0.017
3	0.020	0.020
4	0.035	0.035
5	0.013	0.013
6	0.022	0.022
7	0.020	0.020
8	0.018	0.036
9	0.019	0.019
10	0.015	0.023
11	0.031	0.029
12	0.031	0.024

Table 24: Actual vs. Predicted values for Stocker mortar bars, %

Mix #	Actual	Predicted
1	0.248	0.248
2	0.013	0.013
3	0.059	0.059
4	0.026	0.026
5	0.200	0.200
6	0.028	0.028
7	0.055	0.055
8	0.144	0.133
9	0.003	-0.004
10	0.047	0.072

Appendix D   Cementitious Paste Data

D.1 Titrations

Table 25: Titration for Standardization of NaOH against KHp solutions

End Reaction I:	KHp + NaOH → NaKp + H2O				
# of moles of KHp = g/M.W	**Calculation:**				
	KHp		**NaOH**		
	m1	V1 (ml)	m2	V2(ml)	(V2 from graph)
run 1 0.1170/204.22					
= 0.000573	0.000573	1000	x	5.335	
	x =	0.107387	moles		
	Calculation:				
	KHp		**NaOH**		
	m1	V1 (ml)	m2	V2(ml)	(V2 from graph)
run 2 0.1033/204.22					
= 0.000506	0.000506	1000	x	4.6	
	x =	0.109962	moles		

Average concentration of NaOH solution prepared = 0.108674881 M

Table 26: Titration for Standardization of HCl against NaOH solutions

End Reaction II:	HCl + NaOH → NaCl + H2O			
10 ml of HCl was used for all test runs				
Run 1	ml of NaOH used for titration			
=	8.19			
Calculation:				
	HCl		NaOH	
	ml	V1 (ml)	m2	V2(ml)
x =	10	0.108675	8.19	(V2 from graph)
x =	0.089005	moles		
Run 2	ml of NaOH used for titration			
=	7.99			
Calculation:				
	HCl		NaOH	
	ml	V1 (ml)	m2	V2(ml)
x =	10	0.108675	7.99	(V2 from graph)
x =	0.086831	moles		
Run 3	ml of NaOH used for titration			
=	8.19			
Calculation:				
	HCl		NaOH	
	ml	V1 (ml)	m2	V2(ml)
x =	10	0.108675	8.19	(V2 from graph)
x =	0.089005	moles		

Average concentration of HCl solution prepared = 0.088280228 M

D.2 Pore solution ionic concentrations

Table 27: Ion concentrations for 100% cement sample, mol/L

Day	Na	K	Ca	S	OH
0	0.167727	0.34311	0.019462	0.189936	0.26484
7	0.400917	0.404764	0.002817	0.009543	0.57382
56	0.396698	0.40457	0.004366	0.030307	0.6621
56T	0.537926	0.463534	0.004292	0.275927	0.358417

Table 28: Ion concentrations for 30% cement + 70% slag sample, mol/L

Day	Na	K	Ca	S	OH
0	0.055938	0.063941	0.026024	0.043287	0.158904
7	0.119827	0.106035	0.003887	0.003917	0.185388
56	0.106134	0.092076	0.001747	0.00761	0.158904
56T	0.04515	4.25E-05	8.66E-05	0.000695	0.08828

Table 29: Ion concentrations for 45% cement + 15% slag + 40% fly ash sample, mol/L

Day	Na	K	Ca	S	OH
0	0.070771	0.155608	0.021458	0.08121	0.070624
7	0.186918	0.184177	0.003406	0.002217	0.35312
56	0.132233	0.141055	0	0.005863	0.247184
56T	0.101784	0.109679	0.000393	0.06879	0.050761

Table 30: Ion concentrations for 65% cement + 35% slag sample, mol/L

Day	Na	K	Ca	S	OH
0	0.080905	0.189778	0.022207	0.095057	0.114764
7	0.262738	0.251829	0.003042	0.007613	0.494368
56	0.259898	0.248016	0.001048	0.012861	0.406088
56T	0.021314	0.02394	0.010055	0.011383	0.2207

Table 31: Ion concentrations for 65% cement + 35% fly ash sample, mol/L

Day	Na	K	Ca	S	OH
0	0.094607	0.233207	0.025051	0.123187	0.08828
7	0.240663	0.247466	0.005387	0.001877	0.344292
56	0.199784	0.220342	0.001305	0.004569	0.326636
56T	0.26042	0.273733	0.00121	0.053485	0.300152

Table 32: Ion concentrations for 30% cement + 35% slag + 35% fly ash sample, mol/L

Day	Na	K	Ca	S	OH
0	0.047125	0.082814	0.022713	0.052799	0.079452
7	0.125717	0.109642	0.003516	0.002704	0.17656
56	0.083398	0.083712	0.000704	0.003836	0.123592
56T	0.102432	0.103079	0.001325	0.063873	0.070624

Table 33: Ion concentrations for 54% cement + 23% slag + 23% fly ash sample, mol/L

Day	Na	K	Ca	S	OH
0	0.073446	0.172463	0.02575	0.091595	0.070624
7	0.221898	0.208881	0.002071	0.003237	0.326636
56	0.165421	0.169956	0.001243	0.005717	0.282496
56T	0.182494	0.174386	0.00134	0.081244	0.167732

D.3 Electrical Resistivity

Table 34: Average Electrical Resitivity of Cementitious Pastes(ohm.m)

Cement	1.00	0.30	0.45	0.65	0.65	0.30	0.54
Slag	0.00	0.70	0.15	0.35	0.00	0.35	0.23
Flyash	0.00	0.00	0.40	0.00	0.35	0.35	0.23
Day/Mix ID	1	2	3	4	5	6	7
0	15.727	15.041	8.798	13.500	12.066	18.116	15.853
0.1	27.503	26.069	30.359	23.294	26.779	23.393	19.617
1	32.490	27.493	35.122	29.570	30.959	27.859	22.870
2	40.802	31.626	37.106	33.475	32.555	32.446	26.560
3	50.902	49.834	41.017	40.065	33.740	35.107	28.579
4	55.484	60.081	44.450	47.161	35.285	39.629	30.278
5	58.568	73.413	47.873	52.186	37.530	48.671	37.824
6	61.293	84.608	54.525	55.924	46.165	57.438	43.025
7	63.033	87.624	57.120	57.594	49.485	60.500	45.152
14	34.769	118.112	33.864	49.676	29.720	83.813	44.092
15	36.788	128.676	38.888	53.632	32.599	94.213	48.901
18	37.685	144.378	51.430	58.852	38.644	117.786	58.200
20	36.584	148.864	58.322	59.913	41.682	127.656	61.585
21	37.644	156.409	64.481	62.360	45.189	137.241	65.745
22	37.685	160.284	68.151	63.665	47.310	144.174	68.029
25	38.297	173.131	82.875	67.907	55.671	165.994	77.124
27	39.602	184.959	95.069	72.148	62.605	183.531	84.628
28	39.153	185.570	98.495	72.189	65.174	188.425	86.219
29	39.398	189.445	103.715	73.616	68.314	196.786	89.155
31	39.316	197.806	117.664	76.553	78.511	215.955	96.374
35	40.581	213.508	136.629	81.243	92.989	244.912	108.895
39	42.253	233.696	166.605	85.811	113.381	266.528	123.374
42	42.212	240.630	184.347	90.134	129.084	312.003	136.547
49	43.640	268.363	230.434	98.128	162.731	371.141	164.158
56	44.333	284.677	275.908	101.554	197.398	442.514	191.688
63	39.113	261.634	287.532	88.503	209.633	443.330	194.543
70	39.276	271.830	334.842	95.436	250.826	464.538	217.790
84	44.415	328.317	462.906	109.507	352.788	603.614	295.689
120	45.434	369.917	599.943	119.295	493.087	750.438	375.219

Table 35: Standard Deviation of Electrical Resitivity for Cementitious Pastes(ohm.m)

Cement	1.00	0.30	0.45	0.65	0.65	0.30	0.54
Slag	0.00	0.70	0.15	0.35	0.00	0.35	0.23
Flyash	0.00	0.00	0.40	0.00	0.35	0.35	0.23
Day/Mix ID	1	2	3	4	5	6	7
0	8.331	9.358	6.362	8.511	7.508	7.599	6.587
0.1	5.788	7.328	6.399	6.608	6.398	0.805	0.410
1	3.438	2.728	6.859	0.720	3.761	0.810	0.374
2	3.242	2.846	8.617	1.448	4.647	0.824	0.370
3	3.179	2.519	9.198	2.792	5.295	0.898	0.377
4	2.870	2.352	8.898	3.317	5.351	0.860	0.599
5	2.322	1.920	7.200	3.426	4.702	1.060	0.751
6	1.397	1.327	5.842	3.460	3.015	1.174	0.813
7	3.265	3.421	0.473	2.132	0.709	2.712	1.833
14	0.498	1.285	0.590	1.811	1.772	4.012	0.689
15	0.393	2.148	0.709	1.881	1.920	4.619	0.717
18	0.424	2.447	1.110	2.123	2.231	5.200	1.069
20	0.533	1.869	0.997	2.264	2.342	6.158	0.859
21	0.308	2.891	1.002	2.367	2.631	6.128	0.833
22	0.533	2.447	1.362	2.402	2.698	7.143	0.764
25	0.647	3.406	0.989	2.650	3.088	8.915	1.041
27	0.509	2.891	0.924	2.695	3.738	7.641	1.413
28	0.441	2.891	0.612	2.650	3.704	8.023	1.207
29	0.441	3.139	1.320	2.796	4.112	8.745	1.342
31	0.578	3.688	0.934	2.698	4.193	10.219	1.418
35	0.604	3.406	1.869	3.313	5.008	12.925	1.619
39	0.674	3.237	2.891	1.783	2.547	24.366	7.984
42	0.533	3.933	5.517	4.084	7.443	14.425	2.022
49	1.026	2.547	3.532	5.294	8.565	21.485	2.547
56	0.777	4.945	5.227	5.008	13.422	15.541	3.532
63	0.926	4.592	6.118	0.934	12.377	7.375	8.477
70	1.067	3.688	7.169	5.333	16.000	11.102	3.237
84	1.088	2.547	3.532	5.008	23.161	25.470	5.782
120	0.885	4.632	12.852	5.438	31.242	40.531	9.345

Bibliography

[Al-Akhras, 2006] Al-Akhras, N. M. (2006). Durability of metakaolin concrete to sulfate attack. *Cement and Concrete Research*, 36(9):1727 – 1734.

[Altan and Erdogan, 2012] Altan, E. and Erdogan, S. T. (2012). Alkali activation of a slag at ambient and elevated temperatures. *Cement and Concrete Composites*, 34(2):131 – 139.

[Antiohos et al., 2005] Antiohos, S., Maganari, K., and Tsimas, S. (2005). Evaluation of blends of high and low calcium fly ashes for use as supplementary cementing materials. *Cement and Concrete Composites*, 27(3):349 – 356.

[Bagheri et al., 2012] Bagheri, A. R., Zanganeh, H., and Moalemi, M. M. (2012). Mechanical and durability properties of ternary concretes containing silica fume and low reactivity blast furnace slag. *Cement and Concrete Composites*, 34(5):663 – 670.

[Bakharev et al., 2002] Bakharev, T., Sanjayan, J., and Cheng, Y.-B. (2002). Sulfate attack on alkali-activated slag concrete. *Cement and Concrete Research*, 32(2):211 – 216.

[Bentz et al., 2011] Bentz, D. P., Hansen, A. S., and Guynn, J. M. (2011). Optimization of cement and fly ash particle sizes to produce sustainable concretes. *Cement and Concrete Composites*, 33(8):824 – 831.

[Chatterji, 1994] Chatterji, S. (1994). A discussion of the paper the effectiveness of supplementary cementing materials in suppressing expansion due to asr. part 1. concrete expansion and portlandite depletion by j. duchesne and m.a. brub. *Cement and Concrete Research*, 24(8):1572 – 1573.

[Cornell, 2002] Cornell, J. (2002). *Experiments with mixtures: designs, models, and the analysis of mixture data. 3rd Ed.* John Wiley & Sons Inc.

[Douglas and Pouskouleli, 1991] Douglas, E. and Pouskouleli, G. (1991). Prediction of compressive strength of mortars made with portland cement - blast-furnace slag - fly ash blends. *Cement and Concrete Research*, 21(4):523 – 534.

[Duchesne and Brub, 1994] Duchesne, J. and Brub, M. (1994). The effectiveness of supplementary cementing materials in suppressing expansion due to asr: Another look at the reaction mechanisms part 1: Concrete expansion and portlandite depletion. *Cement and Concrete Research*, 24(1):73 – 82.

[Duval and Kadri, 1998] Duval, R. and Kadri, E. (1998). Influence of silica fume on the workability and the compressive strength of high-performance concretes. *Cement and Concrete Research*, 28(4):533 – 547.

[Fisher and Mackenzie, 1923] Fisher, R. A. and Mackenzie, W. A. (1923). Studies in crop variation. ii. the manurial response of different potato varieties. *The Journal of Agricultural Science*, 13:311–320.

[Ghrici et al., 2007] Ghrici, M., Kenai, S., and Said-Mansour, M. (2007). Mechanical properties and durability of mortar and concrete containing natural pozzolana and limestone blended cements. *Cement and Concrete Composites*, 29(7):542 – 549.

[Guneyisi et al., 2012] Guneyisi, E., Gesoglu, M., Karaoglu, S., and Mermerdas, K. (2012). Strength, permeability and shrinkage cracking of silica fume and metakaolin concretes. *Construction and Building Materials*, 34(0):120 – 130.

[Jr. and Diamond, 1981] Jr., R. B. and Diamond, S. (1981). Expression and analysis of pore fluids from hardened cement pastes and mortars. *Cement and Concrete Research*, 11(2):279 – 285.

[Lane and Ozyildirim, 1999] Lane, D. and Ozyildirim, C. (1999). Preventive measures for alkali-silica reactions (binary and ternary systems). *Cement and Concrete Research*, 29(8):1281 – 1288.

[Li and Zhao, 2003] Li, G. and Zhao, X. (2003). Properties of concrete incorporating fly ash and ground granulated blast-furnace slag. *Cement and Concrete Composites*, 25(3):293 – 299.

[Longuet et al., 1973] Longuet, P., Burglen, L., and Zelwer, A. (1973). La phase liquide du ciment hydrate. *Revue Materiaux Construction Travaux 676 (1973) 3541.*

[Malvar and Lenke, 2003] Malvar, L. and Lenke, L. (2003). Efficiency of fly ash in mitigating alkali-silica reaction based on chemical composition. *ACI Materials Journal*, 103:319–326.

[Massazza, 1993] Massazza, F. (1993). Pozzolanic cements. *Cement and Concrete Composites*, 15(4):185 – 214. ¡ce:title¿Special Issue on Composite Cements¡/ce:title¿.

[McKeen et al., 1998] McKeen, R., Lary, P., Lenke, R., Kiran, P., and Pallachulla, K. (1998). Mitigation of alkali silica reactivity in new mexico. *Technical Report,Materials Research Center, ATR Institute, University of New Mexico.*

[Mindess et al., 2003] Mindess, S., Young, J. F., and Darwin, D. (2003). *Concrete. 2nd Ed.* Prentice Hall, Pearson Education, Inc. Upper Saddle River, NJ 07458,.

[Moser et al., 2010] Moser, R. D., Jayapalan, A. R., Garas, V. Y., and E.Kurtis, K. (2010). Assessment of binary and ternary blends of metakaolin and class c fly ash for alkali-silica reaction mitigation in concrete. *Cement and Concrete Research*, 40(12):1664 – 1672.

[Mostafa et al., 2001] Mostafa, N., El-Hemaly, S., Al-Wakeel, E., El-Korashy, S., and Brown, P. (2001). Characterization and evaluation of the hydraulic activity of water-cooled slag and air-cooled slag. *Cement and Concrete Research*, 31(6):899 – 904.

[Pal et al., 2003] Pal, S., Mukherjee, A., and Pathak, S. (2003). Investigation of hydraulic activity of ground granulated blast furnace slag in concrete. *Cement and Concrete Research*, 33(9):1481 – 1486.

[Poon et al., 2000] Poon, C., Lam, L., and Wong, Y. (2000). A study on high strength concrete prepared with large volumes of low calcium fly ash. *Cement and Concrete Research*, 30(3):447 – 455.

[Radlinski and Olek, 2012] Radlinski, M. and Olek, J. (2012). Investigation into the synergistic effects in ternary cementitious systems containing portland cement, fly ash and silica fume. *Cement and Concrete Composites*, 34(4):451 – 459.

[Rajamane et al., 2007] Rajamane, N., Peter, J. A., and Ambily, P. (2007). Prediction of compressive strength of concrete with fly ash as sand replacement material. *Cement and Concrete Composites*, 29(3):218 – 223.

[Rangaraju and Harish, 2011] Rangaraju, P. and Harish, K. (2011). Effectiveness of fly ash and its blend with lithium admixture in mitigating asr in concrete - role of chemical, physical and mineralogical aspects. *NAVFAC Phase I Technical Report, Technologies and Methodologies in Prevention of ASR in Concrete Pavements*.

[Rangaraju and Math, 2012] Rangaraju, P. and Math, S. (2012). Effectiveness of slag in mitigating asr in concrete - role of chemical, physical and mineralogical aspects. *NAVFAC Phase II Technical Report, Technologies and Methodologies in Prevention of ASR in Concrete Pavements*.

[Rasheeduzzafar and Hussain, 1991] Rasheeduzzafar and Hussain, S. E. (1991). Effect of microsilica and blast furnace slag on pore solution composition and alkali-silica reaction. *Cement and Concrete Composites*, 13(3):219 – 225. ¡ce:title¿Special Issue on Blended Cements¡/ce:title¿.

[S. and Chatterji, 1979] S. and Chatterji (1979). The role of ca(oh)2 in the breakdown of portland cement concrete due to alkali-silica reaction. *Cement and Concrete Research*, 9(2):185 – 188.

[Scheff, 1958] Scheff, H. (1958). Experiments with mixtures. *Journal of the Royal Statistical Society. Series B (Methodological)*, 20(2):pp. 344–360.

[Scheffe, 1963] Scheffe, H. (1963). The simplex-centroid design for experiments with mixtures. *Journal of the Royal Statistical Society. Series B (Methodological)*, 25(2):pp. 235–263.

[Shehata and Thomas, 2002] Shehata, M. H. and Thomas, M. D. (2002). Use of ternary blends containing silica fume and fly ash to suppress expansion due to alkalisilica reaction in concrete. *Cement and Concrete Research*, 32(3):341 – 349.

[Stanton, 1940] Stanton, T. (1940). Expansion of concrete through reaction between cement and aggregate. In *Proceedings,American Society of Civil Engineers*, pages 1781–1811.

[Wang and Chen, 1997] Wang, D. and Chen, Z. (1997). On predicting compressive strengths of mortars with ternary blends of cement,ggbfs and fly ash. *Cement and Concrete Research*, 27(4):487 – 493.

[Zhang et al., 2012] Zhang, T., Yu, Q., Wei, J., and Zhang, P. (2012). Efficient utilization of cementitious materials to produce sustainable blended cement. *Cement and Concrete Composites*, 34(5):692 – 699.

[Zuquan et al., 2007] Zuquan, J., Wei, S., Yunsheng, Z., Jinyang, J., and Jianzhong, L. (2007). Interaction between sulfate and chloride solution attack of concretes with and without fly ash. *Cement and Concrete Research*, 37(8):1223 – 1232.